Real-Time Vehicle Emission Estimation Using Traffic Data

By

Anjie Liu

A thesis

presented to the University of Waterloo

in fulfilment of the

thesis requirement for the degree of

Master of Applied Science

in

Civil Engineering,

Transportation Systems

Waterloo, Ontario, Canada, 2019

Author's Declaration

I hereby declare that I am the sole author of this thesis. This is a true copy of the thesis, including any required final revisions, as accepted by my examiners.

I understand that my thesis may be made electronically available to the public.

Abstract

The current state of climate change should be addressed by all sectors that contribute to it. One of the major contributors is the transportation sector, which generates a quarter of greenhouse gas emissions in North America (Environment and Climate Change Canada, 2018; U.S. EPA, 2018). Most of these transportation related emissions are from road vehicles; as result, how to manage and control traffic or vehicular emissions is therefore becoming a major concern for the governments, the public and the transportation authorities.

One of the key requirements to emission management and control is the ability to quantify the magnitude of emissions by traffic of an existing or future network under specific road plans, designs and traffic management schemes. Unfortunately, vehicular traffic emissions are difficult to quantify or predict, which has led a significant number of efforts over the past decades to address this challenge. Three general methods have been proposed in literature. The first method is for determining the traffic emissions of an existing road network with the idea of measuring the tail-pipe emissions of individual vehicles directly. This approach, while most accurate, is costly and difficult to scale as it would require all vehicles being equipped with tail-pipe emission sensors. The second approach is applying ambient pollutant sensors to measure the emissions generated by the traffic near the sensors. This method is only approximate as the vehicle-generated emissions can easily be confounded by other nearby emitters and weather and environmental conditions. Note that both of these methods are measurement-based and can only be used to evaluate the existing conditions (e.g., after a traffic project is implemented), which means that it cannot be used for evaluating alternative transportation projects at the planning stage. The last method is model-based with the idea of developing models that can be used to estimate traffic emissions. The emission models in this method link the amount of emissions being generated by a group of vehicles to their operations details as well as other influencing factors such as weather, fuel and road geometry. This last method is the most scalable, both spatially and temporally, and also most flexible as it can meet the needs of both monitoring (using field data) and prediction.

Typically, traffic emissions are modelled on a macroscopic scale based on the distance travelled by vehicles and their average speeds. However, for traffic management applications, a model of higher granularity would be preferred so that impacts of different traffic control schemes can be captured. Furthermore, recent advances in vehicle detection technology has significantly increased the spatiotemporal resolutions of traffic data. For example, video-based vehicle detection can provide more details about vehicle movements and vehicle types than previous methods like inductive loop detection. Using such detection data, the vehicle movements, referred to as trajectories, can be determined on a second-by-second basis. These vehicle trajectories can then be used to estimate the emissions produced by the vehicles.

In this research, we have proposed a new approach that can be used to estimate traffic generated emissions in real time using high resolution traffic data. The essential component of the proposed emission estimation method is the process to reconstruct vehicle trajectories based on available data and some assumptions on the expected vehicle motions including cruising, acceleration and

deceleration, and car-following. The reconstructed trajectories containing instantaneous speed and acceleration data are then used to estimate emissions using the MOVES emission simulator. Furthermore, a simplified rate-based module was developed to replace the MOVES software for direct emission calculation, leading to significant improvement in the computational efficiency of the proposed method.

The proposed method was tested in a simulated environment using the well-known traffic simulator - Vissim. In the Vissim model, the traffic activities, signal timing, and vehicle detection were simulated and both the original vehicle trajectories and detection data recorded. To evaluate the proposed method, two sets of emission estimates are compared: the "ground truth" set of estimates comes from the originally simulated vehicle trajectories, and the set from trajectories reconstructed using the detection data.

Results show that the performance of the proposed method depends on many factors, such as traffic volumes, the placement of detectors, and which greenhouse gas is being estimated. Sensitivity analyses were performed to see whether the proposed method is sufficiently sensitive to the impacts of traffic control schemes. The results from the sensitivity analyses indicate that the proposed method can capture impacts of signal timing changes and signal coordination but is insufficiently sensitive to speed limit changes.

Further research is recommended to validate the proposed method using field studies. Another recommendation, which falls outside of this area of research, would be to investigate the feasibility of equipping vehicles with devices that can record their instantaneous fuel consumption and location data. With this information, traffic controllers would be better informed for emission estimation than they would be with only detection data.

Acknowledgements

First and foremost, I would like to thank Dr. Liping Fu, my supervisor, for his guidance and support. From conception to final touches, Dr. Fu has played an important role in this project. He made it possible and guided it to its completion. I would also like to thank Matthew Muresan and Wilson Wang for sharing their expertise in subjects related to my research. Their guidance proved helpful throughout this project.

As the first half of this research was supported by Miovision, I would like to thank Justin Eichel and Sajad Shiravi for their feedback and support in the first half of this project. They gave me a good understanding of the context in which this research is made meaningful.

Finally, I would like to thank all my friends and family for the good times they have given me throughout my Master's. It would have been quite a different experience without them.

Contents

Figures

Tables

Abbreviations

BVWP	Bundesverkehrswegeplan
CFC	Chlorofluorocarbon
CH_4	Methane
CMEM	Comprehensive Modal Emission Model
CO_2	Carbon Dioxide
COPERT	Computer Program to calculate Emissions from Road Transport
EPA	Environmental Protection Agency
GHG	Greenhouse Gas
GIS	Geographic Information System
GPS	Global Positioning System
HBEFA	European HandBook of Emission Factors
MOVES	MOtor Vehicle Emission Simulator
N_2O	Nitrous Oxide
NIM	New Interface for MOVES
PC	Passenger Car
PEMS	Portable Emission Measurement System
RBC	Ring Barrier Control
the Region	Region of Waterloo
SCOOT	Split Cycle Offset Optimisation Technique
TMC	Turning Movement Count
US	United States (of America)
VKT	Vehicle Kilometers
VSP	Vehicle Specific Power

Symbols

General Symbols

t	denotes a point in time
T	denotes a duration of time
x	denotes a position in space
l	denotes a length of distance
v	denotes vehicle speed
F	denotes the fraction of time spent by vehicles in a particular operating mode
E	denotes the quantity of emissions estimated
R	denotes an emission rate used in emission estimation
q	denotes vehicle volume

Subscripts

adv	pertains to advance detections
$stop$	pertains to stop-line detections
$turn$	pertains to detections during turning movements
$exit$	pertains to detections at the exit of an intersection
n	pertains to a vehicle
$n-1$	pertains to the vehicle preceding vehicle n in the platoon
i	pertains to a time step
$passing$	pertains to the section between the stop-line and exit of an intersection
$approach$	pertains to the section between the advance detector and stop-line of an intersection
$1,2$	pertains to the time of arrival at and departure from a detector respectively
h	pertains to the headway between two consecutive vehicles
$cruise$	pertians to cruising motions
s	pertains to the starting point of a segment
f	pertains to the finishing point of a segment

$opMode$	pertains to an operating mode in the MOVES model
$type$	pertains to a vehicle type in the MOVES model
$link$	pertains to an input tuple disaggregated for the MOVES model
pp	pertains to a pollutant process combination
$reconstructed$	pertains to a set of reconstructed trajectories
$original$	pertains to a set of trajectories originally simulated in Vissim

Specific Symbols

$_{\%cruise}$	is the percentile of passing speeds to be considered the cruise speed
m_{lc}	is the number of lane-cycle vehicle groups to sample when determining cruise speeds
$T_{stop,threshold}$	is the threshold for determining whether a detection is long enough to indicate a stop
$p_{stop,cruise}$	is the fraction of the cruise speed that the average speed can reach if a vehicle stops
$T_{h,discharge}$	is the maximum time headway of vehicles discharging from a queue
l_{eff}	is the effective length of a vehicle in Newell's car-following model
T_N	is the time offset in Newell's car-following model
dt	is the time-step increment of discretization
k_3, k_4, k_5	are empirically calibrated parameters for deceleration (Kumar Maurya & Bokare, 2012)
β_0, β_1	are empirically calibrated parameters for acceleration (Y. Zhang, Lv, & Wang, 2013)
$t_{lag,stop}$	is the time a vehicle takes to come to a complete stop after it has already been detected
$t_{lag,start}$	is the time a vehicle has already begun accelerating but is still detected at the detector
p_{adj}	is the proportion to adjust a parameter by when fitting acceleration/deceleration curves
T_{off}	is the time difference between a detection and a reconstructed trajectory
$T_{tolerance}$	is the acceptable value for T_{off}
T_c	is the time length of a particular signal cycle
$\Delta_{\%}$	is the percentage difference between emission estimates from two sets of inputs

Chapter 1 Introduction

As the concerns of climate grows, new methods of reducing greenhouse gas production are sought after. One of the major anthropogenic sources of greenhouse gasses is the transportation sector. In the transportation sector, vehicles contribute to a significant amount of all man-made emissions (Environment and Climate Change Canada, 2018; U.S. EPA, 2018). Attempts have been made from various fronts to reduce vehicle emissions as their production increases; however, it remains a challenge to quantify emissions in many situations. Quantifying emissions is particularly important, because what cannot be measured cannot be managed.

The quantification of vehicle emissions presents a myriad of challenges. From direct measurements to modelling practices, great costs and efforts must be undertaken. Often, trade-offs between cost and accuracy are made. These trade-offs require knowing what is being sacrificed to make the method feasible. When the trade-offs are known, one can decide the choice of method to use and the parameters that govern it. A commonly used method of quantification is modelling. Emissions can be modelled based on vehicle activities at various levels of detail. The modelling methods are based on past research in the relationships between vehicle operations and emission production.

As various transportation related analyses are taking emissions into account, from planning and design to technology, there are improvements to be made and new opportunities to be taken advantage of. This thesis explores using emission modelling to quantify emissions in real-time based on traffic data. The purpose of a real-time emission monitoring method is to enable a way to incorporate emissions into the set of performance metrics used in traffic management. For example, in signal control optimization, traffic controllers may measure vehicle throughput, travel times, or queue lengths to evaluate their traffic control strategies. Emissions are often considered in many transportation management aspects; however, they are rarely considered in microscopic control scenarios due to the difficulties of quantifying emission production at that level of detail.

Due to current technologies, more complex traffic flow-related performance metrics can be measured in real-time in the traffic management industry, allowing traffic control schemes to adapt more intelligently to optimize for traffic flow. The issue of reducing emissions should not be left behind in this progress. As real-time traffic control optimization is enhanced for improving flow, emission production should also be considered as a performance metric.

To address this problem, a method for monitoring emissions in real-time should be developed. Since traffic data is collected for other performance metrics, the same data can be used to model emissions. If emissions can be monitored alongside flow metrics, then traffic control schemes can be optimized for a more wholistic set of objectives that reflect current goals in the transportation sector.

1.1 Motivation

The research presented in this thesis is motivated by the current consensus on climate trends and practices in traffic management. One of the pressing issues looming on the horizon is the persistent climate change that has been picking up momentum since the beginning of the industrial revolution. While the global temperature has fluctuated immensely in the past, its current rate of change is unprecedented, and alarming compared to the last few millennia. It is well-established that climate change is largely due to increasing levels of GHG's in the atmosphere, which is a result of fossil fuel combustion. In Canada and the US, the transportation sector generates 24% and 28% of greenhouse gas emissions respectively, a substantial amount of which is generated by road vehicles (Environment and Climate Change Canada, 2018; U.S. EPA, 2018). As climate change becomes a more pressing issue, traffic control strategies need to adapt to consider its role in climate change.

In addition to increasing global warming, vehicle emissions also degrade air quality. In urban areas, as populations and, consequently, transportation activities become denser, air quality is becoming a growing concern. The degradation of air quality due to traffic activities have been observed to impact the health of residents nearby (K. Zhang & Batterman, 2014). The effects could include increased incidence and severity of respiratory and cardiovascular ailments (Laumbach & Kipen, 2012). It has been shown that measures taken to reduce emission have been able to make a difference in health effects. For example, when efforts were taken to improve air quality during the Beijing Olympics, the average number of outpatient visits for asthma was almost halved (Li, Wang, Kan, Xu, & Chen, 2010). Besides health effects, emissions also reduce visibility and sun penetration, which can cause ecological and aesthetic issues.

Even if transportation modes switch to cleaner fuels and eliminate emissions, there is still the concern of energy consumption, which is highly correlated with emission production. It would still be beneficial to be able to monitor energy consumption, as the energy must be produced somewhere. Energy production, transmission, and storage have their own costs and externalities that contribute to sustainability problems.

1.2 Background

Emission reduction strategies are employed in several different fields ranging across user behaviour, vehicle technology, infrastructure, and control systems. They have varying levels of effectiveness, often depending on how they are implemented. Some examples of emission reduction strategies in the field of traffic controls include speed limit controls on freeways (European Environment Agency, 2013) and designated Low Emission Zones (European Union, 2019). When it comes to traffic controls, one of the challenges is that it is often a dynamic problem. Measures implemented in traffic controls tend to be analysed over a much shorter time frame than those in the areas of economic incentives, regulations, technology, and infrastructure, because the turn-around time is shorter for the cause-and-effect cycle to take place. In traffic controls, the effects can be immediate, and the system can change immediately,

meaning that the effects and changes must be known quickly in order to inform further controls. Furthermore, the effects of traffic controls can be subtle and would require relatively microscopic emission quantification methods to be captured.

Emission quantification is a widely studied field with a diverse set of applications. Areas of applications include testing, alternatives analysis, and real-world monitoring. Typically, testing is performed with equipment that directly measure emissions, such as Portable Emission Measurement Systems (PEMS) or closed facilities with chassis dynamometers (Franco et al., 2013a; Rexeis, Hausberger, Kühlwein, & Luz, 2017; Wu et al., 2015), as described in Sections 2.1.1 and 2.1.2 respectively. Alternatives analyses tend to be performed using simulation models in conjunction with emission models to allow user-defined hypothetical scenarios to be analysed (So, Motamedidehkordi, Wu, Busch, & Choi, 2017). For real-world monitoring applications, both direct measurements and simulation modelling are costly to scale up; therefore, data-driven approaches are usually preferred. Using collected data, highly generalizable models can be used to obtain emission estimates. This approach was used in several studies (Csikós & Varga, 2012; Hang Liu, Tok, & Ritchie, 2011; Park, Ahn, Rakha, & Lee, 2015; Shan et al., 2018; Yao et al., 2012). These methods depend on data sources such as inductive loops, GPS probes, and video cameras. They vary in terms of sensitivity and ability to capture effects of traffic controls. Given the recent advances in data collection and communications technology, methods that use data for modelling can be implemented in real-time if they are sufficiently quick to compute.

1.3 Problem Statement

While many strategies exist for managing vehicle emissions, there are still areas where emissions are not accounted for. One such area is the microscopic and dynamic controls of traffic. In microscopic traffic management, performance metrics such as levels of service, queue lengths, and travel times are often monitored to evaluate signal controls (U.S. Department of Transportation, 2017). Recent technologies allow these metrics to be monitored in real-time so that traffic controls can be adjusted accordingly, such as in adaptive signal control systems like the Split Cycle Offset Optimisation Technique (SCOOT) (Bretherton, Wood, & Raha, 2007). However, it is difficult to incorporate emissions into these performance metrics. To bring emissions into the set of performance metrics used for traffic control, some challenges must be tackled.

Some of the challenges are due to the dynamic nature of traffic systems and the diversity of scenarios that such systems can experience. The focus is on urban traffic, which has complex behaviours and is heavily influenced by controls. As this is a traffic control approach rather than a long-term planning and policy approach, the method must be able to generate results quickly. Furthermore, it should also be easily generalizable.

The practice of traffic management at a microscopic level involves activities such as signal control programming, traffic signage and variable speed limits. As such, the method developed should be sensitive enough to the dynamics of traffic such that the impacts of changes in these types of controls can be accounted for. These changes may include signal timing or speed limit changes.

An obvious approach to emission monitoring may be to measure them directly. However, direct methods, as explained in Sections 2.1.1 and 2.1.2, are difficult to apply to large-scale, microscopic applications. They tend to be reserved for more macroscopic applications (Song, Yao, Zuo, & Lang, 2013) or for testing only (Franco et al., 2013a; Hausberger, Rexeis, Zallinger, & Luz, 2009). On the contrary, simulation-based modelling methods require little equipment and are highly scalable. They are extensively used for emission quantification at different scale levels or as a basis of comparison for developing other emission modelling methods (Csikós & Varga, 2012; Park et al., 2015; Shan et al., 2018), as briefly described in Section 2.1.5. The problem with simulation-based emission modelling is that simulation models are location specific, making this method difficult to generalize. Thus, a data-driven approach, as described in Section 2.1.4, would be more suitable for real-world emission monitoring. A data-driven approach would be applicable where ever data can be obtained without requiring more simulation models to be built.

The previously mentioned SCOOT technique offers an existing data-driven emission monitoring approach for traffic control management. SCOOT can incorporate emissions as a performance metric using an average speed emission model (Grote, Williams, Preston, & Kemp, 2016). While average speed models are commonly used, they tend to be less capable of capturing the effects of different congested situations (Lejri, Can, Schiper, & Leclercq, 2018). There are many existing emission modelling methods that are highly sensitive to vehicular activities, such as software packages like MOVES (U.S. Environmental Protection Agency, 2014) or SIDRA (Akçelik, Smit, & Besley, 2014). These models are sensitive and suitable for microscopic emission modelling. However, microscopic models require lengthy computation or detailed input data, such as simulation outputs, and are difficult to implement at a large scale in real-time in their original state (Lejri et al., 2018). To monitor emissions as part of a traffic network management scheme, the method should be operable in real-time to allow traffic controls to react to the dynamic changes in traffic. Models that are computationally simpler are more suitable for real-time and large scale emission estimation, such as those based on the European Handbook of Emission Factors (Mann, 2016; Ntziachristos et al., 2018; Rexeis et al., 2017). However, these methods are based on highly contextual empirical research, making them difficult to generalize. Furthermore, they are less sensitive and microscopic than the former methods. Even if a more sensitive emission model were applied, the SCOOT system may not be appropriate, since SCOOT uses general flow and occupancy information from loop detector data, which does not provide sufficiently granular vehicle activity data. Another shortcoming is that because vehicle types are not detected by SCOOT, constant vehicle type proportions are used (Bretherton et al., 2007).

New opportunities have been created by the advances in traffic monitoring technology that can record more detailed information than before. For example, computer vision applied to traffic cameras allow vehicle motions to be tracked across an image plane and can provide presence detection at specified locations (Kanhere & Birchfield, 2010). In additional, vehicle types can be roughly classified (Sokemi Rene Emmanuel Datondji, Dupuis, Subirats, & Vasseur, 2016). This introduces a significant improvement to the traditional methods of detection by inductive loops. This opportunity for improved emission monitoring has already been explored by Yao et al. (2012), who used computer vision to detect travel speeds on a freeway segment. Urban intersections, however, exhibit more complex vehicular activities due to stop-and-go traffic. The ability to track each individual vehicle over space and time while knowing

its vehicle type present opportunities for detailed data-driven traffic and emission modelling. These opportunities can be taken advantage of by synthesizing existing knowledge in the practice of emission modelling and traffic management to create methods that are simultaneously sensitive, generalizable, automated, and efficient.

1.4 Research Objectives

The primary objective of this thesis research is to develop a method that can be used to estimate vehicle emissions in real-time for evaluating traffic management and control schemes. This method must be sensitive to traffic activities to capture changes in the control strategies. The particular application scenario is quantification of traffic emissions at urban signalized intersections with varying degrees of traffic volumes, assuming certain types of traffic and signal timing data are available. Such data can be made available through the detection and communications technologies used in traffic monitoring today.

To develop a method, a review of emission modelling techniques was conducted. The review covered an understanding of emission generation models that are used to estimate emissions. It also involved works related to the research objectives stated, such enabling real-time estimations and applications geared toward microscopic traffic movements. Furthermore, the current state-of-the-art in traffic detection was considered, since the developed method would rely on traffic data.

The developed method must be evaluated in terms of its effectiveness under different traffic conditions. It must also be evaluated over changes in controls to see if effects can be captured. To evaluate the method, it needs to be compared to a reasonable level of ground truth such as those from validated traffic and emission simulation models.

1.5 Thesis Structure

First, Chapter 1 sets the context for the research, including 1.1) the motivation for vehicle emission management due to environmental concerns; 1.2) background on the precedents in this area of research; 1.3) a problem statement made to address the needs to be filled by the research in this thesis; and 1.4) a set of research objectives.

Chapter 2 provides a comprehensive review of the relevant literature related to this research. It begins by exploring, at a broad level, different types of emissions quantification methods that have been used (2.1), ranging from measuring methods to modelling methods (2.1.1 to 2.1.5). Then, focus is placed on the modelling methods (2.2), including an overview of the physics of emission production(2.2.1), a review of commonly used emission models and software in practice (2.2.2), and methods developed to model emissions in real-time (2.3). The literature review closes with a section on various traffic management strategies that have been studied or implemented (2.3).

The research methodology in Chapter 3 describes in detail how the research was conducted. It begins by describing the Vissim model that was built as a test-bed for the research activities (3.1). The Vissim model is described in terms of the data used to build, calibrate, and validate the model (3.1.1 to 3.1.2). Then, descriptions are provided for detector simulation (3.1.3) and alternative models that were created for sensitivity analyses (3.1.4). Following the Vissim model descriptions, the methodology for reconstruction vehicle trajectories is explained (3.2). The primary and the alternative simplified trajectory reconstruction methods are formulated in sections 3.2.1 and 3.2.2. Finally, the emission estimation process is described (3.3) by explaining how inputs for the MOVES model are generated from the data and from the trajectory reconstruction process (3.3.1) and how the real-time emissions estimation method is set up and executed (3.3.2).

Results presented in Chapter 4 include examples of the reconstructed trajectories (4.1), emission rates for real-time emission estimation (4.2), and finally evaluations for the proposed method (4.3 and 4.4). Results for the primary trajectory reconstruction method (4.3) include performance evaluations of the method in field conditionals (4.3.1). The effects of advance detector locations, estimate aggregation, truck penetration, signal timing, signal coordination, and speed limits are explored in sections (4.3.2 to 4.3.7 respectively).

Chapter 5 summarizes the main findings of the research (5.1) and discusses related topics (5.2 to 5.3). The findings cover the general adequacy of the proposed emission monitoring method (5.1.1), the patterns observed in the effects of different traffic control schemes (5.1.2), and how the primary and simplified methods compare (5.1.3). After the findings, the applications and limitations of the proposed method is discussed (5.2) and recommendations for future research are made in (5.3). The recommendations include further work that can be done to improve this method (5.3.1), validations using field studies (5.3.2), and possible opportunities for emission monitoring outside of the immediate area of research (5.3.3).

Chapter 2 Literature Review

The literature review focuses on emission modelling methods and examples of emission monitoring frameworks used in the literature, especially those that use traffic data to perform estimations in real-time. Additional relevant material, such as the physics of emission production and a brief overview of various emission quantification methods, are also included. This section ends with considerations of traffic management strategies and technologies that relate to this research.

2.1 Emission Quantification Methods Overview

Several types of approaches have been used for quantifying vehicle emissions, from direct measurements to modelling techniques. Each method has advantages and disadvantages which are summarized in Table 1, from directness on the left to versatility on the right. In general, methods that are direct and accurate tend to require costly measures such as equipment and are difficult to scale up when deployed independently. In contrast, methods that are easier to scale up on a spatial, temporal, or penetrative scale normally require modelling efforts, requiring certain assumptions on how individual system components operate. These assumptions may result in estimation errors, which could become a major concern depending on the purpose of the application. Since this research is focused on quantifying emissions for traffic management purposes such as signal programming, it is important for the method to be highly sensitive to traffic dynamics. It would also be ideal if the method could generate results quickly. Thus, the methods of emission quantification are compared in terms of how fast they can operate on a continuous basis while performing highly detailed estimations. The following section provides a detailed discussion on each of these methods.

Table 1: Emission Quantification Methods Comparison

Comparison of Emission Monitoring Methods with Regard to Traffic Control Management				
Method	**Direct Measurement**	**Indirect Measurement + Modelling**	**Modelling based on Field Traffic Data**	**Modelling based on Traffic Simulations**
Examples	Portable Emission Measurement Systems Chassis Dynamometer Facilities	Stationary air quality sensors + dispersion modelling	Model traffic flow using traffic data, then estimate emissions with traffic model	Use simulated traffic behaviour for emission estimation
Pros	• Accurate • Little additional data required	• Provides direct measurement of air quality • Constant, location-specific monitoring	• No equipment required where traffic data is available • Minimal modelling efforts required for additional sites of application	• Versatile • No equipment required • High level of detail attained
Cons	• Equipment or closed facility required • Costly to scale up by volume, spatial coverage, and time	• Equipment required on site • External factors must be accounted for to find the direct impact of traffic controls on the emissions	• Modelling traffic introduces sources of error. • Additional data required (e.g. road, weather, vehicle types, etc.)	• Simulations can be time-demanding • A model must be created for every site of application • Additional data also required.

2.1.1 Direct Measurement in Closed Facilities

The most direct way to quantify emission is to measure the emissions from the tail-pipe of a vehicle when it is operated in a closed environment where a chassis dynamometer is used to simulate the loads of vehicle operation through roller acting on the driving tires, as shown in Figure 1. This is a method used to perform emissions testing to develop emission factors (Franco et al., 2013b). Emission factors are emission production rates that indicate how much emissions are generated under what type of driving activities. With direct measurements under controlled conditions, the emission quantities are

very accurate. However, due to the testing process and facilities required, this method is expensive and arduous. Thus, it is limited to occasional testing for research or regulatory purposes rather than continuous monitoring. Furthermore, it is not suitable for on-road measurements, as it must be performed in closed facilities.

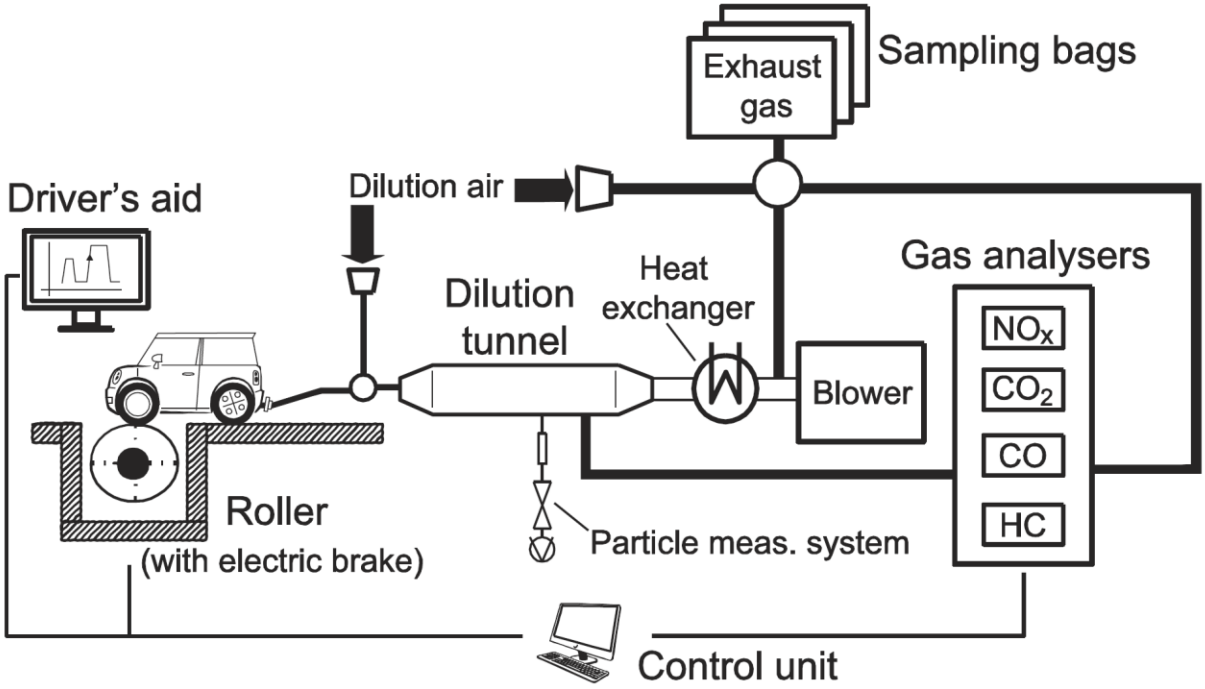

Figure 1: Chassis Dynamometer Emission Testing Framework (Franco et al., 2013b)

2.1.2 Direct Mobile Measurement

Another direct quantification method is to measure emissions from the tail-pipe of a vehicle while it is on the road. This method requires the installation of a Portable Emission Measurement System (PEMS) on the vehicle, as illustrated in Figure 2. Like the previous method, this method provides accurate results through direct measurement under real on-road traffic environment. PEMS data have been used for emission modelling at the mesoscopic level by Song et al. (2013) and Samaranayake et al. (2014). While this method is more versatile than closed facility testing, it is still difficult to scale up, as the equipment is costly, and it is impractical to install it on a large number of vehicles. Typically, it is installed on probe vehicles, and further extrapolation is necessarily to model the general emission activity of all vehicles in relation to the probe vehicle activities. This method is most applicable for mesoscopic or macroscopic emission monitoring. Challenges would arise from using this method for microscopic monitoring if the penetration of probe vehicles with PEMS installed is insufficient to represent the general traffic. As with closed facility testing, this method is mostly used for serving the research purpose of developing emission factors.

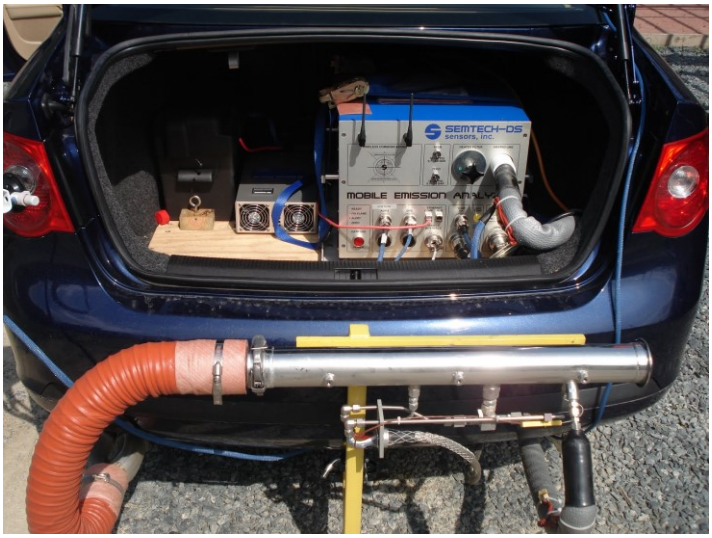

Figure 2: Portable Emission Measurement System (PEMS) (Sensors Inc., 2016)

2.1.3 Indirect Stationary Measurement

Another measurement technique used involves measuring air pollutant through stationary roadside devices. These devices are most suitable for air quality monitoring. However, for traffic emission monitoring, more steps are required to produce adequate results. As soon as emissions leave the tail-pipe of a vehicle, they begin to disperse. As result, a dispersion model is required to estimate the amount of emissions from vehicles based on measurements at roadside equipment. In relating the measured air pollutants to the traffic activities, the dispersion model must account for the external factors of weather and environment as well as other possible non-traffic emitters. For example, Amirjamshidi et al. (2013) used roadside measurements were to infer vehicle emissions. Stationary measurements can also be used in unique, semi-closed conditions such as tunnels (Smit, Ntziachristos, & Boulter, 2010), where dispersion modelling requirements are different.

An advantage of this method is that sensors are fixed at the location of concern to provide constant monitoring, regardless of the vehicle activities. Furthermore, it can also serve as an air quality monitor. A disadvantage would be the requirement of expensive equipment that made this method difficult to scale up. A further disadvantage is the additional data and modelling required to account for external, environmental factors affecting the emission measurement.

2.1.4 Emission Modelling Using Traffic Data

A significant number of past efforts have devoted to developing models to estimate emissions using various types of traffic data, such as loop detector data, GPS probe data, video detection, and Bluetooth/Wi-Fi detector data. Depending on the nature of the traffic data, traffic modelling efforts may

be required to obtain sufficient traffic activity information as required by the underlying emission estimation process.

For example, Hang Liu, Tok, and Ritchie (2011) developed a system to estimate vehicle emissions using inductive loop detector data. The detectors use inductive vehicle signature technology to classify vehicle types. The vehicle speed input consisted of average speeds for each vehicle class as measured by the loop detectors. Additional information such as temperature and humidity were provided by local weather stations. The traffic activity data are then input into the MOVES model for emission estimation.

In a similar example, Csikós and Varga (2012) also developed a method to estimate emissions using loop detector data in real time. The research was conducted using Vissim simulations. The real-time emissions modelling was based on COPERT IV, which provides emission factors for various vehicle classes pertaining to average speeds travelled over a segment. This method was also aimed at a macroscopic spatial level, performed on a simulation model of a freeway. While the developed method operated at a macroscopic level, it was validated through microscopic modelling. The microscopic emission estimates were generated using the Vissim add-on, EnViVer (PTV Vissim, n.d.), which is based on Versit+, an emission modelling approach and dataset from PEMS testing (Ligterink, 2016). This model is a distance-based model where emission factors specific to pollutants, vehicle classes, and speed-time profiles are applied to lengths of road segments corresponding to the speed-time profile, multiplied by traffic volumes of the vehicle class on that segment (Linton, Grant-Muller, & Gale, 2015).

Shan et al. (2018) developed a method to estimate emissions using GPS probe data. The method aimed to quantify emissions at a microscopic level, which required detailed vehicle trajectories. However, GPS data is sparse, so the trajectories must be reconstructed from the known data points. The trajectories were reconstructed into four driving modes – cruise, acceleration, deceleration, idling – with the help of historical data. Emission were modelled using MOVES. This work focused on the reconstruction of vehicle trajectories.

Another instance of using GPS probe data was studied by Park et al. (2015); however, in addition to GPS probe data, they investigated the effects of having GPS-embedded onboard equipment that can also provide instantaneous speed data. Such a data source would provide high resolution speed data without the need to model it. In this case, the accuracy of the emission estimates lies in the penetration rate of vehicles equipped with data collection. This research was performed using Vissim simulations and included a study of the effects of varying levels of probe vehicle penetration rates.

Yao et al. (2012) used video detection data was to monitor vehicles on a freeway. Computer vision was used to obtain vehicle speed and acceleration on a freeway as input for emission estimation. The research was focused on calibrating the computer vision software to obtain accurate speed measurement, which requires accounting for camera distortion. This method was performed on cases with relatively straight travel paths. While this application is similar to the focus of this thesis, the vehicle behaviour on a freeway is very different from that of a signalized urban corridor.

2.1.5 Emission Modelling Using Simulation Data

When modelling emissions using simulation data, the quality and abundance of data is not an issue, as the simulation can be programmed to provide whatever data required for emission modelling. The challenge lies in creating the simulation model to a degree that satisfactorily represent the real-world situation, such that the emissions calculated as a result are valid. This method has been explored by coupling simulation software with emission modelling software, which can be used as a "ground truth" scenario in research investigating the effects of modelling with limited data. Traffic simulators such as the popular Vissim can record a plethora of vehicle data for every simulation step, which provides a simulated ground truth for the traffic activities, while detector data simulated by the model provide a limited scope of data. This technique was used by Csikós and Varga (2012), Shan et al. (2018), Park et al. (2015), Jamshidnejad et al. (2017), and Zhao and Sadek (2013).

Xu et al. (2016) coupled a Vissim simulation with MOVES to analyse the sensitivity of emissions to simulation parameters in Vissim. They found that the emissions are sensitive to the vehicle type distribution in the fleet, as expected. It was also found that the range of the look-ahead distance in the car-following model and the range of the accepted deceleration rate can impact emissions. However, it was noted that there may be a discrepancy between behaviours in Vissim and in actuality, which were not confirmed in that study.

Any traffic simulator can be used in a simulation and modelling approach. So et al. (2017) used an existing framework of the traffic simulator Aimsun (Aimsum, 2010) with the emission model PHEM (Hausberger et al., 2009). The existing framework was compared with an enhanced version where a vehicle dynamics model, CARSIM (Mechanical Simulation, 2017), is inserted in the process between the traffic simulation and the emission model. Another simulator, Paramics (Smith, Duncan, & Druitt, 1995), was integrated with MOVES in a study to investigate methods for extrapolating probe vehicle data to estimate total vehicle emissions (Zhao & Sadek, 2013).

The simulation and emission modelling integration approach can be computationally demanding for large networks. Hence, work was undertaken by Muresan, Hossain, and Fu (2016) to investigate ways of reducing the computation burden while preserving adequate results. A trajectory clustering method was proposed that balances trade-offs between the quality of results and the computation cost of generating them. That study was performed with the integration of Vissim and MOVES.

2.2 Emission Modelling Theory and Methods

The problems of estimating vehicular emissions have been studied extensively in the past due to its large share in the overall emission inventory, covering many topics ranging from the mechanism of vehicle emission production to the modelling of vehicle emissions. First, some of the physical factors that impact emission generation are reviewed. Then, several emission models for practical applications are discussed.

2.2.1 Physical Basis of Vehicle Energy Consumption

Before considering emission models, it is important to understand what factors affect emission production and how they are related. The amount of emissions that a vehicle generates is closely related to the amount of fuel consumed; as such, they can be estimated as a proportion of the latter (U.S. Environmental Protection Agency, 2016a). The amount of fuel consumed by a vehicle during its operation is directly related to the energy consumed by the vehicle, which depends on the energy required to overcome the vehicle's load and the energy efficiency of the vehicle. Energy efficiency is a product of the engine's thermodynamic and mechanical efficiency and the transmission efficiency. These factors are mostly related to the type and model of the vehicle with little to do with the infrastructure or traffic management; thus, we focus on the first factor, vehicle load, in this literature review.

According to Ross (1997), the vehicle load is a sum of the power required to overcome

- Rolling resistance
- Air drag
- Vehicle inertia
- Road grade
- Vehicle accessory power demand

represented in Equation 1 as:

$$P_{load} = P_{rolling} + P_{drag} + P_{inertia} + P_{grade} + P_{acc.} \quad (1)$$

where the individual terms are defined as:

$$P_{rolling} = C_r m g v$$

$$P_{drag} = \frac{1}{2}\rho C_d A v^3$$

$$P_{inertia} = \frac{1}{2} m^* \frac{v^2}{t}$$

$$P_{grade} = m\ g\ v\ sin\theta$$

where

P is the power required [kW]

C_r is a unitless rolling resistance coefficient [-]

m is the vehicle mass [tonnes]

g is the gravitational constant [m/s^2]

v is the vehicle's instantaneous travel speed [m/s]

ρ is the air density [kg/m^3]

C_d is a unitless drag coefficient [-]

A is the frontal area of the vehicle [m^2]

m^* is the effective inertia of the vehicle, which accounts for moving parts; $m^* \approx 1.03m$

θ is the angle of the road grade

The coefficients C_r and C_d are found empirically and are also specific to the vehicle make and model. The factor that is the most important to traffic management – that is, the factor manageable through traffic controls – is vehicle speed. Thus, to quantify vehicle emissions for applications in traffic management, it is critical to capture the vehicle speed at high temporal resolutions. Other factors are also important as they play into the complex interdependencies of emission generation; for example, a vehicle's mass affects its resulting behaviour. Additional characteristics that affect emission generation include fuel supply and technology, vehicle mechanics, weather, driving behaviours, etc. Some of these factors, such as those related to the drivers and environment, can be partially accounted for through the vehicle's speed. In any case, in terms of data requirements, high resolution vehicle speed profiles are of the greatest importance.

2.2.2 Emission Modelling in Practice

Significant efforts have been devoted to developing empirical models and methods for estimating mobile emissions. Models of different granularity and spatiotemporal aggregation levels have been developed. They vary by the assumptions made on available data for the characteristics of the mobile sources such as vehicle type, speed profile, fuel technology, and road grade (Boulter, McCrae, & Barlow, 2006; Franco et al., 2013b). Many of the emission models developed incorporate mechanistic-based models combined with empirical factors. In these models, the mechanistic functions represent the physical process of emission production, while the empirical factors account for vehicle and network characteristics. Emission models that are solely based on empirical factors also exist.

The progression of emission modelling developments appeared to be leaning more towards empirical approaches. This seems to be resulting from an attempt to incorporate more and more factors, most of which are difficult to model mechanistically. Still, most of the models reviewed have both mechanistic and empirical components, aside from the models based on the European Handbook of Emission Factors (HBEFA) as explained in section 2.2.2.4. From an instinctive perspective, mechanistic models may appear to be more modular, flexible, and versatile for transitioning through times of technological change. However, the nature of emission production is so complex that it is difficult for models to function in purely mechanistic form. Thus, empirical factors will always be required to account for processes that are not represented mechanistically. These factors need to be calibrated to keep the model current. Considering the need for updating empirical factors, models that are more simplistic in their functional form may be easier to calibrate.

The literature on emission models shows the dependence on data availability in estimating the emissions produced by traffic. The models perform best using high resolution traffic data, such as instantaneous speeds (Bowyer, Akcelik, & Biggs, 1985; Swanson, Talbot, & Dumont, 2010). Thus, in the interest of obtaining accurate results, high resolution traffic data should be used, i.e. second-by-second vehicle speed and acceleration profiles. These profiles, referred to as vehicle trajectories, are normally not directly measured in their entirety by traffic detectors. However, measurements from traffic detectors can be used to reconstruct the trajectories, whether the measurements come from mobile sources such as GPS data (Shan et al., 2018; Sun, Hao, Ban, & Yang, 2015) or stationary sources (Laval, He, & Castrillon, 2012).

2.2.2.1 Vehicle Power Model

An example of a highly mechanistic approach can be seen in the methods introduced in a fuel consumption analysis guide by Bowyer, Akcelik, and Biggs (1985). The early models are still in use, but minor changes were introduced. A previous study shows this model significantly overestimating emissions (Demir, Bektaş, & Laporte, 2011); however, this issue may have been rectified as the model parameters were recently calibrated for newer vehicle fleets (Akçelik et al., 2014). The guide presented different formulations, including formulations that use one function based on instantaneous vehicle speed, formulations that divide vehicle operation into four modes (acceleration, deceleration, cruising, and idling), and formulations that use average speeds.

The instantaneous model in this collection of methods is the basis for the SIDRA software package (Akçelik et al., 2014), a traffic signal timing and analysis, which is widely used in Australia. The current version of the instantaneous model is formulated as

$$f_t = \frac{dF}{dt} = \alpha + \beta_1 R_T v + [\beta_2 a P_1]_{a>0} \ , \quad P_t > 0 \qquad (2)$$

$$= \alpha \ , \qquad P_t \leq 0$$

$$P_T = \min(P_{max}, P_C + P_1 + P_G)$$

$$P_C = b_1 v + b_2 v^3$$

$$P_1 = \frac{M_V a \, v}{1000}$$

$$P_G = 9.81 M_v \left(\frac{G}{100}\right)\left(\frac{v}{1000}\right)$$

$$\alpha = \frac{f_i}{3600}$$

where

f_t	is the instantaneous fuel consumption rate [mL/s]
P_T	is the total tractive power [kW]
P_{max}	is the maximum engine power [kW]
P_C, P_I, P_G	are the components of power for cruise, inertia, and grade respectively [kW]
G	is the road grade [-]
M_V	is the vehicle mass including loads [kg]
v	is the instantaneous speed [m/s]
a	is the acceleration rate [m/s^2]
f_i	is the constant idle fuel consumption rate [mL/h]
α	is the constant idle fuel consumption rate [m/s^2] applicable to all modes
$b_1, b_2, \beta_1, \beta_2$	are parameters for rolling resistance, aerodynamic drag, and efficiency

From this model, it can be seen that a similar set of variables are included compared to the physical model of fuel consumption. Notably, instantaneous vehicle speed and acceleration, as well as vehicle mass and road grade are vital factors in both models. Once fuel consumption is known, an emission production factor relating the greenhouse gas to the fuel can be multiplied to the fuel consumption to calculate emissions (U.S. Environmental Protection Agency, 2016a).

2.2.2.2 Comprehensive Modal Emission Model (CMEM)

The Comprehensive Model Emissions Model (CMEM) was developed in Europe to address additional vehicular factors, such as a variety of vehicle types and the vehicle's operating condition (Scora & Barth, 2007). The structure of the model finds the tailpipe emissions as a function of the engine power demand, engine speed, air/fuel ratio, fuel rate, emissions from the engine, and the catalyst pass fraction. The factors are not stand-alone variables but have interdependencies. Their relationships can be found in the development document for CMEM (Barth et al., 2009). In CMEM, there are also four modes of operation: variable soak time start, stoichiometric operation, enrichment, and enleanment. Compared to the four modes from the previous modal model, these modes are based on the conditions of the vehicle's engine (e.g. its air/fuel ratio) rather than its movement profile. There is evidence that this model may under-estimate emissions significantly (Jaikumar, Shiva Nagendra, & Sivanandan, 2017), although an earlier study shows this model overestimating emissions (Demir et al., 2011). Smit et al. (2010) showed modal models like CMEM overestimating some emissions and underestimating others in a study that groups similar model types together.

2.2.2.3 MOtor Vehicle Emission Simulator (MOVES)

One of the most widely used emission models is the MOtor Vehicle Emission Simulator (MOVES) developed by the US's Environment Protection Agency (EPA). It was created to be a standard of practice for estimating mobile emissions (Swanson et al., 2010). MOVES is an improved version of the previous EPA models such as MOBILE5 and MOBILE6. One of the key improvements is the introduction of Vehicle Specific Power (VSP) (Frey, Unal, Chen, & Song, 2003), which is a normalized function for quantifying the power consumed by a vehicle (Jiménez-Palacios, 1999). Similar to the SIDRA model, VSP is assumed to be a function of the vehicle speed, vehicle mass, road grade, and other coefficients related to vehicle properties, formulated in Equation 3 as

$$VSP = \left(\frac{A}{M}\right)v + \left(\frac{B}{M}\right)v^2 + (a + g\sin\theta)v \tag{3}$$

where

VSP is Vehicle Specific Power

A is the rolling resistance coefficient $[\mathrm{kW{\cdot}s/m}]$

B is the mechanical rotating friction coefficient $[\mathrm{kW{\cdot}s^2/m^2}]$

C is the aerodynamic drag coefficient $[\mathrm{kW{\cdot}s^3/m^3}]$

M is the vehicle's mass [tonnes]

v is the instantaneous vehicle speed [m/s]

a is the instantaneous vehicle acceleration [m/s^2]

g is the gravitational constant [m/s^2]

θ is the road grade percentage [-]

Based on the VSP function value as well as vehicle speed and acceleration, vehicle activities can be grouped into Operating Modes, of which the resulting distribution is used by MOVES to estimate the total emissions of different types. The details of the operating mode bins are in Appendix A – Operating Mode Bins. The parameters for calculating VSP have been recalibrated since its inception and can be found in the Population and Activity of On-Road Vehicles technical report for MOVES (U.S. Environmental Protection Agency, 2016b). Other developments in MOVES that differentiate it from its predecessors include a binning methodology, which reduces the need for regression modelling and makes the model more data-oriented (Frey et al., 2003). MOBILE, the earlier version, was shown to belong to a group of average speed models that over- or underestimate emissions by 10-15%, which was in the mid-range of performance for the models in that study. In the latest efforts to validate MOVES, it was found that the estimation accuracy varies between vehicle ages, with newer vehicle resulting in

much more accurate estimates (Choi & Koupal, 2011). This is favourable since there is a much greater proportion of new vehicles in the local vehicle fleet (Statistics Canada, 2009).

2.2.2.4 European Handbook of Emission Factors

A highly empirical model is recommended in the German Federal Transport Plan or Bundesverkehrswegeplan (BVWP). It includes a handbook for conducting cost-benefit analyses of transportation projects, which describes a method for emission estimation (Mann, 2016). This model is based on the European Handbook of Emission Factors (HBEFA), which is periodically updated with new data (Rexeis et al., 2017). It is unique from the emission models presented in this review, because it calculates emissions as a product of purely empirical emission factors. Blocks of traffic disaggregated by space and time are multiplied by their corresponding emission factor, as shown in Equation 4.

$$\Delta EM_{FG(Vb),sf} = \sum_{FG}\sum_{h}\sum_{s}\left(\Delta FL_{FG(Vb),h,s} \times efl_{FG(Vb),HST,Z,v_{max},sf}\right) \times 10^{-3} \quad (4)$$

where

ΔEM is the difference in emissions between the baseline and alternative cases [tonnes/year]

sf is a pollutant index (NO_X, CO, HC, PM)

$FG(Vb)$ is a vehicle class index

h pertains to an interval in the temporal disaggregation

s pertains to stretch in the spatial disaggregation

ΔFL is the difference in vehicle activity between the baseline and alternative cases in VKT

efl is the emission factor corresponding to the vehicle activity [g/vehicle-km]

HST is the street type index

Z is the traffic condition index

To calculate emission using this model, traffic must be discretized into segments by traffic state, road type, and vehicle classes. The emission factor for each traffic state pertains to a specific vehicle type, road type, traffic state, speed limit, and pollutant. All of the required factors are provided with the handbook. These emission factors were developed using empirical data collected through PEMS and chassis dynamometer testing over many stages of development. Due to resource constraints, testing could not be performed for all possible driving situations. Instead, testing data was used to calibrate the PHEM model, which was then used to calculate emission factors for further driving situations (Rexeis, Hausberger, Kühlwein, & Luz, 2013). The PHEM model is an instantaneous power-based emission model that treats vehicle power demand as the sum of several power load components (Hausberger et al.,

2009). Its form is similar to that of the vehicle power consumption model formulated by Ross (1997), described in Section 2.2.1.

The HBEFA model, due to its simple form, can be computed easily and used at all levels of aggregation. However, it is highly dependent on the already-calibrated emission factors. Emission factors require extensive effort to develop (Franco et al., 2013b) and are difficult to generalize. As such, it is difficult to adopt such a model outside of the context for which it was developed.

2.2.2.5 COPERT IV

COPERT IV (Computer Program to calculate Emissions from Road Transport) is a software package created for standard practice in Europe by the European Environment Agency (Ntziachristos et al., 2018). It recommends three tiers of methodology. The methodologies range in the quality of estimates. Tier 3 has the highest quality but also requires the most data to use.

In Tier 1, emissions are calculated based on aggregate fuel consumption data according to Equation 5.

$$E_i = \sum_j \sum_m FC_{j,m} \times EF_{i,j,m} \tag{5}$$

where

E_i is the emission of pollutant i [g]

$FC_{j,m}$ is the fuel consumption of vehicle category j using fuel m [kg]

$EF_{i,j,m}$ is the fuel consumption-specific emission factor of pollutant i for vehicle category j and fuel m [g/kg]

The fuel consumption and emission factors are based on data aggregated by country. This is the most aggregate method to be used when only aggregate fuel consumption data is available.

If VKT for different vehicle categories and technologies is available, the Tier 2 method defined by Equation 6 can be used:

$$E_{i,j} = \sum\left(TM_{j,k} \times EF_{i,j,k}\right)$$

$$\text{Or} \tag{6}$$

$$E_{i,j} = \sum\left(N_{j,k} M_{j,k} \times EF_{i,j,k}\right)$$

where

$TM_{j,k}$ is the total annual distance driven by vehicles in category j and technology k [veh-km]

$EF_{i,j,k}$ is the emission factor of pollutant i for category j and technology k [g/veh·km]

$M_{j,k}$ is the average annual distance per vehicle in category j and technology k [km/veh]

$N_{j,k}$ is the number of vehicles in category j and technology k

Tier 2 is a method that calculates emission based on distance travelled but is insensitive to traffic states and detailed vehicle activities. The calculation uses factors that account for different types of vehicles operating with different technology classes. The vehicle types and technology classes follow standard European classifications (Ntziachristos et al., 2018).

If further information such as vehicle speeds are known, the Tier 3 method can be used. In Tier 3, vehicle speed distribution profiles can be accounted for in the hot emissions formulae in Equation 7:

$$E_{HOT;i,k,r} = N_k \times M_{k,r} \times e_{HOT;i,k,r} \tag{7}$$

$$e_{HOT;i,k,r} = \int \left[e(v) \times f_{k,r}(v)\right] dv$$

where

$E_{HOT;i,k,r}$ is the hot emissions

N_k is the number of vehicles

$M_{k,r}$ is the distance driven per vehicle

$e_{HOT;i,k,r}$ is the emission factor

v is the vehicle speed

$e(v)$ is the dependency of $e_{HOT;i,k,r}$ on the the speed

$f_{k,r}(v)$ is the equation describing the frequency distribution of the vehicle speeds

i, k, r pertain to a certain pollutant, vehicle technology, and road type respectively

While COPERT models do not mechanistically represent physical processes that generate emissions, a high-resolution speed profile can be taken into consideration. There is evidence that the COPERT model may underestimate emissions; this evidence came from a study using distance-based emission factors, i.e. the Tier 2 method (Jaikumar et al., 2017). Similar results were observed in (Demir et al., 2011) where COPERT was one of two emissions models that underestimated field measurements out of six models tested. Although the software is open-source, some of the required data for using the software requires purchase.

2.3 Real-Time Emission Estimation Methods

Several methods for real-time emission estimation based on the MOVES model have been developed. These methods typically involve first generating emission rates for a basic set of input variable combinations that account for certain variables, alternating the calculation algorithm used by MOVES, or a combination of both. Real-time methods that use other emission models have also been used.

2.3.1 Pre-Generating Emission Rates with MOVES

To avoid having to run the MOVES software, Haobing Liu, Xu, Rodgers, Akanser, and Guensler (2016) created a matrix of emission rates using MOVES that can be used to save computing time. The matrix was generated by feeding MOVES combinations of the input variables. It was shown that the matrix method could estimate emissions in less than 1% of the time required by running the MOVES software interface. The matrix was developed for Operating Mode Distribution as well as speed inputs. To develop a sufficient variety of factors, 146 853 MOVES runs were required for each region of interest. The factors were sensitive to ranges of humidity at 5% intervals, temperatures at 1°F intervals, 31 vehicle model years, 13 vehicle types, and different fuel types. This method was used by Xu et al. (2016) for estimating emissions from Vissim simulations in real time.

Hang Liu et al. (2011) developed a real-time emission monitoring system as well. To enable real-time emission estimates, similar to the work of Haobing Liu et al. (2016), a look-up table of emission rates was pre-generated using MOVES. However, not all combinations of inputs were accounted for. The look-up table contained emission rates by distance that account for different vehicle classes, average speeds, temperatures, and humidity. To account for combinations of speed, temperature, and humidity, multi-dimensional interpolation was used.

A method based pre-generated emission rates was also used by Yao et al. (2012), where computer vision obtained speed profiles of vehicles to generate Operating Mode Distribution inputs. The computer vision works in real-time, as does the emission estimation. In this case, data such as vehicle age distribution, fuel data, and meteorological data were held constant, similar to previous cases.

2.3.2 Alternative Emission Estimation Algorithms for MOVES

In the development of a real-time emission monitoring framework, Park et al. (2015) created a New Interface for MOVES (NIM). They made an important statement about the MOVES inputs regarding real-time estimation by noting that the Operating Mode Distribution is the most important input for real-time estimation, since it is dynamic, while other inputs remain relatively constant over a small spatial-temporal scale. Thus, the NIM only uses the Operating Mode Distribution as an input. The NIM is a Python-based software that accesses the MOVES database to retrieve information for emission estimation. Its role in the overall emission monitoring framework is illustrated in Figure 3. A model that is only required to be sensitive to the Operating Mode Distribution would take significantly less time to run.

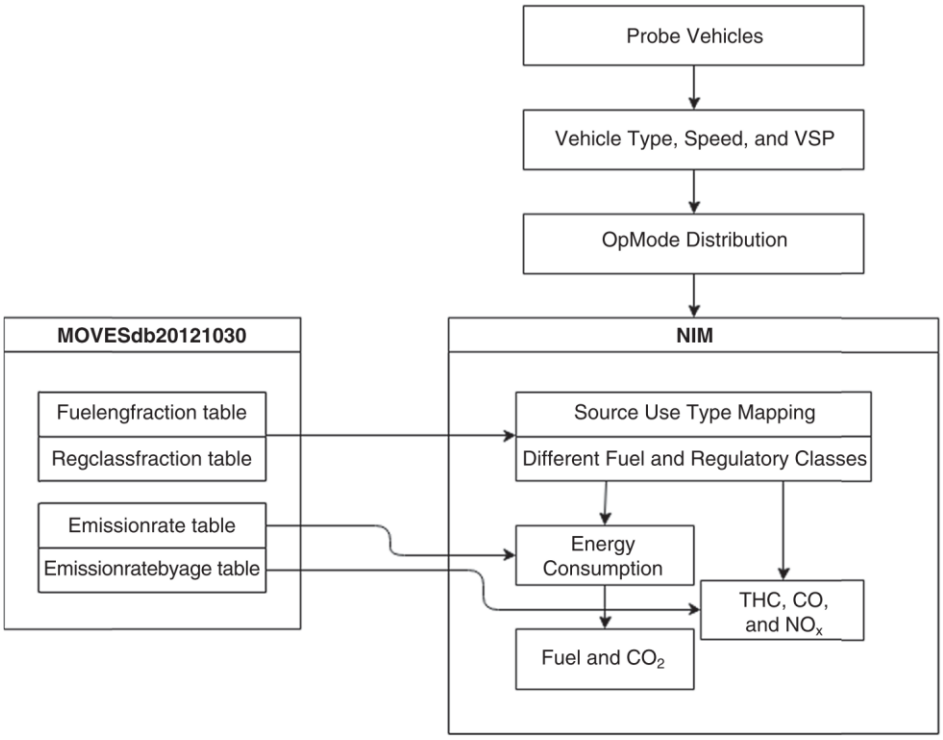

Figure 3: New Interface for MOVES (NIM) in an Emission Monitoring Framework (Park et al., 2015)

2.3.3 Other Emission Models

Jamshidnejad et al. (2017) proposed a method that generates real-time emission estimates by coupling a traffic flow model with the microscopic emission model, VT-micro. The resulting method developed was considered a mesoscopic emission monitoring framework, since it was applicable to any macroscopic flow model and microscopic emission model. VT-micro is a microscopic emission model that uses instantaneous vehicle speeds and acceleration.

Macroscopic real-time emission monitoring was also used by Csikós & Varga (2012), where an emission factor is applied to average speeds from real-time measurements. The emission factors were obtained from the COPERT model and validated with Versit+Micro through a Vissim add-on.

2.4 Traffic Management Technology

Traffic management requires monitoring traffic through the detection of on-road vehicles. The detection of vehicles often includes detection of vehicle-related properties such as speed and vehicle classification. The most commonly used sensor technology for vehicle detection is inductive loop sensing due to its accurate presence detection and reliability. Its cost is also relatively low compared to other

types of sensors. Inductive loop technology uses wires embedded in pavement that detect the presence of vehicles as they pass over. Other pavement embedded technologies include magnetometers and magnetic sensors, the latter of which is less sensitive to vehicle presence than inductive loops. These are used as alternatives to the inductive loops when the road structure or condition does not permit loops. (Federal Highway Administration, 2017)

Methods non-invasive to pavement are also available. For example, microwave, infrared, ultrasonic, and acoustic sensors can be used to detect vehicles. Microwave, infrared, and ultrasonic technologies can be used as radars, where a device transmits energy, then measures its reflection, referred to as active sensing. Acoustic and also infrared technologies are used in passive sensing, where energy is not transmitted but only detected from vehicles and other objects. These methods have varying levels of reliability depending on the surrounding environment and weather conditions. Furthermore, aside from active infrared sensing, these methods can be unreliable for vehicle detection at certain speeds. However, it is an advantage to not require pavement alterations to install these sensors. (Federal Highway Administration, 2017)

Inductive loops can detect the presence of vehicles where the detectors are installed, but has trouble classifying the vehicles and recognizing repeated detections of the same vehicle. Lacking this information presents challenges in determining detailed vehicle activity profiles. Vehicle activity modelling methods developed in the past were designed without this information available.

Currently, advances in detection technology is providing more detailed data, allowing vehicle tracking. This allows multiple detections of the same vehicle to be associated. An example is computer vision applied to traffic cameras, an emerging traffic monitoring technology already in use, but also still being improved (Sokemi Rene Emmanuel Datondji et al., 2016). While it is currently unable to provide accurate second-by-second trajectory information due to camera distortion (S. René E. Datondji, Dupuis, Subirats, & Vasseur, 2016; Sokemi Rene Emmanuel Datondji et al., 2016), it can provide detections of vehicles in specified locations, and these locations in the image plane can be matched to the real world (Kanhere & Birchfield, 2010). Furthermore, computer vision can differentiate the vehicle type in terms of rough categories (Sokemi Rene Emmanuel Datondji et al., 2016).

Other recent developments in vehicle detection include Bluetooth and Wi-Fi sensing. These methods rely on sensors that receive the MAC (Media Access Control) address of devices in a vehicle such as mobile phones. Like video-based detection, they can re-identify vehicles using the unique identities of devices. The re-identification of vehicles at multiple locations allows these sensors to monitor travel times between these locations. A similar technique can be applied to ANPR (Automatic Number Plate Recognition), where license plates are captured by camera and recognized at specified locations. (José, Díaz, Belén, González, & Wilby, 2016) While vehicle re-identification technologies can provide macroscopic travel time data, they are unable to track vehicle movement in detail, unlike video-based detection.

Chapter 3 Research Methodology

As discussed in Chapter 1, one of the major difficulties in emission quantification is how to obtain real world ground truth data, for both emission production and detailed vehicle activity information. In this research we propose to address this challenge by introducing a simulation-based approach, which couples two well validated simulation models: Vissim for traffic simulation (PTV Group, 2015) and MOVES for emission estimation (US EPA, 2015). This method is adopted as a testbed environment for generating the "ground truth" emissions estimates, which are then used to develop real-time emission estimation model. To save time in the research process and to achieve a real-time calculation method, a shortcut method for running MOVES was developed. Thus, the emission estimation process does not require running the MOVES software, but the results are practically identical to those generated by the MOVES software.

The overall framework of the research is illustrated in Figure 4. First, a Vissim model is created using field data, which simulates the traffic controls, vehicle activities, and data collection using assumed sensor settings. The outputs from the traffic simulation provide the assumed traffic data required for the emission model, such as traffic flow, signal timings, and high-resolution vehicle activity data. This way, the original vehicle trajectories are known in detail. The process follows two main paths: one path, indicated with solid lines, showing how the "ground truth" emissions are estimated and the other, indicated with dashed lines, through which the real-time emission modelling method is tested. In the end, the emission estimates from both paths are compared to evaluate the adequacy of the proposed real-time modelling method.

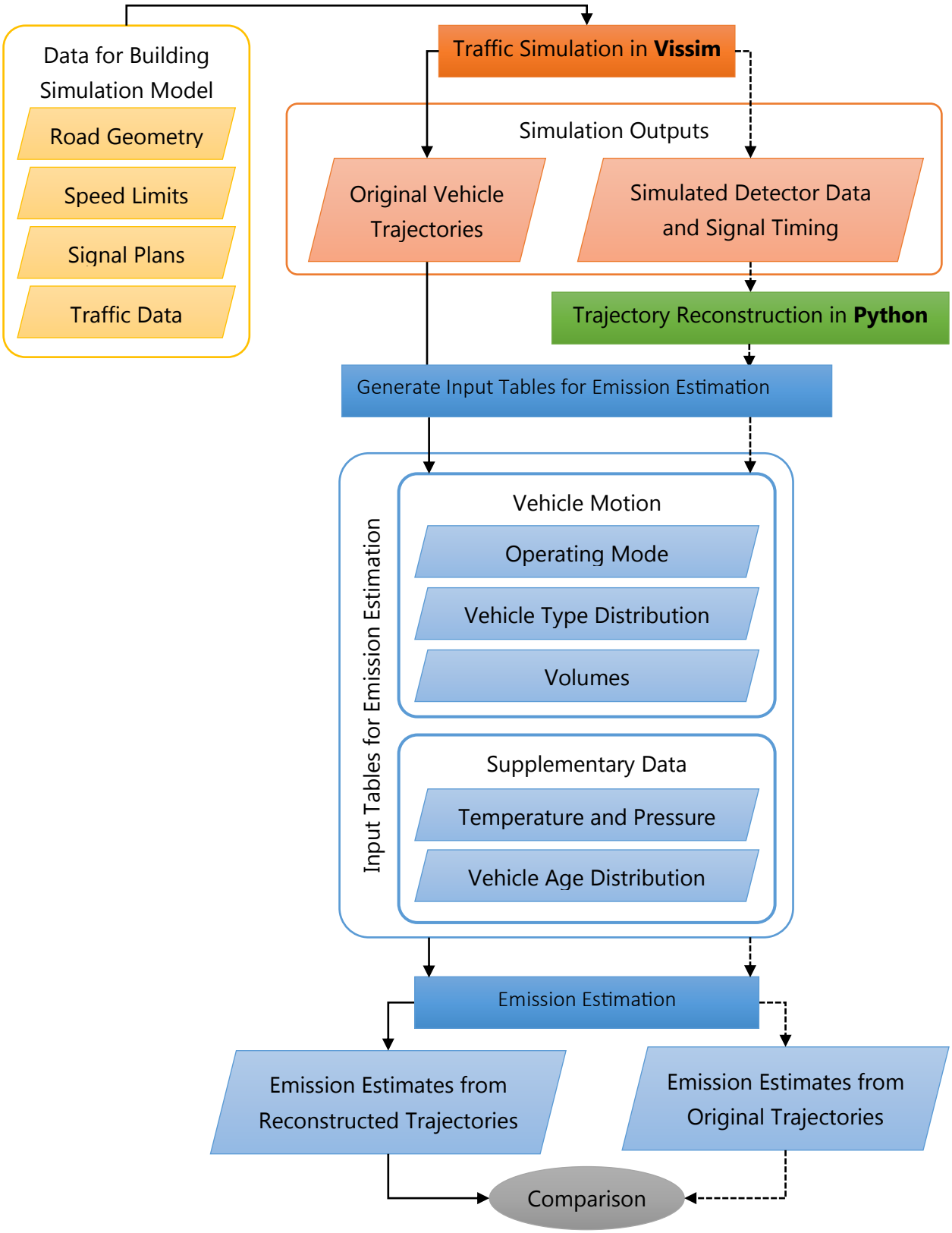

Figure 4: Research Framework

3.1 Vissim Model

The traffic simulation model was created in PTV Vissim 7 (PTV Group, 2015). Details of this model, including the site it is based on, characteristics of the network, and on-site traffic detection are described below. The subsections describe how data was used to create the model (3.1.1), how the model is used to simulate detector data for the research (3.1.3), how the model was validated (3.1.2), and how alternative scenarios of the original Vissim model was created for sensitivity analyses (3.1.3).

Site Description

The case study is based on an urban corridor located in Cambridge, Ontario, Canada, as shown in Figure 5. This site was chosen because it represents a typical urban corridor with traffic signals and because traffic data was available to calibrate and validate a simulation model based on this site. It runs along Hespeler Road spanning from Dunbar Road to the Highway 401 eastbound ramp. From south to north, the major roads intersecting with Hespeler in this segment are Dunbar Road, Sheldon Drive, Bishop Road, Pinebush Road, and the Highway 401 Eastbound Ramp. Between these five major intersections are four minor intersections that serve as entrance/exits to retail parking lots.

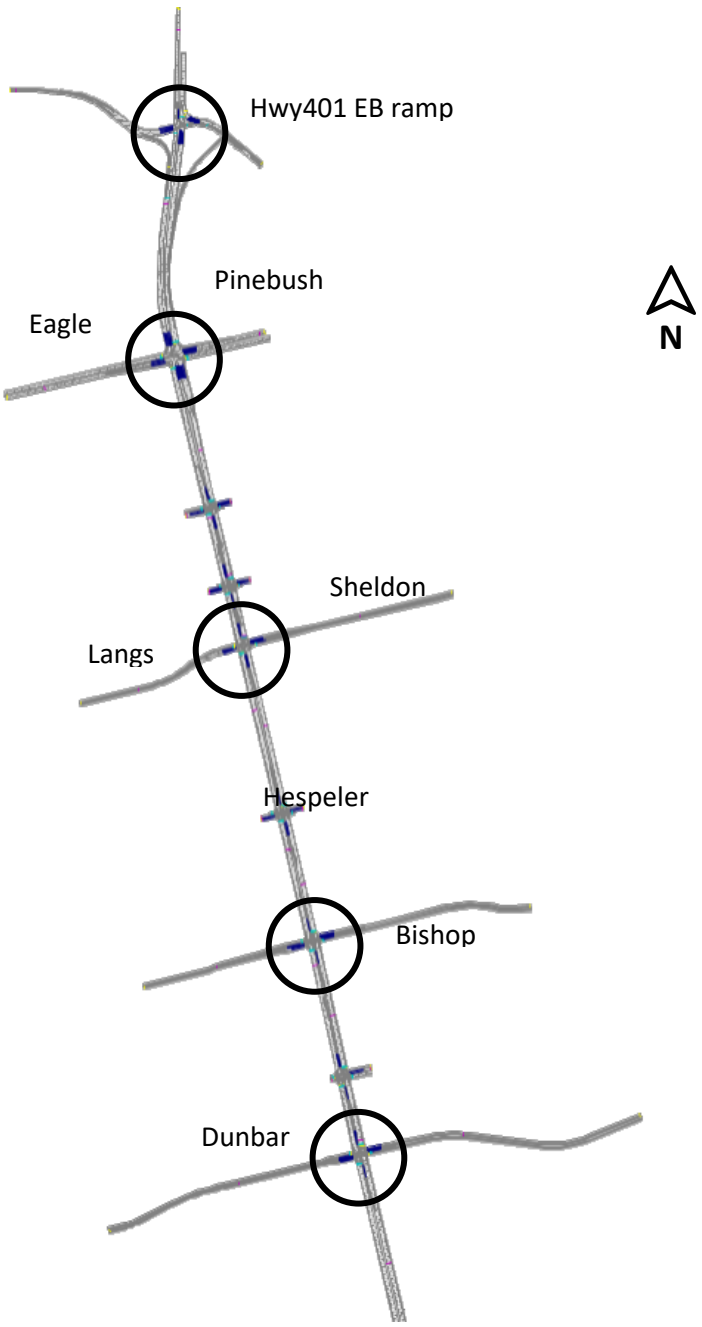

Figure 5: Case Study Traffic Corridor (Circled are major intersections.)

Traffic Network Description

Most of the corridor is a three-lane road with left-turn storage lanes and actuated signal control at intersections. Apart from the Pinebush intersection, the minor direction approaches have two thru lanes or fewer and the signal actuation is partial, with minor thru movements and all left-turn movements actuated. At Pinebush, both major and minor directions are fully actuated with two left-turn storage lanes.

On-Site Traffic Detection

The major intersections of the corridor were implemented with a set of video-based counting and presence detection as well as Wi-Fi detectors. The video-based system provides volumes and turning movement counts, while the Wi-Fi detectors provide travel time measurements. Inductive loop detectors are used for signal actuation and for queue length detection, but the loop detector data was not used in this research.

3.1.1 Input Data

The data used to construct the Vissim model are listed in Table 2 with their sources and purposes. The Vissim model is intended to be as realistic as reasonably possible given the available data so that studies conducted in the model would be valid for the existing conditions of the site. Most of the data were used for model-making, except for the travel speed measurements which were used for model validation.

Table 2: Data for Building Vissim Model

Information		Source	Format	Modelling Application
Road geometry		Google Maps	Image in JPEG	Constructing road links, lanes, stop-line positions
Speed limits		Region of Waterloo	GIS shape file	Inserting speed decision markers
Signal plans		Region of Waterloo	Tables in PDF	Programming signal controls for all intersections
Positions of loops detectors for signal actuation		Region of Waterloo	Setback descriptions in email	Placing detectors for signal actuation
Turning Movement Counts	**Major Intersections**	Video-based TMC	Spreadsheets in Excel	Specify vehicle input volumes Specify route decision ratios for intersection movements
	Minor Intersections	Traditional TMC	Tables in PDF	
Travel Speeds between major intersections		Wi-Fi Detectors	Spreadsheets in Excel	Validate the Vissim model based on travel time distributions

3.1.1.1 Geometry

The road geometry was constructed based on Google Map images. Several screenshots were stitched together to cover the entire site (Figure 6). This stitched image was used as a background in Vissim to

trace the links and lanes (Figure 7). The built-in map background available did not provide enough clarity to build accurate lane layouts; thus, high-resolution Google Maps screenshots were used.

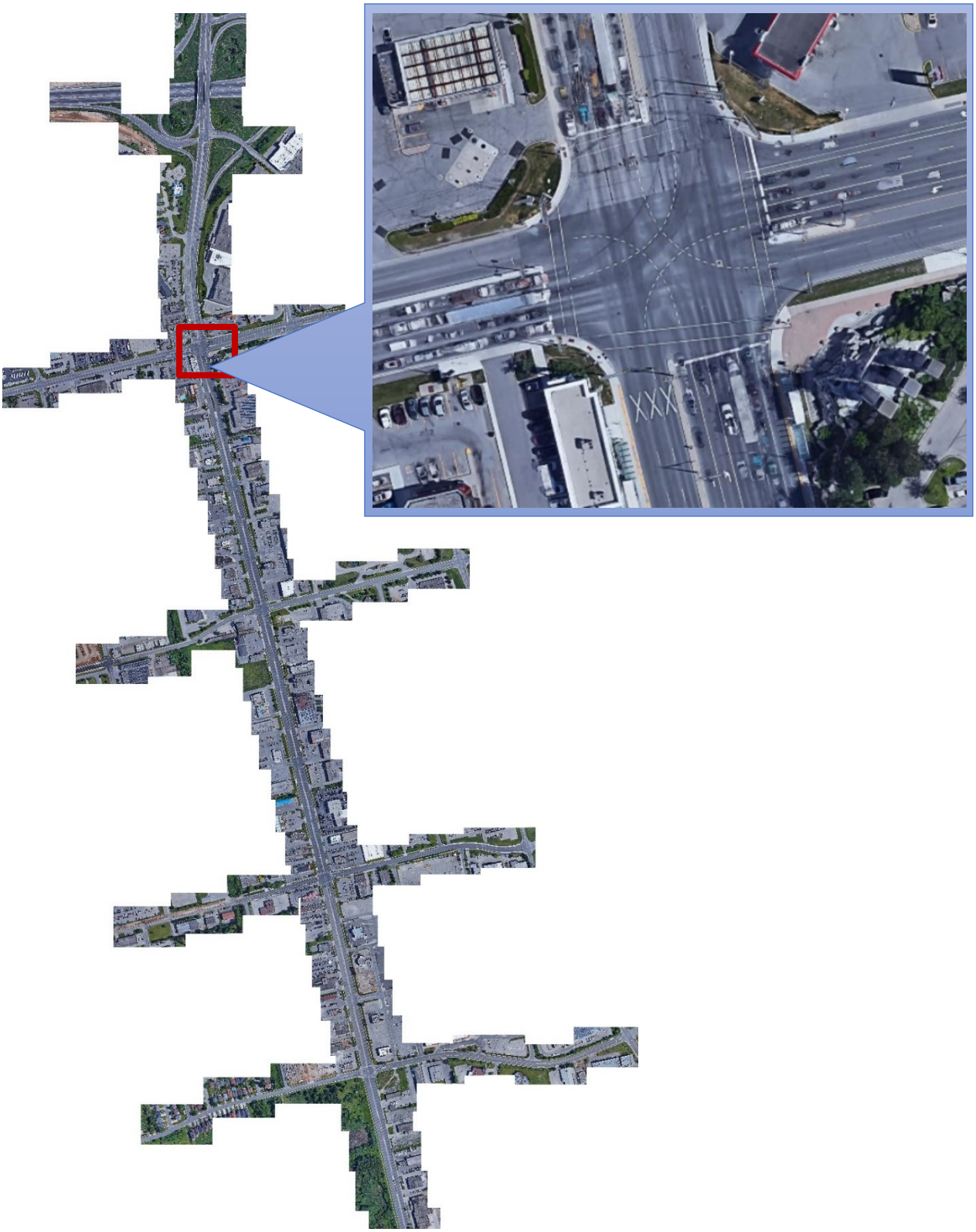

Figure 6: Google Maps Background for Building Vissim Model

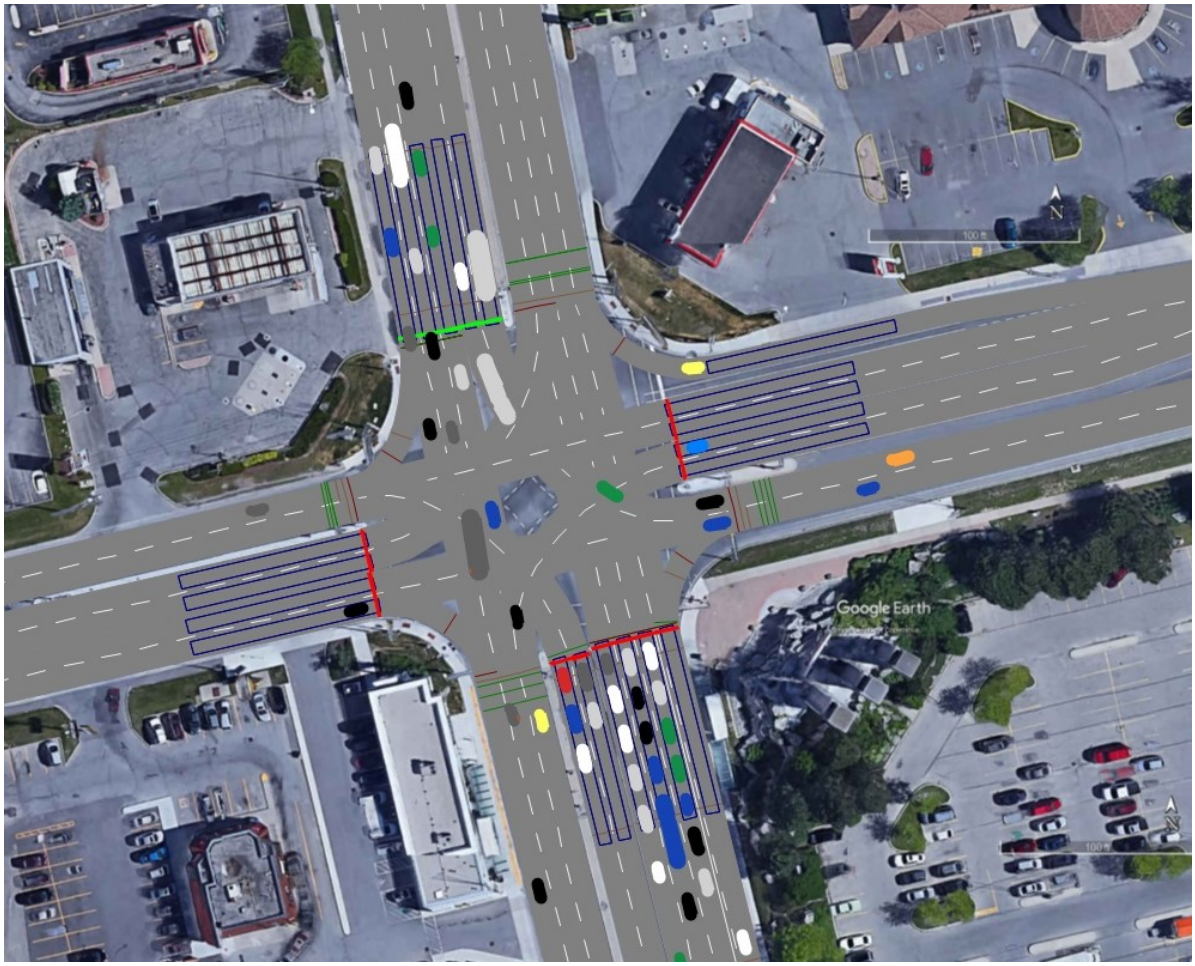

Figure 7: Screenshot from Vissim Simulation – Pinebush Intersection

3.1.1.2 Speed Limits

Speed decision markers were inserted at all entry points into the network and at links where the speed limit changes from its upstream link. The markers were set to define link speeds according to information provided in the open data catalogue of the Region of Waterloo (henceforth referred to as the Region). This information was obtained in the form of Geographic Information System (GIS) shapefiles. As shown in Figure 8, the corridor running north-south has a speed limit of 60 km/h with most east-west approaches having a speed limit of 50 km/h. For the minor intersection, the east-west approaches come from parking lots, and are assumed to have an approach speed of 25km/h until they reach the intersection.

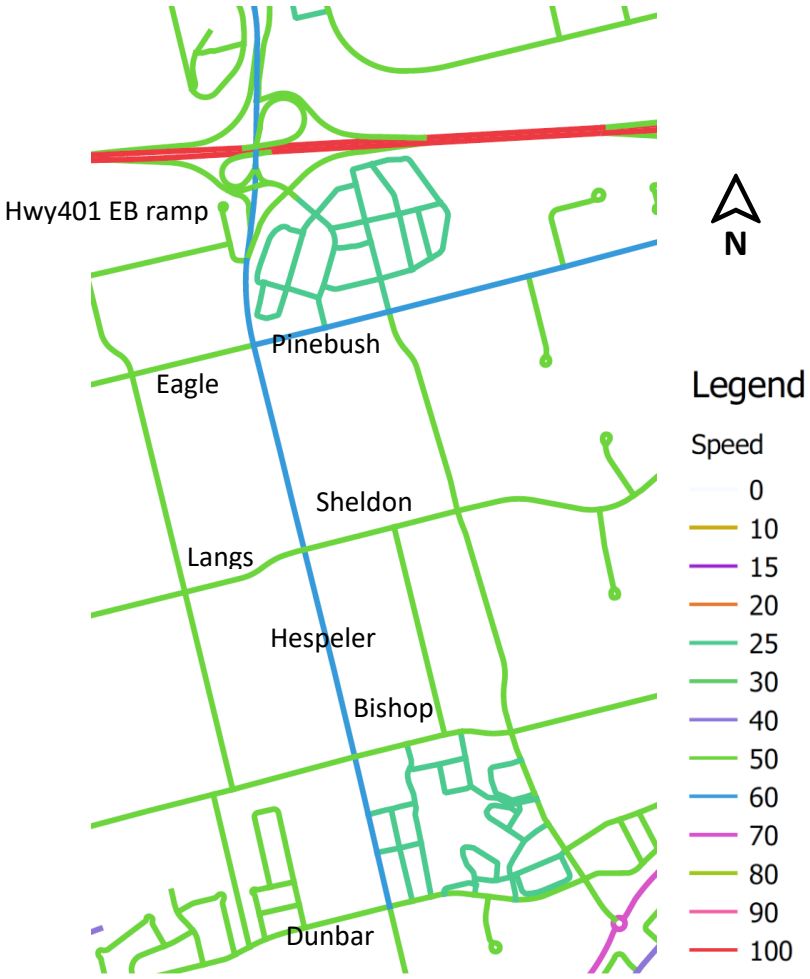

Figure 8: Speed Limits – Hespeler Corridor from Dunbar to Hwy401

3.1.1.3 Signal Control

Signal plans were obtained from the Region for all intersections, with a sample included in Appendix B – Sample of Signal Plan. The Region also described the positioning of signal actuation detector loops in Appendix C – Signal Actuation Detector Loop Layout . These were used to program the signal controllers in Vissim through the Ring Barrier Control (RBC) tool with detector actuation.

3.1.1.4 Traffic Volumes and Turning Ratios

The vehicle input volumes and turning ratios were based on turning movements counts (TMC) provided by the Region. A sample is provided in Appendix D – Sample of Turning Movement Count Data. Video-based TMC was available for major intersections on one day only – June 8, 2016. TMC's for all intersections were available from different dates over the past several years; these were used for the remaining minor intersections. In the Vissim model that is based on field conditions, the vehicle inputs are specified per hour according to the TMC data. Due to the availability of data, the following hours

were simulated: 7-10am, 3-6pm, and 8-10pm, denoted henceforth as the morning period, afternoon period, and evening period, respectively. These hours had data available across all intersections.

3.1.2 Model Validation

In the Vissim model, travel speeds were measured between major intersection from the upstream stop-line to the downstream stop-line. The distribution of travel times from the simulation were then compared to the distribution of travel times in the field as measured by the Wi-Fi-detectors. It should be noted that the Wi-Fi-detectors have a detection range of several meters, so they are not as precise as the simulated travel time detectors. Thus, the distribution of field travel times is expected to be more widespread than those measured in the simulation. Furthermore, the placement of the Wi-Fi detector could influence the measurements taken. They are typically placed at the corner of an intersection inside a cabinet among other electronic equipment.

The distribution of travel times for all segments between major intersections for all simulated hours are shown in Figure 9. The comparison was also disaggregated by period in Appendix E – Comparison of Field and Simulation Travel Times. Wi-Fi detectors also have a low detection rate. The difference in sample size between the simulation and field data are illustrated by scaling the distribution plots by sample size in Figure 10. Scaled plots disaggregated by hour are also included in Appendix E – Comparison of Field and Simulation Travel Times.

The field data is shown to have a much lower sample size and wider spread than the simulation travel time measurements, as expected. However, it is still evident that the travel times of the simulation and field data generally fall within the same ranges with a similar overall distribution. When disaggregated by hour, the same consistency is seen for most segments in most hours.

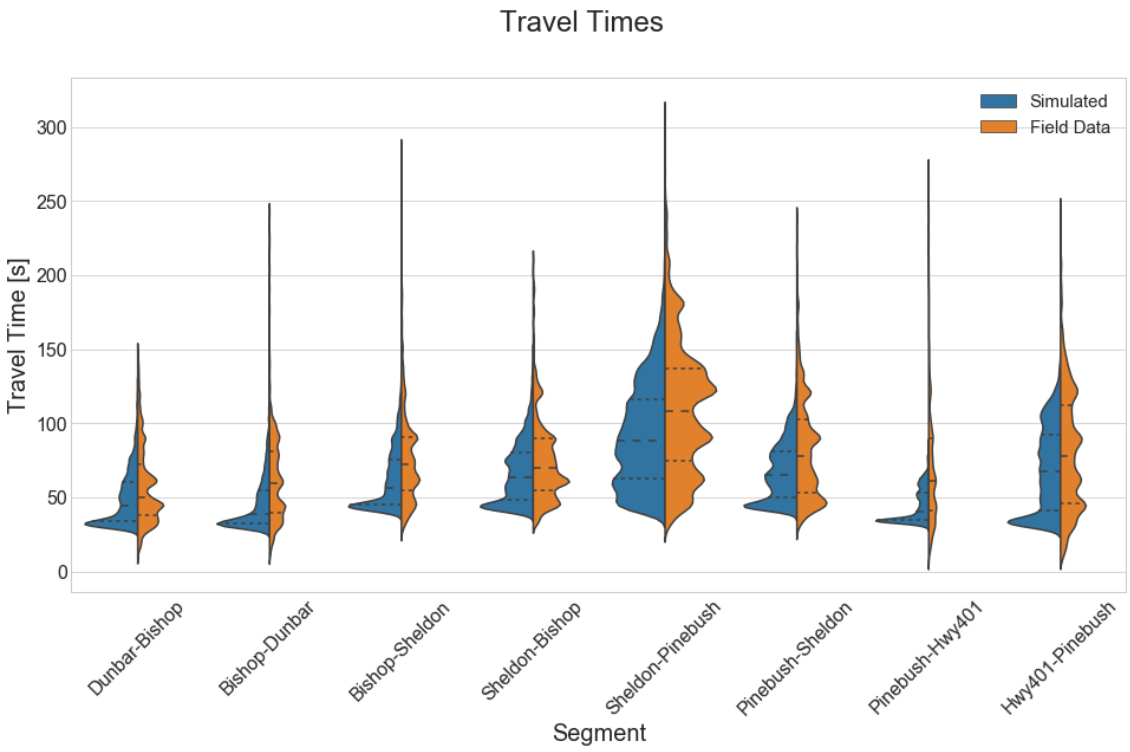

Figure 9: Comparison of Field and Simulation Travel Times for Validation – Equal Area Plots

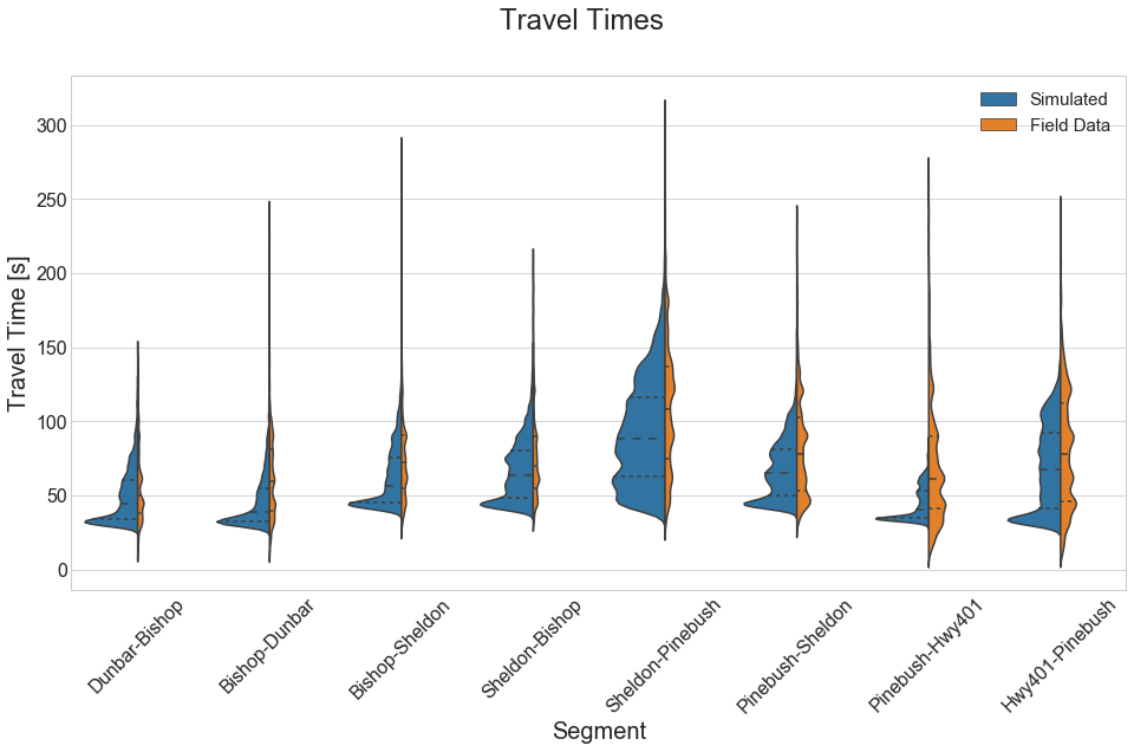

Figure 10: Comparison of Field and Simulation Travel Times – Area Scaled by Counts

3.1.3 Detector Simulation

Aside from simulating vehicle activities, the Vissim model can also simulate detectors. The data assumed to be available includes vehicle presence detection at the positions near an intersection that can be specified by the users. Furthermore, multiple detections of the same vehicle can be known as detections of the same vehicle. In Vissim, the data collection feature was used to generate this data. Data collection points were placed at the following locations with respect to an intersection approach: an advance location upstream from the intersection, the location of the stop-line, and the exit at the end of the intersection, as indicated in Figure 11. Detectors were placed according to this scheme for the approach of each major intersection that is preceded by another major intersection. Only one advance detector would be used in the method, but several advance detectors were placed in the model to investigate the effects of the location of the advance detector. The various locations considered were at 25, 50, 75, and 100m setbacks. In addition, detectors were placed for turning movements to detect stops made during permissive turns, shown in Figure 12.

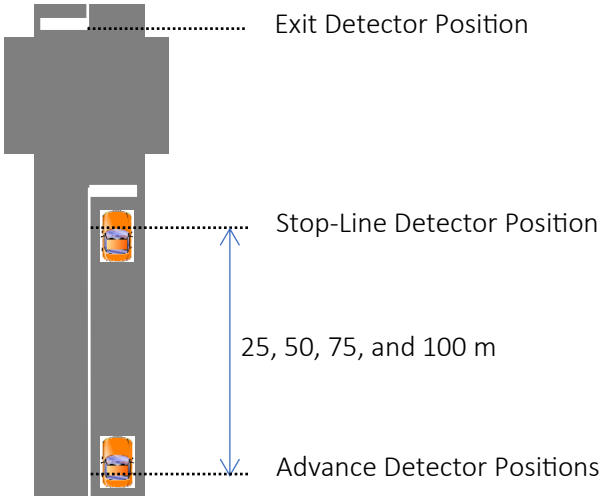

Figure 11: Detector Locations

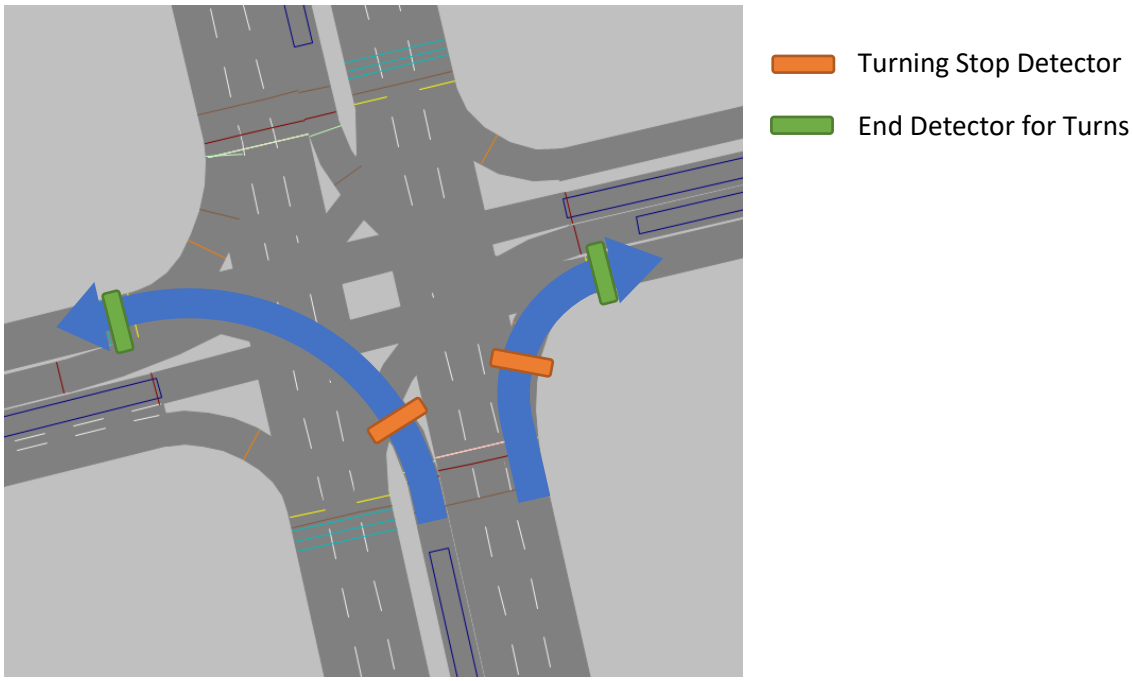

Figure 12: Detector Locations for Turning Movements

3.1.4 Alternative Scenarios Created for Sensitivity Analysis

Aside from the Vissim model created according to the field data, additional Vissim models were created for sensitivity analysis. The additional Vissim model scenarios and their properties are summarized in Table 3. Each alternative scenario is used to analyse the sensitivity of the proposed method to various factors.

Table 3: Alternate Vissim Model Scenarios

Alternative Scenario		Simulation Model Variables			
Scenario Number	**Scenario Description**	**Vehicle Input: Volumes**	**Vehicle Input: Vehicle Types**	**Signal Plans**	**Speed Limits**
0	Field Conditions	As per TMC data	As per TMC data	As provided by the Region	As found in the Region's data
1	Volume Variations	Gradually Increasing	Constant: 95% PC 5% HGV	Constant: Morning period signal plans	Constant: As per data
2	Fleet Variations	Constant: Average of Scenario 0	0% to 30% HGV at 5% increments	Constant: Morning period signal plans	Constant: As per data
3	Signal Coordination	Same as Scenario 1	Constant: 95% PC 5% HGV	Coordinated for NB thru, Otherwise based on morning period signal plans	Constant: As per data
4	Signal Variations	Constant: Average of Scenario 0	Constant: 95% PC 5% HGV	Thru green increases from 30s to 65s at 5s increments, Otherwise based on morning period signal plans	Constant: As per data
5	Speed Limit Variations	Same as Scenario 1	Constant 95% PC 5% HGV	Constant: Morning period signal plans	3 models, each with all speed limits at 50, 60, or 70 km/hr
6	Detector Location Variations	Same as Scenario 1	Constant 95% PC 5% HGV	Constant: Morning period signal plans	Constant: As per data

3.1.4.1 Scenario 0 – Field Conditions

The Vissim model for Scenario 0 is based on field conditions. The vehicle input volumes and types were specified for the hours of 7-10am, 3-6pm, and 8-10pm according to TMC data from the field. Vehicles were classified in terms of Light Duty Vehicles, Buses, Single-Unit Trucks, and Articulated Trucks in the video-based TMC data. In the older manual TMC data, Single-Unit and Articulated Trucks were not differentiated. Due to their small percentage (<5%), they were specified as Single-Unit Trucks in the

simulation model. The equivalent vehicles used in the Vissim model are Passenger Cars, Buses, Heavy Goods Vehicles, and Articulated Heavy Goods Vehicles. The signal plans are specified as per the signal plan documents provided by the Region for the corresponding time periods. The speed limits are set as per the Region's data as well.

Scenario 0 is simulated in one continuous simulation. Each time period (morning, afternoon, and evening), including the first time period, is preceded by a warm-up period. Simulation data from the warm-up period is not used. The warm-up time for the beginning of the simulation and the beginning of each subsequent time period is half an hour and one hour, respectively. The warm-up time of half an hour was determined by examining the travel times between major intersections at 5-minute intervals. For all intersections, the travel time distributions do not show significant changes in pattern after half an hour into the simulation or sooner. Thus, half an hour is allowed for warming up. In between periods, an hour is used conservatively for the transition between traffic conditions from the previous period to the next.

3.1.4.2 Scenario 1 – Volume Variations

In Scenario 1, the volume of the vehicle inputs increases gradually over the course of the simulation. The purpose of this simulation is to provide results over a range of volumes so that the sensitivity of the proposed method to different volumes can be examined. To specify vehicle input volumes for Scenario 1, the field volumes across all available hours – as specified in Scenario 0 – were averaged, and then input volumes ranging from 25% to 200% of the average were found at 25% increments. This creates eight levels of input volumes, resulting in a gradual increase of approach volumes. One simulation is run continuously with the input volume increasing by one level every half an hour.

The rest of the variables were held constant. The vehicle input fleet distribution was set at 95% PC and 5% HGV continuously. Oher vehicle types were omitted for simplicity, as they account for a very small percentage (<5%). The signal plan follows that of the morning period continuously. The speed limits remained unchanged from Scenario 0.

3.1.4.3 Scenario 2 – Fleet Variations

Scenario 2 was created to investigate the effects of having different proportions of HGV's in the fleet. The amount of HGV's increase from 5% of the input volume to 30% at 5% increments every half hour, after a warm-up period of half an hour. In the Scenario 2 simulations, the input volumes are held constant at the average of values from Scenario 0 – Field Conditions for each input. The signal plan and speed limits are held constant as in Scenario 1.

3.1.4.4 Scenario 3 – Signal Coordination

In Scenario 3, the simulation inputs vary across two variables: volume and signal timing. The volume follows the same input scheme as in Scenario 1. The difference between Scenario 1 and 3 is that the signal plan in Scenario 3 is coordinated for the northbound direction according to the offsets in Table 4.

This scenario was used to compare the results of coordinated and uncoordinated signal plans, across different volumes.

Table 4: Signal Offsets for Coordination

Intersection	Distance from Previous Intersection [m]	Distance from Dunbar [m]	Speed [km/h]	Signal Offset [s]
Dunbar	0	0	63	0
Cambridge Centre	190.7	190.7	63	11
Bishop	331.4	522.1	63	30
Shoppers	316.6	838.7	63	48
Sheldon-Langs	412.4	1251.1	63	71
Burger King	145.6	1396.6	63	80
Blackshop	193.4	1590.1	63	91
Pinebush-Eagle	363.4	1953.4	63	112
Hwy401	564.9	2518.3	63	144

3.1.4.5 Scenario 4 – Signal Variations

The simulation model in Scenario 4 holds the input volumes and vehicle types constant. The varying variable is the green interval for the thru movements of the corridor direction at all intersections. The thru green interval increases from 30s to 65s at 5s increments every half hour period after a half hour warm-up period.

3.1.4.6 Scenario 5 – Speed Limit Variations

In Scenario 5, three simulation models are used to investigate the effects of three speed limits. All models are based on the Scenario 1 model, with the only difference being the speed limit. In each of the three models of Scenario 5, all speed limits are set at 50, 60, or 70 km/hr.

3.1.4.7 Scenario 6 – Detector Location Variations

Scenario 6 is not performed in its own separate model; rather, it involves performing the trajectory reconstruction using detector data from detectors at different positions. All of the simulation models have multiple advance detectors as described in section 3.1.3. The trajectory reconstruction is performed using advance detection from the detectors at a 25m setback from the stop-line detectors, then 50m, 75m, and 100m.

3.2 Trajectory Reconstruction

As discussed in literature review, one of the key factors affecting the amount of emissions that could be generated by a vehicle is its motion patterns such as acceleration, braking and cruising. As a result, in order to accurately estimate traffic emissions, an ideal approach would be one that can accurately reconstruct the trajectories of individual vehicles in a traffic stream based on the available sensor data. In this research, we assume that the available data consists of vehicle presence detection at specified locations and signal timing records. The detection of the same vehicle at multiple locations is assumed to be associated; thus, repeated detections are known. Furthermore, it is assumed that the detection technology can roughly classify the vehicle type. This data alone is insufficient for microscopic emission modelling, as microscopic emission modelling requires higher resolution data, such as instantaneous vehicle speed and acceleration at small time intervals. Thus, a reasonable approach would be reconstructing the vehicle trajectories using known information from the detectors.

There are various levels of detail at which the trajectories can be reconstructed, each having repercussions for the emission estimates generated using them. In the reconstruction method presented here, vehicle acceleration and deceleration functions and car-following principles are used. The acceleration and deceleration functions, found in the literature, were empirically developed (Bogdanović & Ruškić, 2013; Kumar Maurya & Bokare, 2012). The car-following principles came from Newell's car-following model (Treiber & Kesting, 2013). This reconstruction process can be seen as an effort to fill in the missing information of vehicle trajectories between detections.

An alternative method that assumes constant average speed between detectors was also explored. To interpolate the average speeds, signal timing information is not required. This alternative is much simpler and faster, but the estimation errors are expected to be greater. However, depending on the purpose at hand, it may be appropriate.

3.2.1 Trajectory Reconstruction using Acceleration

The first proposed trajectory reconstruction method is based on the general motion patterns of vehicles and their car-following behaviour when approaching an intersection, as conceptually illustrated in Figure 13. It first segments each trajectory into stretches of acceleration, deceleration, cruising, and idling based on detections. The method involves performing a set of algorithms on the data from a platoon of vehicles passing through one intersection approach during one signal cycle. The required information includes presence detection and the signal timing for the cycle of interest. The locations of detectors, as previous explained in section 3.1.3, are at an advance location upstream from the intersection, the stop-line of the intersection approach, the stopping point on a left- or right-turn curve, and the point of exit at the end of the intersection.

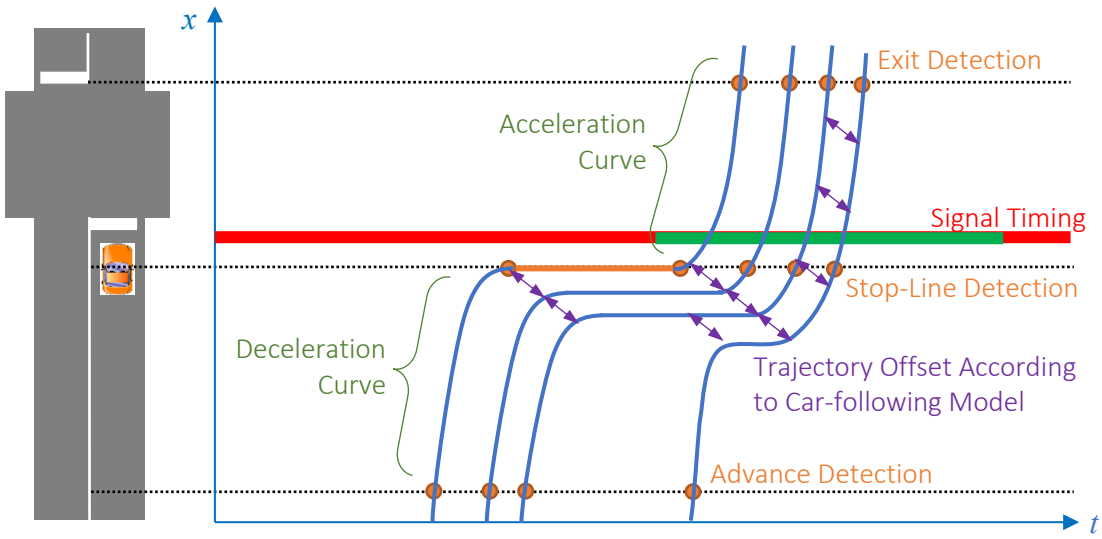

Figure 13: Conceptual Illustration of Vehicle Trajectory Reconstruction with Acceleration

Figure 14 and Figure 15 show the overall process for the proposed trajectory reconstruction method. The reconstruction method outlined in Figure 14 is performed for all vehicles passing through the stop-line of each thru movement lane, while Figure 15 applies to left-turn lanes. The thru movement lanes are processed before the left-turn lanes. The two processes shown are similar, except that for the left turn lanes it accounts for more instances of possible stops during the turn. Differences in Figure 15 are coloured in red. This is due to the possibility of having permissive left-turn phases without any protected left-turn phase in the cycle, which can happen if the protected phase is not actuated. This is different from right-turn lanes in the major direction, which are shared with thru lanes in the major direction and will always have a protected phase in each cycle. At the end of the algorithm, complete trajectories from the exit of the upstream intersection to the exit of the current intersection are constructed. Another difference is that the cruise speed is found using thru-movement vehicles, which is omitted in the left-turn reconstruction process.

Detailed formulations of the individual components in the flowcharts are provided in sections 3.2.1.1 to 0. Some general patterns about the nomenclature used in the formulation are listed below.

t	denotes a point in time
T	denotes a duration of time
x	denotes a position in space
l	denotes a length of distance
$_{adv,stop,turn,exit}$	are used as subscripts pertaining to the advance, stop-line, turning, and exit detectors respectively

n	pertains to a certain vehicle
$n-1$	pertains to the vehicle preceding vehicle n in the platoon
i	pertains to a time step
$1,2$	denotes the beginning and end times of a vehicle detection

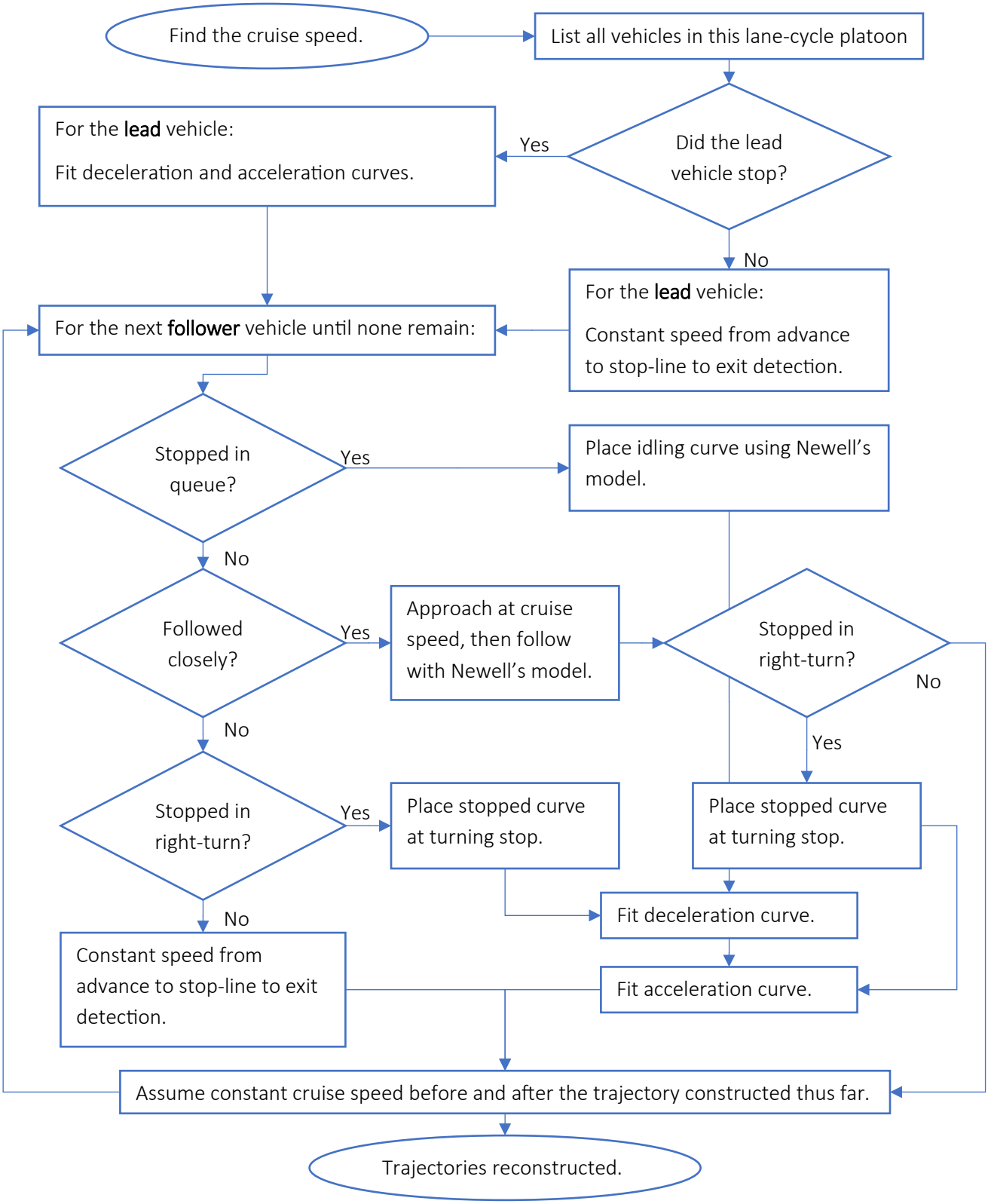

Figure 14: Trajectory Reconstruction Method Overview for Thru Movement Lanes

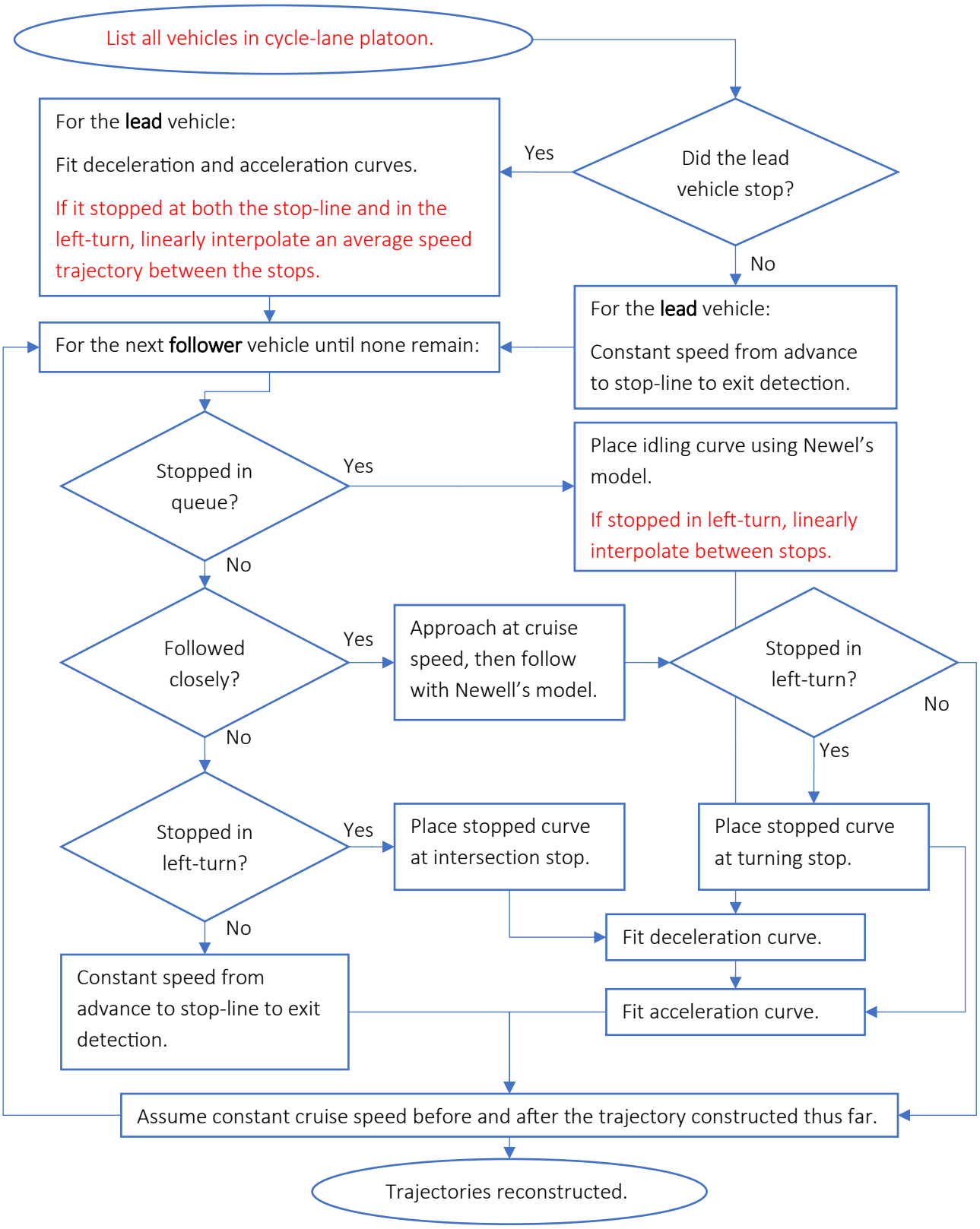

Figure 15: Trajectory Reconstruction Method Overview for Left-Turn Movements

3.2.1.1 Determining the Cruise Speed

To find the cruise speed, the average speeds of vehicles passing through an intersection from the stop-line detector to the exit detector are considered. From a sample of average passing speeds, the cruise speed would be a high percentile of all the speeds, as vehicles in the lower speed range likely slowed down due to queuing. When finding the cruise speed, the sample of average passing speeds must incorporate vehicles that passed through in free flow. Thus, a large enough sample size is needed. However, in theory, the cruise speed depends on the level of congestion, which can change from cycle to cycle. The samples of average passing speeds should be taken from a sufficient number of cycles such that vehicles passing in free flow are captured, but an overly large sample could result in a cruise speed that is too aggregated.

The average passing speed is found according to Equation 8, illustrated in Figure 16.

$$v_{passing,n} = \frac{l_{passing}}{T_{passing,n}} = \frac{x_{exit} - x_{stop}}{t_{exit2,n} - t_{stop2,n}} \tag{8}$$

where

$v_{passing,n}$ is the average speed of vehicle n from the stop-line to the exit detector

$l_{passing}$ is the distance between the stop-line to the exit detector

$T_{passing,n}$ is the time it took vehicle n to travel from the stop-line to the exit detector

x_{stop}, x_{exit} are the positions of the stop-line and exit detectors respectively

$t_{stop2,n}, t_{exit2,n}$ are the times vehicle n left the stop-line and exit detectors respectively

(Subscripts 1 and 2 denote the beginning and end of a detection respectively.)

The cruise speed was found as the 95% percentile of all thru movement passing speeds in the current intersection approach for the past m_{lc} lane-cycle platoons, as in Equation 9. A value of It was found that the value of m_{lc}does not have a great impact on the overall performance.

$$v_{cruise} = P_{\%cruise}\{v_{passing,n} \mid n \in all\ vehicles\ in\ the\ last\ m_{lc}\ lane-cycles\} \tag{9}$$

where

$_{\%cruise}$ is the percentile of passing speeds to be considered the cruise speed

v_{cruise} is the determined cruise speed

m_{lc} is the number of lane-cycle vehicle groups to sample

Values of $_{\%cruise} = 95$ and $m_{lc} = 10$ were used.

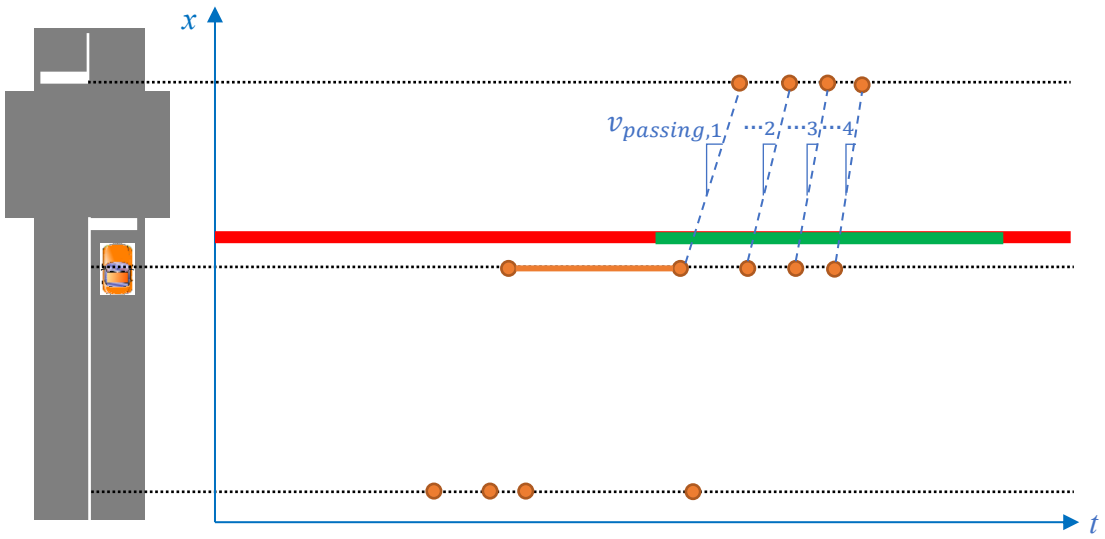

Figure 16: Finding the Cruise Speed

3.2.1.2 Decision Conditions

The process for making the decisions in the flow charts in Figure 14 and Figure 15 are explained in this section.

Did the lead vehicle stop?

Lead vehicles are identified as the first vehicle to pass through a stop-line after a green phase begins. For a detected lead vehicle n $(n = 1)$, it is easy to determine if the vehicle has arrived in the red interval and thus stopped at the stop-line. This can be done by checking if the passing time of the vehicle over the stop-line detector is over a specific threshold, $T_{stop,threshold}$.

Did a follower vehicle stop in queue?

For follower vehicles, whether they came to a complete stop in the queue is determined by the approach speed of the vehicle over the distance from the advance to stop-line detector. If this speed is sufficiently less than the cruising speed, the vehicle is considered to have come to a full stop. This is checked using Equation 10 and illustrated in Figure 17.

$$v_{approach,n} = \frac{l_{approach}}{T_{approach,n}} = \frac{x_{stop} - x_{adv}}{t_{stop2,n} - t_{adv2,n}} \tag{10}$$

If $v_{approach} < p_{stop-cruise} \times v_{cruise}$, the vehicle idled in queue.

where

$v_{approach,n}$	is the average approach speed of vehicle n from the advance to the stop-line detector
$l_{approach}$	is the distance between the advance and stop-line detectors
$T_{approach,n}$	is the time it took vehicle n to travel from the advance to the stop-line detector
x_{stop}, x_{adv}	is the positions of the stop-line and advance detectors respectively
$t_{stop2,n}, t_{adv2,n}$	is the time vehicle n left the stop-line and advance detectors respectively
$p_{stop,cruise}$	is the threshold fraction of the cruise speed that the average speeds of vehicles cannot exceed if they had stopped. A value of $p_{stop,cruise} = 0.5$ was used.

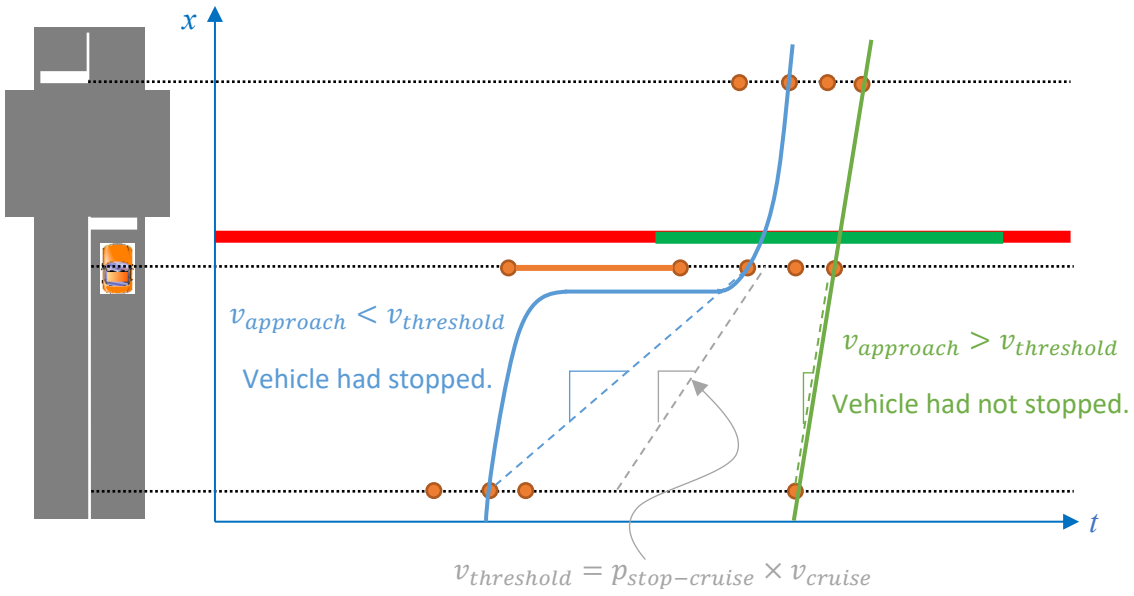

Figure 17: Determining Whether a Vehicle Stopped While Approaching an Intersection

Did a follower vehicle follow closely?

If the vehicle was found to have not stopped in queue, then it is checked whether the vehicle was following the preceding vehicle closely behind when passing the stop-line. This check is performed by comparing the time headway between the current and preceding vehicle to a threshold time headway according to Equations 11 and 12, as illustrated in Figure 18.

$$T_h = t_{stop2,n} - t_{stop2,n-1} \quad (11)$$

$$If\ T_h < T_{h,discharge} \rightarrow vehicle\ followed\ closely \quad (12)$$

where

T_h	is the headway between the current and preceding vehicle when crossing the stop-line
$T_{h,free}$	is the minimum headway for vehicles following in free-flow conditions
$T_{h,discharge}$	is the maximum time headway of vehicles discharging from a queue. A value of $T_{h,discharge} = 1.2s$ was used.

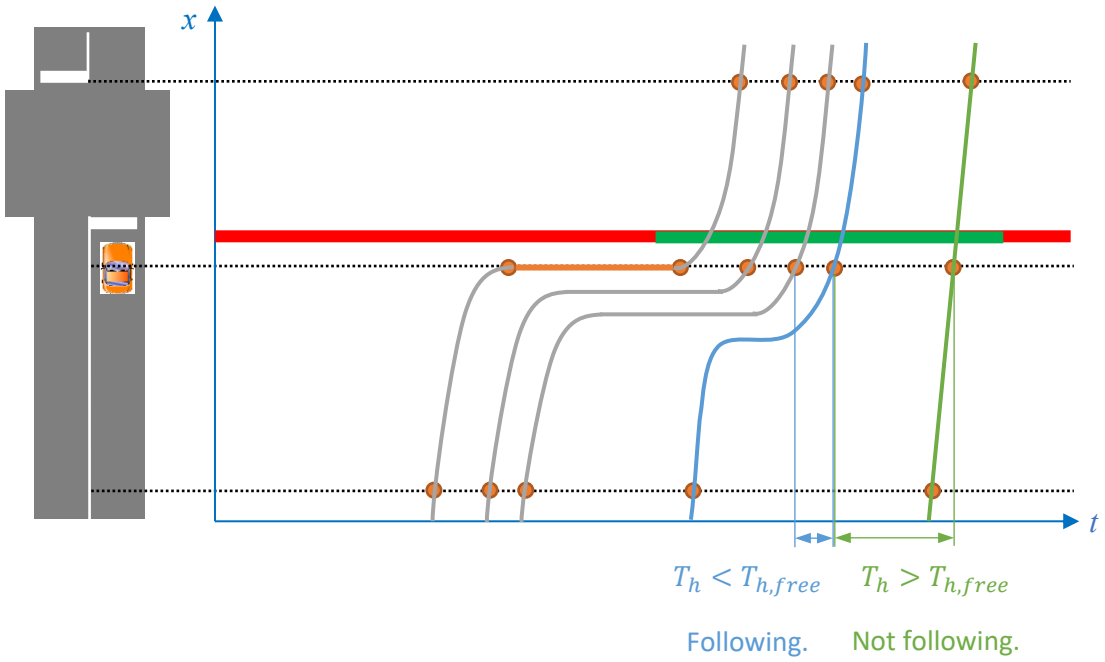

Figure 18: Determining Whether a Vehicle is Following Its Predecessor

Did a vehicle stop during a turn?

Whether a vehicle stopped during a turn is determined the same way as whether a lead vehicle stopped at the stop-line. If the detection of the vehicle at the turning detector lasts longer than $T_{stop-threshold}$, the vehicle is considered to have stopped there.

3.2.1.3 Newell's Car-Following Model

Newell's model was chosen to model the car-following behaviour in this method because of its simplicity (Treiber & Kesting, 2013). It was also shown to be able to generate adequate emission estimates despite its simple form (Vieira da Rocha et al., 2015). In Newell's model, the follower is assumed to always maintain a constant time and distance offset from the preceding vehicle. The distance offset is referred to as the effective length of the preceding vehicle, l_{eff}. The effective length depends on the vehicle length and following distance. In this research, a vehicle length is set for each vehicle class considered, based on the vehicle properties in Vissim, listed in Table 5. To find the time offset, find i such that Equations 13 and 14 are satisfied.

$$x_{i,n-1} \approx x_{stop} + l_{eff,n-1} \tag{13}$$

$$T_N = t_{i,n-1} - t_{stop2,n} \tag{14}$$

where

$l_{eff,n-1}$ is the effective length of vehicle $n-1$

T_N is the time offset

Newell's model is used to determine the idling position and idling end-time of vehicles in queue. For vehicle n, the x and t coordinates of the start of the idling curve is found according to Equations 15 and 16, as illustrated in Figure 19.

$$t_{stop2,n} = t_{stop2,n-1} + T_N \tag{15}$$

$$x_{stop,n} = x_{stop,n-1} - l_{eff,n-1} \tag{16}$$

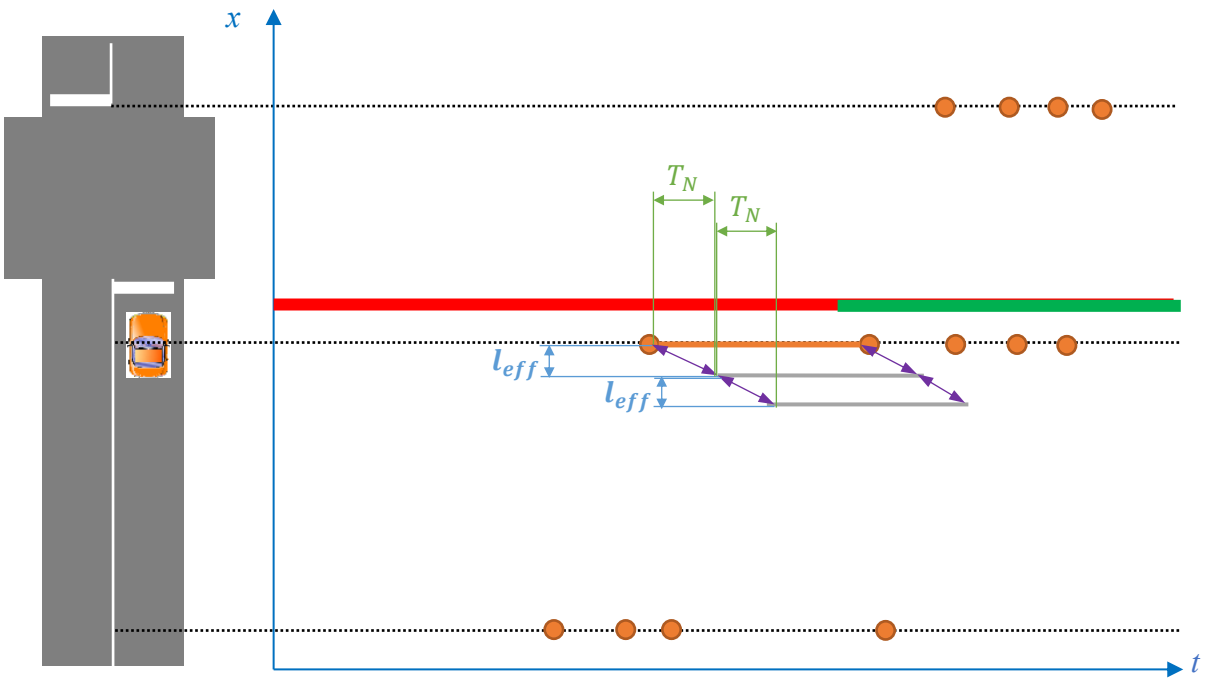

Figure 19: Newell's Car-Following Model

Table 5: Effective Vehicle Lengths for Newell's Car-Following Model

Vehicle Type	Effective Vehicle Length l_{eff} [m]
Passenger Car	5.5
Single Unit Truck	11.5
Combination Truck	13.5
Transit But	13

3.2.1.4 Modelling Following Motions

In the case where a vehicle is found to have followed closely, the following formulation is used. Typically, the vehicle would approach the intersection in a free-flow cruising mode but begin to follow closely once it is near the preceding vehicle. The cruise portion of the trajectory is described in Equations (17-18) and the car-following portion is described in Equations (19-22).

$$t_i = t_{i-1} + dt \tag{17}$$

$$x_i = x_{i-1} + v_{cruise} dt \tag{18}$$

$$for\ i = \{1,2, \dots k\}\ until \begin{Bmatrix} t_{k+1,n} < t_{i,n-1} + T_N \\ and \\ x_{k+1,n} > x_{i,n-1} - l_{eff,n-1} \end{Bmatrix}$$

Then,

$$t_{i,n} = t_{i,n-1} + T_N \tag{19}$$

$$x_{i,n} = x_{i,n-1} - l_{eff,n-1} \tag{20}$$

$$v_{i,n} = v_{i,n-1} \tag{21}$$

$$a_{i,n} = a_{i,n-1} \tag{22}$$

where

i	denotes a time-step
n	denotes the current vehicle
$n-1$	denotes the preceding vehicle
t_i	is the time at time-step i
x_i, v_i, a_i	are the position, speed, and acceleration of the vehicle at t_i
dt	is the time-step increment. A value of $dt = 1s$ was used.

3.2.1.5 Modelling Deceleration Motions

As indicated in Figure 14 and Figure 15, the deceleration motion of a vehicle is modelled if it is determined to have come to a complete stop. A deceleration curve is defined by its startpoint, endpoint, and a curve function. The startpoint and endpoint are both defined by a time and position coordinate. The curve function used is an empirical function calibrated in a study of the deceleration behaviours of vehicles at an intersection (Kumar Maurya & Bokare, 2012). Kinematic relationships are used to determine related factors.

When the endpoint time and position of the deceleration curve are specified, such as for a lead vehicle detected to have stopped at the stop-line, the following process is used to fit a deceleration curve:

Consider a continuous set of k time intervals of step size dt over the segment of deceleration with an initial speed of $v_0 = v_{cruise}$ and an initial acceleration rate of $a_0 = 0$ at $t_0 = 0$. For time interval i $(i = 1,2, \dots k)$, Equations 23-26 define the deceleration curve.

$$-a_i = -k_3 {v_{i-1}}^2 + k_4 v_{i-1} + k_5 \tag{23}$$

$$v_i = v_{i-1} + \frac{a_i + a_{i-1}}{2} dt \tag{24}$$

$$x_i = x_{i-1} + \frac{v_i + v_{i-1}}{2} dt \tag{25}$$

$$t_i = t_{i-1} + dt \tag{26}$$

$$for\ i = \{1,2, \dots k\}\ such\ that\ v_k = 0$$

where

i	denotes a time-step
t_i	is the time at time-step i
x_i, v_i, a_i	are the position, speed, and acceleration of the vehicle at t_i
k_3, k_4, k_5	are empirically calibrated parameters (Kumar Maurya & Bokare, 2012)
dt	is the time-step increment. A value of $dt = 1s$ was used.

To match the end of the deceleration curve to the beginning of the stopped curve:

Shift x_i so that $x_i \rightarrow x_i + x_{stop} - x_k$, and

Shift t_i so that $t_i \rightarrow t_i + t_{stop1} - t_k + t_{lag,stop}$

$t_{lag,stop}$	is introduced to account for the time a vehicle is already detected at the stop-line but has not come to a complete stop. $t_{lag,stop} = 2s$ was used.
x_{stop}	is the position of the stop-line detector. It is replaced by x_{turn} for cases where the vehicle stopped during a turn without stopping at the stop-line
t_{stop1}	is the time the vehicle left the stop-line detector. It is replaced by t_{turn1} for cases where the vehicle stopped during a turn without stopping at the stop-line

Then adjust the deceleration curve so that it matches the advance detection, as illustrated in Figure 20.

If $x_0 > x_{adv}$, then extrapolate the trajectory by cruise speed to the advance detector position according to Equations 27-30

$$T_{cruise} = \frac{x_0 - x_{adv}}{v_{cruise}} \tag{27}$$

$$t'_{adv} = t_0 - T_{cruise} \tag{28}$$

$$T_{off} = t_{adv1} - t'_{adv} \tag{29}$$

If $x_0 < x_{adv}$, then find i where x_i is closest to x_{adv}

$$T_{off} = t_{adv1} - t_i \tag{30}$$

where

T_{cruise}	is the time spent cruising from the advance detector before decelerating
t'_{adv}	is the extrapolated time of being at the advance detector
T_{off}	is the difference between the detected time at the advance detector and the time in the trajectory reconstructed so far

If $T_{off} > 0$, decrease k_3 and increase k_4, k_5 by a proportion p_{adj}.

If $T_{off} < 0$, increase k_3 and decrease k_4, k_5 by a proportion p_{adj}.

Values of $p_{adj} = 0.05s$ and T_{off} were used. Note that lower values of T_{off} generate more accurate trajectories but require significantly more computation effort. Plus, the value of p_{adj} must be small enough that the trajectory can be fitted with T_{off} of the detections.

This section is repeated until $T_{off} < T_{tolerance}$, where $T_{tolerance}$ is the acceptable discrepancy between the detected time and reconstructed trajectory time.

In some cases, the endpoint position is specified but the time is not, such as for a follower vehicle idling in a queue. Its position in the queue can be found, but its time of entering the queue is not detected. In such cases, a previously modelled deceleration curve is used. The position of the curve is shifted so that the endpoint position of the deceleration curve matches the specified idling position. The time of the curve is shifted so that it matches the advance detection of that vehicle.

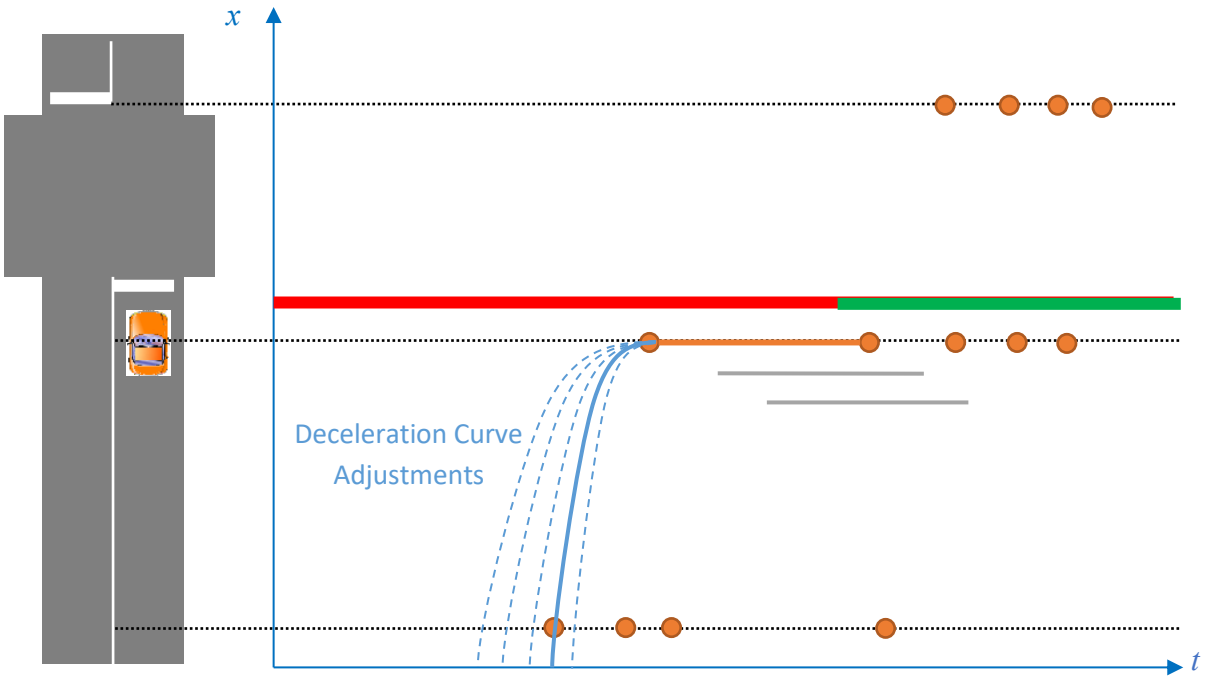

Figure 20: Fitting Deceleration Curves

3.2.1.6 Modelling Acceleration Motions

The modelling of acceleration motions is performed to that of deceleration motions. The acceleration curves are modelled according to Equation 31 as a sequential process using a set of kinematic equations similar to those for the deceleration process (Equations 24-26).

$$\text{Let } v_0 = v_{cruise}, a_0 = 0, x_0 = 0, and\ t_0 = 0$$

$$a_i = \beta_0 + \beta_1 v_{i-1} \tag{31}$$

$$v_i = v_{i-1} + \frac{a_i + a_{i-1}}{2} dt \tag{24}$$

$$x_i = x_{i-1} + \frac{v_i + v_{i-1}}{2} dt \tag{25}$$

$$t_i = t_{i-1} + dt \tag{26}$$

$$for\ i = \{1,2, \dots k\}\ such\ that\ v_k = v_{cruise}$$

where

β_0, β_1 are empirically calibrated parameters (Y. Zhang et al., 2013)

To match the end of the stopped curve to the beginning of the acceleration curve:

Shift x_i so that $x_i \rightarrow x_i + x_{stop}$, and

Shift t_i so that $t_i \rightarrow t_i + t_{stop2} - t_{lag,start}$

$t_{lag,start}$ is introduced to account for the time a vehicle is detected at the stop-line but has already begun accelerating. $t_{lag,start} = 2s$ was used.

x_{stop} is the position of the stop-line detector. It is replaced with x_{turn} for cases where the vehicle accelerated from stopping during a turn

t_{stop2} is the time the vehicle leaves the stop-line detector. It is replaced with t_{turn2} for cases where the vehicle accelerated from stopping during a turn

Then adjust the acceleration curve so that it matches the exit detection, as illustrated in Figure 21.

If $x_k < x_{exit}$, then extrapolate the trajectory by cruise speed to the exit detector position according to Equations 32-35.

$$T_{cruise} = \frac{x_{exit} - x_k}{v_{cruise}} \tag{32}$$

$$t'_{exit} = t_k + T_{cruise} \tag{33}$$

$$T_{off} = t_{exit2} - t'_{exit} \tag{34}$$

If $x_0 < x_{adv}$, then find i where x_i is closest to x_{adv}

$$T_{off} = t_{exit2} - t_i \tag{35}$$

where

T_{cruise} is the time spent cruising from the advance detector before decelerating

t'_{exit} is the extrapolated time of being at the advance detector

T_{off} is the difference between the detected time at the advance detector and the time in the trajectory reconstructed so far

If $T_{off} > 0$, decrease β_0 and increase β_1 by a proportion p_{adj}.

If $T_{off} < 0$, increase β_0 and decrease β_1 by a proportion p_{adj}.

The same values of p_{adj} and T_{off} as the deceleration modelling method were used. This section is repeated until $T_{off} < T_{tolerance}$, where $T_{tolerance}$ is the acceptable discrepancy between the detected time and reconstructed trajectory time.

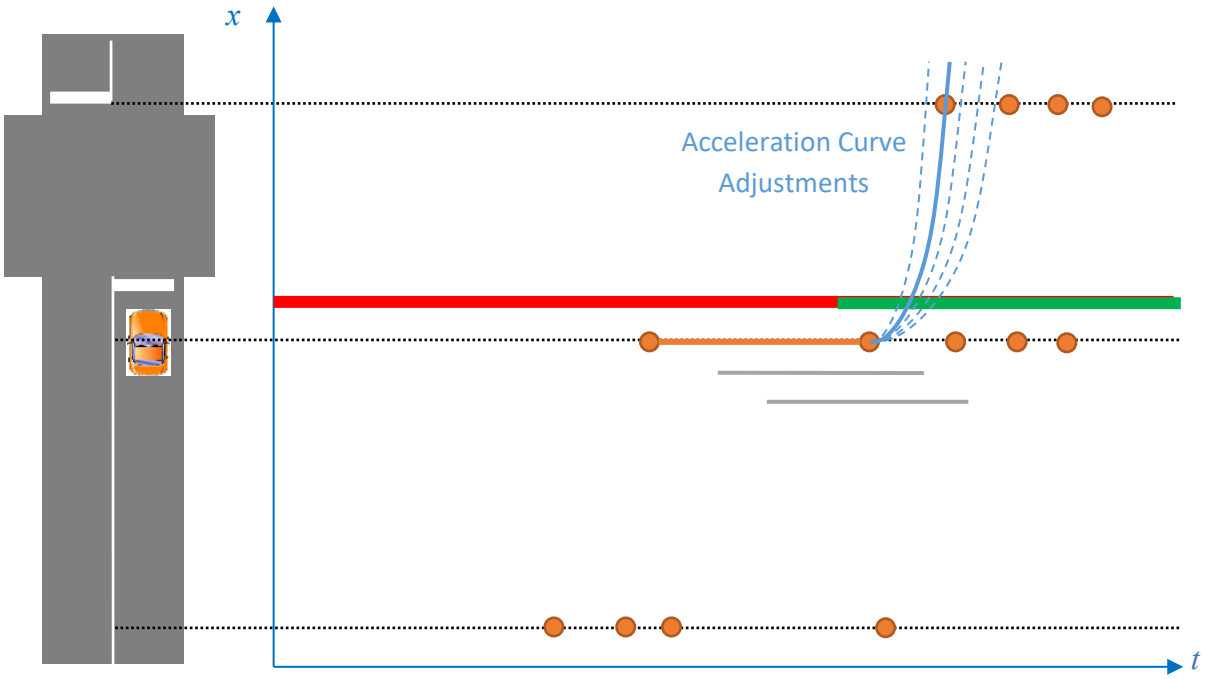

Figure 21: Fitting Acceleration Curves

3.2.1.7 Modelling Linear Constant-Speed Motions

This section describes the linear interpolation indicated in the flow charts. It is used between idling curves at the stop-line and turn detectors, and for free-flow movements between detectors. The formulation is the same as that in equations (3) and (4). For linear interpolation between two points in time and space, the kinematics properties are found using Equation 36.

$$v = \frac{x_f - x_s}{t_f - t_s} \tag{36}$$

where

v is the constant speed between the points

x_f, x_s are the positions of the end and start points respectively

t_f, t_s are the points in time for the end and start points respectively

In the case of interpolating between two idling curves, the end of the first curve is the startpoint and the beginning of the second curve is the endpoint of the interpolated segment. In the case of free-flow movement through the intersection, this interpolation formulation is applied with the advance detection as the startpoint and the stop-line detection as the endpoint, then with the stop-line detection as the startpoint and the exit detection as the endpoint.

3.2.2 Trajectory Reconstruction Using Average Speed Interpolation

A simpler method is investigated where the vehicle trajectories are linearly interpolated between the detections. The detected idling curves are taken as is. Between detections, the trajectory is interpolated as an average speed trajectory, as illustrated in Figure 22. In this method, the formulation in section 0 is used for all spaces between detections.

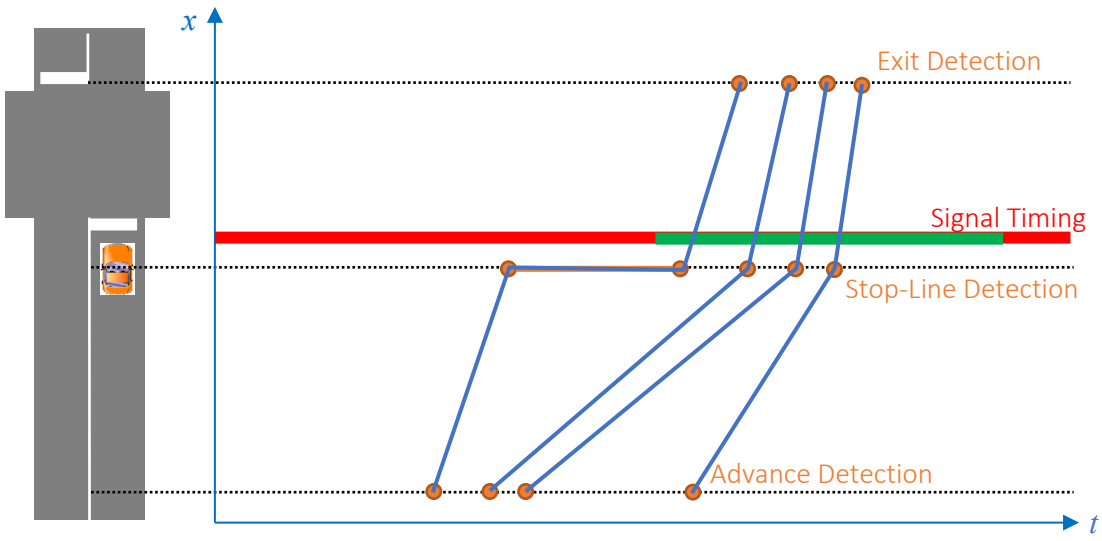

Figure 22: Conceptual Diagram of Trajectory Reconstruction with Linear Interpolation

3.3 Emission Estimation

The second major component of our proposed traffic emission estimation method is the simulation model MOVES that is used to determine the emission amounts of different types using vehicle trajectories – either simulated or reconstructed – as inputs. The following section provides a detailed

discussion about the MOVES model and the inputs required. To improve the computational efficiency, a simplified method is lastly introduced, which could be used to calculate emission directly without the need to run the MOVES software.

3.3.1 Generating Inputs for MOVES

MOVES is a software system developed by EPA that can be used to estimate traffic generated emissions at various levels of scales, ranging from project level to national level. In this research, we use MOVES for project level analysis.

To generate emission estimates, the MOVES software requires a range of inputs as listed in

Table 6. Running MOVES requires selecting a region-specific domain from its database or creating a custom one. Since no domains were available for Canadian regions, and creating one is an onerous task, MOVES was run using the Erie County domain.

With these inputs, MOVES is used to generate emission estimates disaggregated by vehicle type, pollutant, and pollutant process. Further disaggregation is enabled by disaggregating the input data prior to feeding it into MOVES using unique link numbers, as explained in section 3.3.1.3. The emission estimates are aggregated over the vehicles crossing the stop-line in one lane of one intersection approach during one signal cycle.

Table 6: MOVES Input Tables and Sources of Information

Input Table	Source of Information	Notes Regarding Input Table Creation
Age Distribution	Statistics Canada (Statistics Canada, 2009)	Available data was extrapolated for unavailable data
Fuel Supply	Default MOVES database for Erie County, New York	Available information from the closest region was used.
Fuel Usage Fraction		
Alternative Vehicle Fuel Technology		
Fuel Formulation		
Meteorology	Open online archives (Thorsen, 2018)	Temperature and pressure for Cambridge was found for each hour of the day
Links	Vissim simulation	The vehicle records from the simulation output provides second-by-second vehicle profiles including speed, acceleration, vehicle type, and their place in the network.
Link Source Types		
Operating Mode Distribution		

3.3.1.1 Local Regional Data – Vehicle Age Distribution and Meteorology

Where available, data for the local context was used, such as vehicle age distributions from Statistics Canada (Statistics Canada, 2009) and meteorological data from open sources (Thorsen, 2018). It was assumed that the current age distribution of vehicles is not significantly different from the time of the data. MOVES accepts age distributions spanning a 30-year range, but data only provided a distribution spanning less than 20 years, so the remaining years' distribution were extrapolated, as shown in Appendix F – Vehicle Age Distribution Extrapolation. The meteorological data, i.e. temperature and relative humidity, were specified on an hourly basis for the city of Cambridge, Ontario.

3.3.1.2 Default Data Provided in MOVES – Fuel Information

For the Fuel Supply, Fuel Usage Fraction, Alternative Vehicle Fuel Technology, and Fuel Formulation input tables, the default data included in the MOVES software for Erie County was used, as it is the closest U.S. county to Cambridge. This data was not easily obtainable. Moreover, it does not significantly impact the method of emission monitoring developed in this research.

3.3.1.3 Vehicle Activities – Links, Link Source Types, Operating Mode Distribution

In addition to the inputs on vehicle age distribution, meteorology, and fuel information, the last set of inputs to MOVES is related to vehicle operations including Links, Link Source Types, and Operating Mode Distribution, which concern the activities of the vehicles generating the emissions. When estimating emissions for the purpose of traffic management, these inputs are the most important. The format for these input tables are generated according to the templates created by MOVES and following the Input Guidelines for Motor Vehicle Emissions Simulator Model, Volume 2: Practitioners' Handbook: Project Level Inputs (Porter et al., 2015). When generating the input templates with MOVES, the user must select pollutants, processes, vehicle types, and fuels of interest to include in the MOVES run outputs. The pollutants selected were CO_2, N_2O, CH_4, and any prerequisite pollutants for estimating those pollutants as determined by MOVES in the selection interface, which were Total Energy Consumption and Total Gaseous Hydrocarbons. The processes selected were running exhaust and crank-case exhaust, which occur during on-road driving. The vehicle types selected were Passenger Cars, Single Unit Short-Haul Trucks, Combination Short-Haul Trucks, and Transit Buses. The fuels selected were Gasoline and Diesel Fuel. Only the Urban Unrestricted road type is used. The follow section provides a detailed description of these input tables.

Links Table

Table 7 is an example of part of a Links input table. In a Links table, one tuple is required for each "link", identified with a user-specified linkID value. A "link" is how inputs are disaggregated in MOVES and outputs are disaggregated correspondingly. As such, the linkID can be used as an abstract property to disaggregate input and output data. It can represent an actual link in the traffic network or any disaggregated portion of the input traffic activity. In this research, the linkID was used to differentiate between vehicle activities approaching different intersections from different directions, which lane they

passed the stop-line in, what turning movement they made, and which cycle they passed the stop-line in. For example, in a linkID of 21634: the 2 indicates an approach – Dunbar southbound; the 1 indicates second lane from the right (counts begin at 0); the 634, being greater than 500, indicates a left turn movement; and 634-500=134 indicates the 134th signal cycle of the dataset. This convention was developed before the real-time emission calculation method, when MOVES runs were required, which only allows a maximum of 5 digits in the linkID. The countyID, zoneID, and roadTypeID are values corresponding with settings chosen for the MOVES run and are held constant in this research. The linkLength values correspond with the distance vehicles travel in the individual "link". The linkVolume is the number of vehicles traversing the link in the time period of concern. The linkAvgSpeed is the speed of all vehicles in the "link" averaged over the time and distance of concern. It is not used if the Operating Mode Distribution table is provided. The linkDescription is an optional field. The linkAvgGrade, the average grade across the "link", is held at 0 for simplicity, as it does not affect the methodology developed in this research.

Table 7: Links Input Table Example

linkID	countyID	zoneID	roadTypeID	linkLength	linkVolume	linkAvgSpeed	linkDescription	linkAvgGrade
10001	36029	360290	5	171.604	2	36.79739757		
11001	36029	360290	5	171.604	2	26.49264088		
10002	36029	360290	5	171.604	2	30.24914179		
11002	36029	360290	5	171.604	2	37.64627249		
10502	36029	360290	5	171.604	1	35.2919002		
10003	36029	360290	5	171.604	1	38.19702487		
…	…	…	…	…	…	…		

Link Source Types Table

Table 8 is an example of part of a Link Source Types input table. "Source Type" refers to the type of vehicle that is the source of emissions. A tuple is required for vehicle type – specified by the sourceTypeID – on each "link" – specified with the linkID. The sourceTypeHourFraction is a decimal fraction indicating what proportion of vehicular travel time on a "link" is contributed by a particular source type. The fractions of all source types on any "link" must add up to 1.

Table 8: Link Source Types Input Table Example

linkID	sourceTypeID	sourceTypeHourFraction
10001	21	1
11001	52	0.66666667
11001	21	0.33333333
10002	21	1
…	…	…

Operating Mode Distribution Table

The Operating Mode Distribution (OMD) is an optional input table for MOVES available at the project level. It provides the traffic activity data at the highest level of detail available for MOVES inputs. In the OMD, a tuple is required for each source type, link, pollutant process, and operating mode combination. That is, for each pollutant process of each vehicle type on each link, there must be a tuple for each of the operating modes. Table 9 shows part of an OMD table for a single vehicle type on a single link for a single pollutant process across all operating modes. The pollutants and processes of interest are identified by a single polProcessID. The required polProcessID's were identified by having MOVES generate an OMD template after selecting the pollutants and processes of interest mentioned earlier in this section.

Table 9: Operating Mode Distribution Input Table Example

sourceTypeID	hourDayID	linkID	polProcessID	opModeID	opModeFraction
21	85	10001	101	0	0.19047619
21	85	10001	101	1	0
21	85	10001	101	11	0
21	85	10001	101	12	0
21	85	10001	101	13	0
21	85	10001	101	14	0
21	85	10001	101	15	0
21	85	10001	101	16	0
21	85	10001	101	21	0
21	85	10001	101	22	0.04761905
21	85	10001	101	23	0.42857143
21	85	10001	101	24	0.0952381
21	85	10001	101	25	0.0952381
21	85	10001	101	27	0
21	85	10001	101	28	0.14285714
21	85	10001	101	29	0
21	85	10001	101	30	0
21	85	10001	101	33	0
21	85	10001	101	35	0
21	85	10001	101	37	0
21	85	10001	101	38	0
21	85	10001	101	39	0
21	85	10001	101	40	0
…	…	…	…	…	…

The operating mode is a categorization of vehicle activity by speed, Vehicle Specific Power (VSP), and acceleration. The operating mode bins relevant to this research and their corresponding boundary conditions as provided by the MOVES software are in Appendix A – Operating Mode Bins. The bin boundary conditions were in the template generated by MOVES. The opModeFraction is the fraction of time spent in one operating mode by all the vehicles of one type on one link. These fractions must be repeated for each pollutant process of interest. Vehicle Specific Power is a measure of the power consumption of a vehicle at an instantaneous moment. It is a function of the vehicle's instantaneous speed and acceleration, vehicle mass, mechanical coefficients, and road grade, as described in equation (2). Parameter for the function are provided in the report Population and Activity of On-road Vehicles in MOVES2014 (U.S. Environmental Protection Agency, 2016b).

A modified version of this function is provided by the report for heavy duty vehicles. The coefficients A, B, C, and vehicle mass M for various types are also provided in this report. The vehicle speed and

acceleration come from the Vissim simulation or trajectory reconstruction. Although road grade has been ignored in this research process, it can be easily accounted for in the VSP if it is known.

To calculate the amount of vehicle-time spent in each VSP and speed bin, individual vehicle data at one-second intervals are used. In the case of using the originally simulated vehicle trajectories, vehicle records are output at one-second intervals. In the case of using the reconstructed trajectories, trajectories are reconstructed or discretized into one-second interval datapoints. The operating mode fraction for a single link, vehicle type, and pollutant process is then found according to Equation 37.

$$F_{opMode,type,link} = \frac{\sum T_{opMode,type,link}}{\sum T_{type,link}} \tag{37}$$

where

F is the operating mode fraction

T is the collective driving time of all vehicles

$opMode$ pertains to a specific operating mode

$type$ pertains to a vehicle type

$link$ pertains to a "link" or input disaggregation

The operating mode fractions for a set of operating modes is repeated for all pollutant processes, aside from the running exhaust of CH_4 and N_2O, which are not split into operating modes. The fractions of all operating modes for each link, vehicle type, and pollutant process combination must add up to 1.

3.3.2 Real-Time Emission Estimation

Running the MOVES software to calculate emissions is by no means a real-time calculation method, especially when the dataset is large. Aside from navigating the interface, the run itself involves a complex algorithm with some processes requiring multiple iterations. For example, in order to gain a full understanding of the inner working of the MOVES system, an attempt was made to visualize the whole MOVES algorithm in detail with the processes relevant to the three greenhouse gasses of interest, as described in the MOVES documentation (U.S. Environmental Protection Agency, 2015). The effort was abandoned due to its complexity, as evident in the partial visualization shown in Appendix G – Partial Visualization of the MOVES Algorithm.

A simplified approach is therefore developed to replicate the main functions of the MOVES software without running the software directly. The basic idea is to categorize each of the individual inputs to the MOVES system (i.e., emission influencing factors), create combinations based on the categories of all inputs, and then determine the emission rate for each combination. For example, in this research, we consider three main emission influencing factors including Traffic Volume (q), Vehicle Types ($type$) and

Operating Mode ($opMode$), the total emission that are expected to be generated by a given type of traffic/vehicle on a given link ($link$) can be estimated according to Equation 38.

$$E_{type,pp,link} = \sum\left(F_{opMode,type,link} R_{opMode,type,pp}\right) q_{type,link} \quad (38)$$

where

$type$	pertains to a vehicle type
$opMode$	pertains to an operating mode
$link$	pertains to a "link" or input disaggregation
pp	pertains to a pollutant process
$E_{type,\ pp,\ link}$	is the emission quantity estimated for a given type of vehicles, on a given link for a given pollutant process [g]
$F_{opMode,\ type,\ link}$	is the proportion of motions that are in a given operating mode
$R_{opMode,\ Type}$	is the unit emission rate [g/veh/hr]
$Q_{type,\ link}$	is the total volume of vehicle type on link [veh/hr]

It should be noted that MOVES includes a large number of factors as shown in Figure 18. If all of these factors are considered in classification, it would result into an unmanageable number of combinations. Fortunately, many of these factors in MOVES can be held constant when the scope of our analysis is limited to a traffic project level with short timeframes (e.g., by minutes or hours) and small spatial coverage (e.g., a traffic corridor or a district). Examples of such factors include fuel type, temperature and humidity, and vehicle age distribution, which can all be assumed to be uniform or constant across alternative traffic management schemes. To model emissions for the purpose of traffic management, the model should be able to differentiate between changes in emissions caused by traffic management strategies and those caused by external factors such as weather and changing fleets. Holding external factors constant in the modelling process and only being sensitive to traffic activity factors would aid the analysis of relationships between traffic management strategies and emissions. As a result, similar to the work of Park et al. (2015), it was decided that the Volumes and Operating Mode Distribution is the only input that the method must be sensitive to over a small spatial-temporal scale.

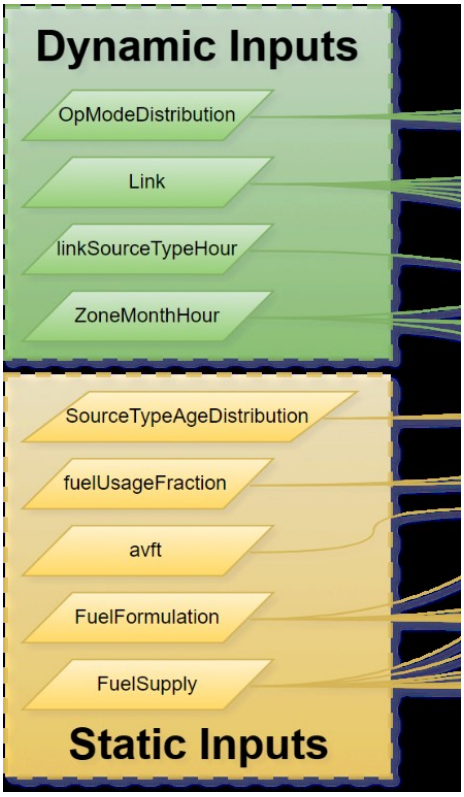

Figure 23: Dynamic and Static Inputs for MOVES

3.3.2.1 Generating Emission Rates for Real-Time Emission Estimation

In the proposed simplified emission estimation method described in the previous section (Equation 38), the emission rates for individual classes must be available or obtained in advance. In this research, we obtained the estimates of these rates by feeding basic combinations of the inputs of interest into the MOVES software. This method is similar to that of Xu et al. (2016), but with much fewer input combinations. One link was created for each vehicle type and operating mode combination, with the linkID being a concatenation of the vehicle type ID and operating mode ID. Thus, for 4 vehicle types and 25 operating modes, a total of 4x25=100 links were created. For each link, the Links, Link Source Types, and Operating Mode Distribution tables were populated as described below.

Input Tables

The input tables were populated so that the unit emission rate per vehicle for each vehicle type, pollutant process, and operating mode would be generated by MOVES. One link must be specified for each vehicle type and operating mode combination. In the Links table, for each link, which represents one vehicle type and one operating mode, a volume of 1 is entered. In the Link Source Types table, for each link, the corresponding vehicle type and a source type fraction of 1 is entered. In the Operating Mode Distribution table, for each link, the corresponding vehicle type was specified, and an entry was created for each pollutant process. The opModeID was named the mode corresponding with the link

and a fraction of 1 was assigned. Thus, each tuple pertains to one vehicle type and one pollutant process operating in a single operating mode. Table 10 shows entries for vehicle type 21 for operating modes 0 and 1. The table continues in the same pattern for the remaining operating modes, and the pattern is repeated for each vehicle type. For 4 vehicle classes, 23 operating modes, 3 pollutants of interest and 2 prerequisite pollutants resulting in 6 pollutant processes, the required combinations of inputs are

$$4 \times 23 \times 6 = 552$$

This produces 552 emission rates to be used as factors in the real-time calculation.

Table 10: Part of the Operating Mode Distribution Input Table for Generating Emission Rates

sourceTypeID	hourDayID	linkID	polProcessID	opModeID	opModeFraction
21	85	2100	101	0	1
21	85	2100	501	0	1
21	85	2100	601	0	1
21	85	2100	9001	0	1
21	85	2100	9101	0	1
21	85	2100	515	0	1
21	85	2101	101	1	1
21	85	2101	501	1	1
21	85	2101	601	1	1
21	85	2101	9001	1	1
21	85	2101	9101	1	1
21	85	2101	515	1	1
…	…	…	…	…	…

The remaining input tables required for MOVES were populated with default or average values. This produces rates that differ by vehicle type, operating mode, and pollutant process, but all correspond with the same values for fuel, meteorological, and age distribution data.

Emission Rates by Class

The emissions estimates output by the MOVES software can be disaggregated by pollutant process and vehicle type. It cannot disaggregate the outputs by operating mode, but since the inputs assigned one operating mode per link and named the linkID's accordingly, it is clear which emission values correspond with which operating mode. Table 11 shows part of the MOVES output after generating emissions rates to be used in real-time calculations. For example, in the first row, the emissionQuantity is the rate of emission for pollutant 91 (Atmospheric CO_2) generated by vehicle type 61 (Combination Short-Haul Truck) operating in mode 40 (Cruise/Acceleration; 30<=VSP; 50<=Speed) per vehicle.

Table 11: Part of the MOVES Output that Generated Emission Rates

linkID	pollutantID	processID	sourceTypeID	roadTypeID	emissionQuantity
6140	91	1	61	5	4949810000
6139	91	1	61	5	4049850000
6138	91	1	61	5	3149890000
6137	91	1	61	5	2249920000
6135	91	1	61	5	1437490000
…	…	…	…	…	…

3.3.2.2 Validation of the Rate-based Method

The proposed rate-based method was validated by performing an estimation on a set of fictional input tables using the MOVES software and also using the simplified rate-based method. The results for both methods are shown in Table 12. The results obtained from the real-time estimation method are practically equal to those generated using the MOVES software with errors less than 0.001%. The small error is likely due to the MOVES algorithm mostly consisting of multiplying various values together. Pre-multiplying these factors should not cause a big difference in the results. The process is also much faster, since it only requires multiplying the input values by a few factors. A large dataset that normally takes hours to process can be process in a few minutes.

Table 12: Comparison of Real-Time Emission Estimates with MOVES Generated Emission Estimates

linkID	pollutantID	processID	sourceTypeID	MOVES Generated Emission Estimates	Real-Time Calculated Emission Estimates	Error
1	1	1	21	197.45	197.449988	-0.000006%
1	5	1	21	24.9094	24.90937355	-0.000106%
1	5	15	21	0.325275	0.325275389	0.000120%
1	6	1	21	2.50384	2.50384	0.000000%
1	90	1	21	869946	869946.51	0.000059%
1	91	1	21	12102600000	12102596600	-0.000028%
1	1	1	42	360.725	360.7247075	-0.000081%
1	5	1	42	36.3234	36.323382	-0.000050%
1	5	15	42	0.0320243	0.032024345	0.000141%
1	6	1	42	1.86278	1.8627825	0.000134%
1	90	1	42	3024710	3024714.295	0.000142%
1	91	1	42	41085100000	41085116175	0.000039%
1	1	1	52	314.313	314.312949	-0.000016%
1	5	1	52	16.3821	16.3820951	-0.000030%
1	5	15	52	0.068828	0.068827842	-0.000230%
1	6	1	52	1.77858	1.77858	0.000000%
1	90	1	52	1170130	1170135.035	0.000430%
1	91	1	52	16012100000	16012090000	-0.000062%
1	1	1	61	64.8381	64.838117	0.000026%
1	5	1	61	8.54957	8.5495574	-0.000147%
1	5	15	61	0.00483098	0.004830987	0.000145%
1	6	1	61	0.413891	0.413891	0.000000%
1	90	1	61	734323	734323.2245	0.000031%
1	91	1	61	9968950000	9968948900	-0.000011%

Chapter 4 Results

4.1 Example of Reconstructed Trajectories

One of the key components of our proposed emission estimation method described previously is the reconstruction of vehicle trajectories based on presence detection data of individual vehicles at multiple locations when passing an intersection or a corridor. As a result, our first analysis of the results from the simulation experiments is to compare the time-space diagrams of the vehicle trajectories from the reconstructed versus the original trajectories from the simulation. Figure 24 shows an example of the comparative trajectories in which the original simulated trajectories are shown as green lines, the simulated detector data is shown in pink at the positions where detection is specified, and the reconstructed trajectories are plotted in orange on top of the original trajectories. The reconstructed trajectories were discretized into second-by-second numerical data for emission modelling. The discretization is plotted in black points. Each point, plotted in space and time, is associated with an instantaneous speed and acceleration. Further extrapolations of the trajectories beyond the detectors are only shown in terms of the discretized points.

As shown in Figure 24, for most cases, the reconstructed trajectories closely resemble the originally simulated trajectories. However, there are cases where the reconstruction algorithm fails to identify the actions taken or makes the wrong assumption. There are also cases where the reconstruction algorithm is not able to model the vehicle behaviour as it does not fall clearly into any of the categories of driving behaviours modelled. Examples of these cases are circled in red.

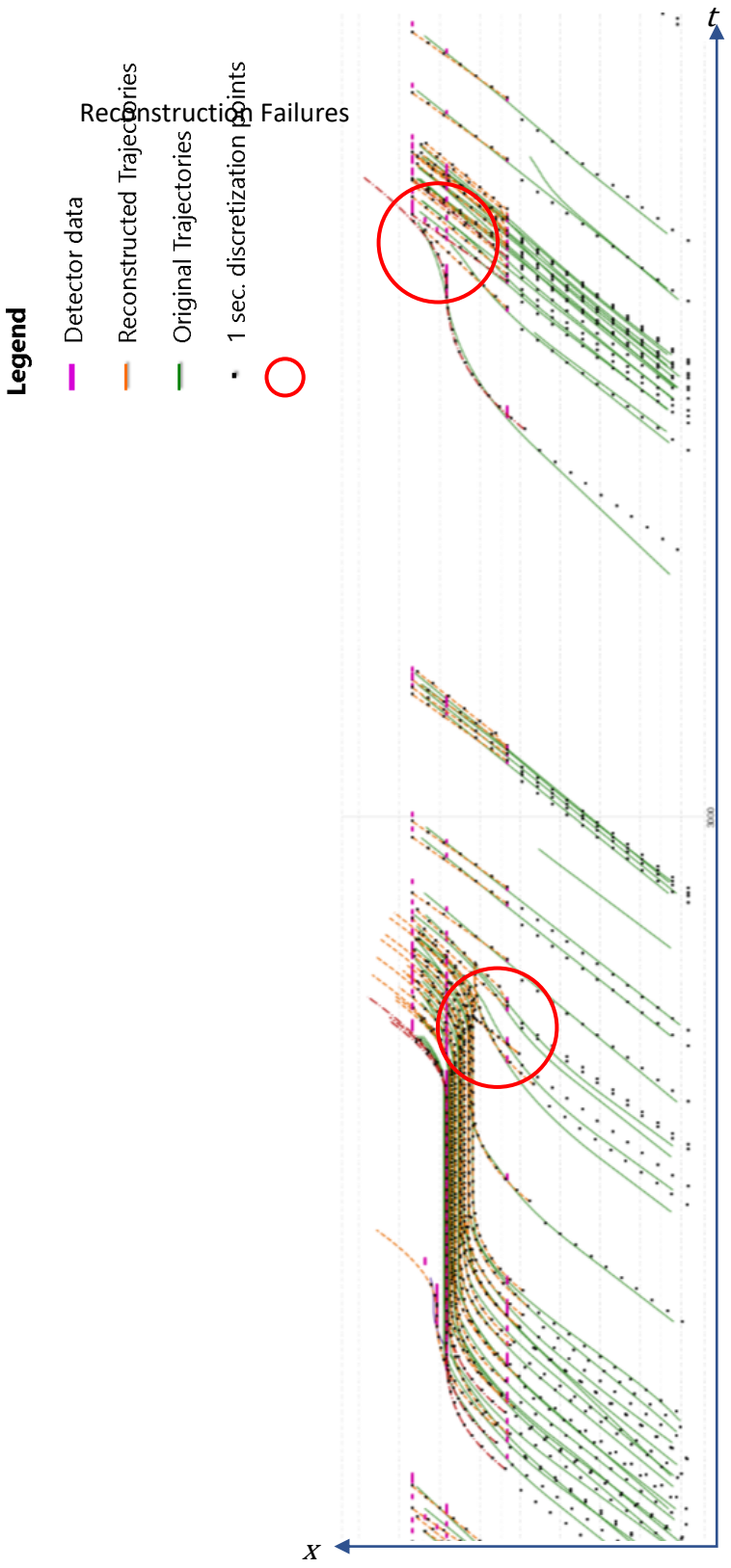

Figure 24: Sample Trajectories: Original vs. Reconstructed

4.2 Emission Rates for Real-Time Calculations

The second important component of our proposed method is the emission rates of different emission types that were generated from MOVES for real-time calculations. Emission rates are provided for each operating mode. Descriptions of the operating modes are provided in Table 13, summarized from the MOVES outputs in Appendix A – Operating Mode Bins. As shown in Figure 25, for carbon dioxide emissions, the rates gradually increase as VSP and speed increase. The rates are very low for braking and idling in comparison to other driving modes. Passenger cars emit far less carbon dioxide than the heavier vehicle types. On the contrary, the emission rates for nitrous oxide are constant across operating modes, as shown in Figure 26, and only differ by vehicle type, suggesting that they are dependent on factors other than speed and power. Single Unit Trucks emit far more nitrous oxide than the other vehicle types. For methane, different rates are required for tailpipe and crankcase emissions. Figure 27 shows that heavy vehicles emit relatively constant rates of methane in most operating modes, with braking and idling modes emitting less; however, the contrast is not as stark as that of carbon dioxide. Passenger cars actually emit slightly more methane in the braking mode than some other modes and have a sharper climb in rates towards the higher VSP modes. Figure 28 shows that Single Unit Trucks and Passenger Cars have some of the highest rates of crankcase methane emission, especially at higher VSP modes.

Table 13: Operating Mode Descriptions

Mode	0	1	11	12	13	14	15	16	21	22	23	24	25	27	28	29	30	33	35	37	38	39	40
Description	Braking (<-2 mph/s)	Idling	Coasting	Cruise/Acceleration	Cruise/Acceleration	Cruise/Acceleration	Cruise/Acceleration	Cruise/Acceleration	Coasting	Cruise/Acceleration	Cruise/Acceleration	Cruise/Acceleration	Cruise/Acceleration	Cruise/Acceleration	Cruise/Acceleration	Cruise/Acceleration	Cruise/Acceleration	Cruise/Acceleration	Cruise/Acceleration	Cruise/Acceleration	Cruise/Acceleration	Cruise/Acceleration	Cruise/Acceleration
Speed [mph]	–	-1 – 1	1 – 25						25 – 50									> 50					
VSP [kW/t]	–	–	< 0	0 – 3	3 – 6	6 – 9	9 – 12	> 12	< 0	0 – 3	3 – 6	6 – 9	9 – 12	12 – 18	18 – 24	24 – 30	> 30	< 6	6 – 12	12 – 18	18 – 24	24 – 30	> 30

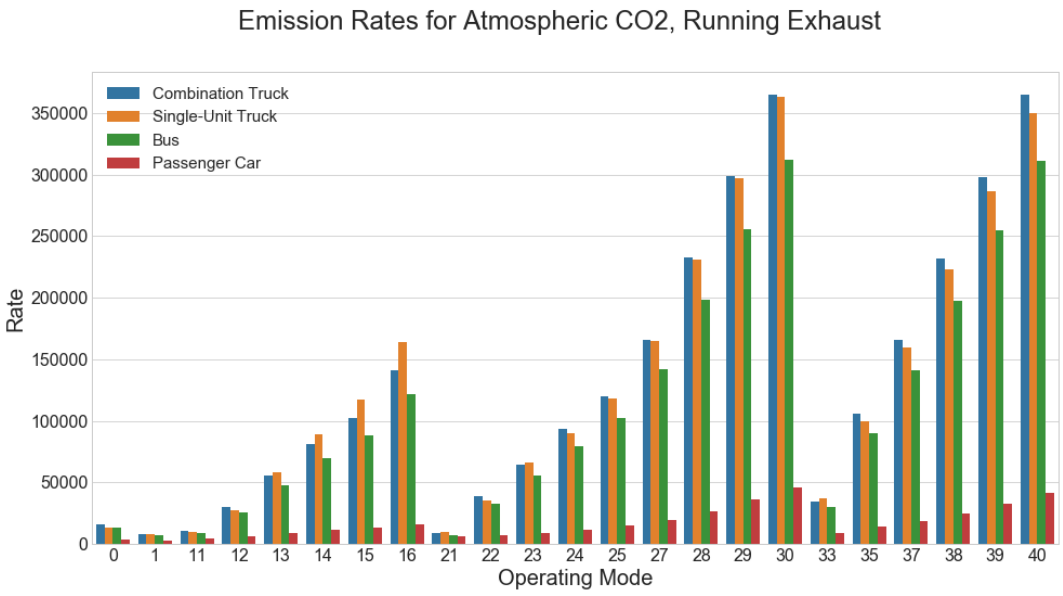

Figure 25: Emission Rates for Carbon Dioxide due to Running Exhaust

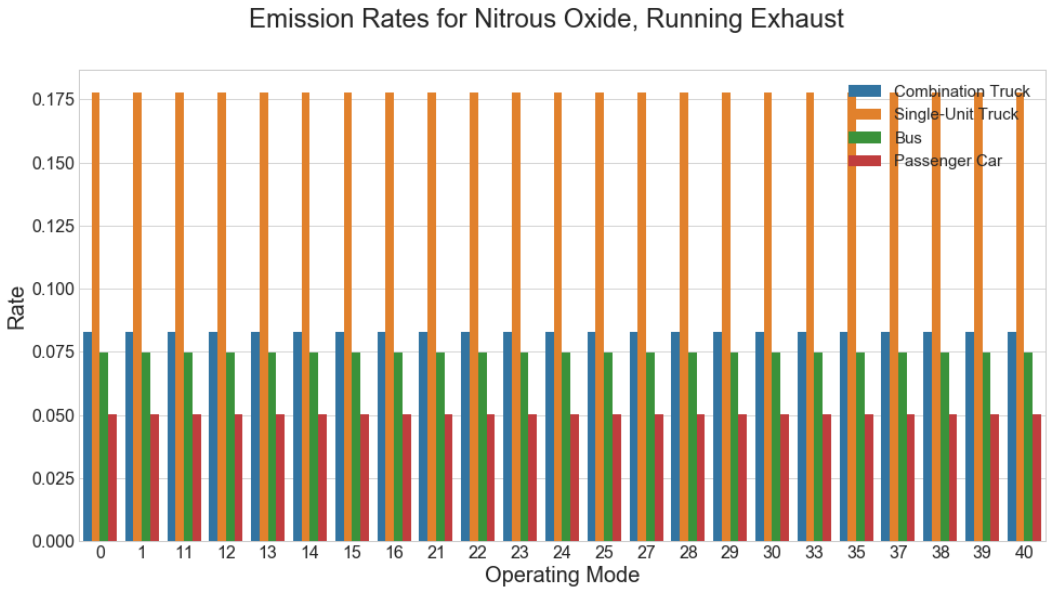

Figure 26: Emission Rates for Nitrous Oxide due to Running Exhaust

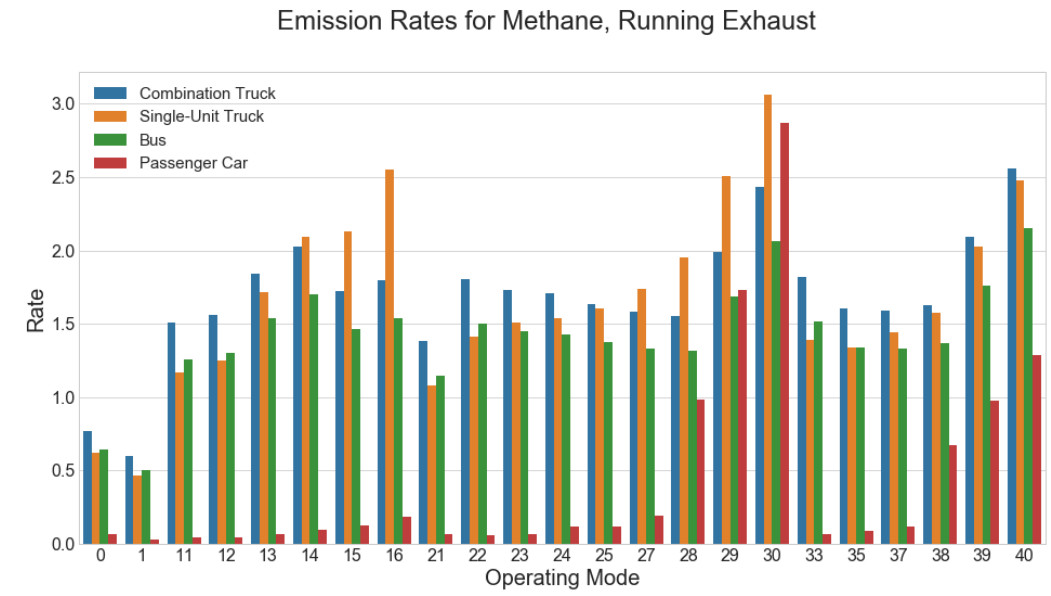

Figure 27: Emission Rates for Methane due to Running Exhaust

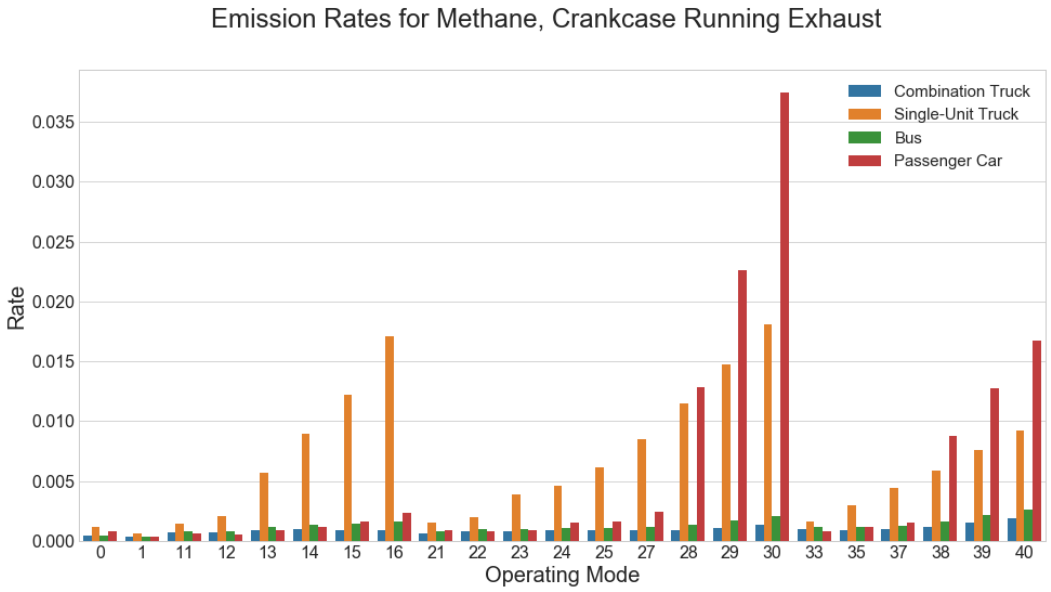

Figure 28: Emission Rates for Methane due to Crankcase Running Exhaust

4.3 Model Evaluation and Sensitivity Analysis

As shown in **Error! Reference source not found.** in the previous section, the MOVES rates generated w ere able to produce emission estimates within a negligible error margin. As a result, the differences between emissions estimated through the proposed method and through simulations come from the trajectory reconstruction process alone. This section discusses how well the trajectory reconstruction performs. To evaluate the adequacy of the trajectory reconstruction method, the emissions calculated using the reconstructed trajectories were compared to the emissions calculated using the simulated trajectories using a "relative difference" measure defined as

$$\Delta_{\%} = \frac{E_{reconstructed} - E_{original}}{E_{original}}$$

where

$\Delta_{\%}$ is the relative difference [%];

$E_{reconstructed}$ is the emission quantity estimated from the reconstructed trajectories;

$E_{original}$ is the emission quantity estimated from the originally simulated trajectories.

This section pertains to the trajectory reconstruction method that uses acceleration. The alternative trajectory reconstruction method that only uses average speeds is evaluated in section 4.4. First, the overall performance of the model in the field conditions is evaluated in section 0. Then, the subsequent sections investigate the effects of changing different parameters in the traffic network.

Emissions estimates were disaggregated at the level of individual lanes and signal cycles. In each analysis, unless specified otherwise, one data point represents the emissions of one pollutant from all vehicles of one type of vehicles passing through one lane during one cycle.

4.3.1 Performance in Field Conditions

The performance of the trajectory reconstruction method applied to the field conditions (described in section 3.1.4.1) were investigated on an hourly basis. Firstly, the emissions from the simulated trajectories of the field conditions are explained in section 0. Again, each point represents all vehicles of one type crossing a lane at one intersection approach during one signal cycle. Then comparisons were made between the emissions from the simulated and reconstructed trajectories in section 4.3.1.2.

4.3.1.1 Characteristics of the Simulated Trajectory Emissions

First, the distribution of emission estimates for field conditions by lane, movement, and hour are examined. The emission estimates from the originally simulated trajectories are shown for all vehicle types and pollutants in Appendix H – Emissions from Simulated Trajectories of Field Conditions. For the

passenger cars, there are generally more emissions produced for thru movements than left-turns, likely due to higher volumes of thru movements. For single-unit trucks, however, the dominating movement in terms of emissions produced depends on the hour. For combination trucks and transit buses, thru movements do not dominate emission production for any period. The periods having the greatest amounts of emission are the afternoon peak hours from 15:00-18:00 for passenger cars, and there is less contrast between the periods for other vehicle types. For all periods, there are far greater sample points for passenger cars due to all lanes and cycles having passenger cars, whereas other vehicle types may not be observed at every lane during every cycle. However, the quantities of emissions from other vehicle types tend to be greater in magnitude due to their mass.

There is a noticeable discretization in a large portion of the nitrous oxide quantities for passenger cars, as shown in Appendix H – Emissions from Simulated Trajectories of Field Conditions. This is most likely due to the constant emission rates of nitrous oxide across all operating modes as shown in Figure 26. For lane and cycle vehicle groups consisting of all passenger cars, the nitrous oxide emission rate would be applied to a whole number volume. This occurs frequently for passenger cars, whereas it is rare for all vehicles of one lane over an entire cycle to be only consisted of any other vehicle type. Thus, the emission quantities of other vehicle types do not exhibit this pattern.

4.3.1.2 Comparison of Emissions between Simulated and Reconstructed Trajectories

Figure 29 to Figure 31 show the distribution of emissions calculated from the simulated and reconstructed trajectories. The lines in the violin plots represent the median and quartiles. Overall, the differences are within 10% except for methane for passenger cars and during a few hours of the day for carbon dioxide.

The estimates for nitrous oxide estimates have the lowest errors (Figure 30). This is no surprise as the nitrous oxide emission rates are constant across all operating modes as shown in Figure 26. Thus, there is less chance for variation.

Figure 31 shows that estimates for the methane emissions of passenger cars had rather high differences, which may be attributed to the emission rates used to calculate them. As seen in Section 4.2, the emission rates for most pollutant and vehicle types are relatively insignificant for operating modes 0 and 1 – braking and idling. However, for the case of methane emitted by passenger cars, the emission rates are rather high compared to many other modes. In this case, the modelling of deceleration behaviour and idling times becomes more important. Of the two, modelling deceleration behaviour is a more likely culprit for a source of error. It should be noted again that the deceleration functions used were calibrated to field data, which may differ from simulated trajectories.

To explore whether the modelling of deceleration is a significant source of error, the Operating Mode Distributions were compared in Figure 32. The distribution of the operating modes shows that the fractions for modes 0 and 1 are significantly different between the simulated and reconstructed trajectories, indicating that braking and idling modes were indeed modelled less accurately than other modes. Mode 23 is also relatively highly allocated. The high proportion of operating mode 23 may be the result of generalizing several driving modes, and perhaps some of the braking activities, as one

speed. The higher proportions of modes 0 and 1 in the morning and afternoon peak hours suggest these are the hours where stop-and-go traffic occurs the most as compared to the evening peak hours, likely due to higher levels of congestion.

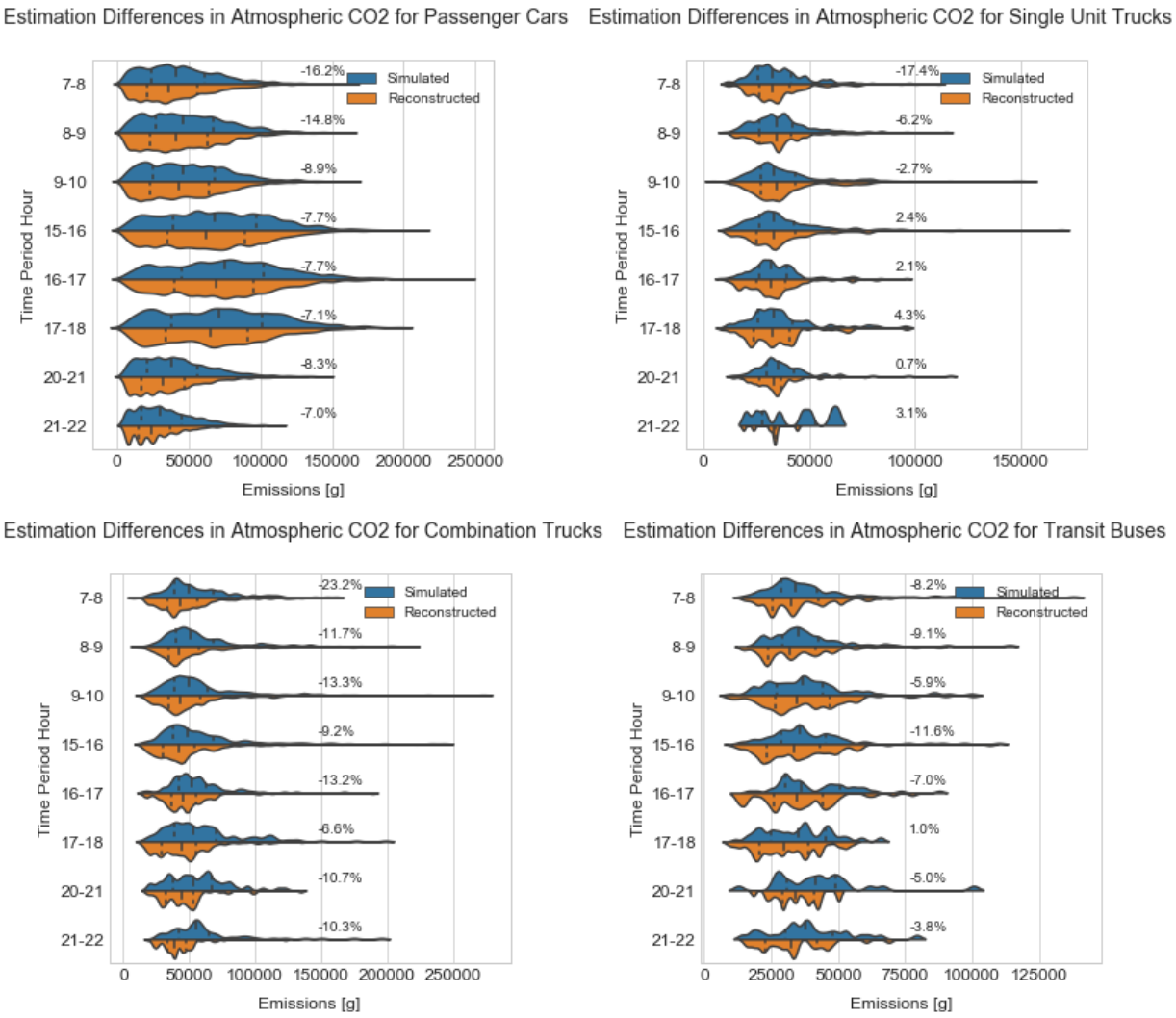

Figure 29: Performance Across Field Condition Hours for Carbon Dioxide

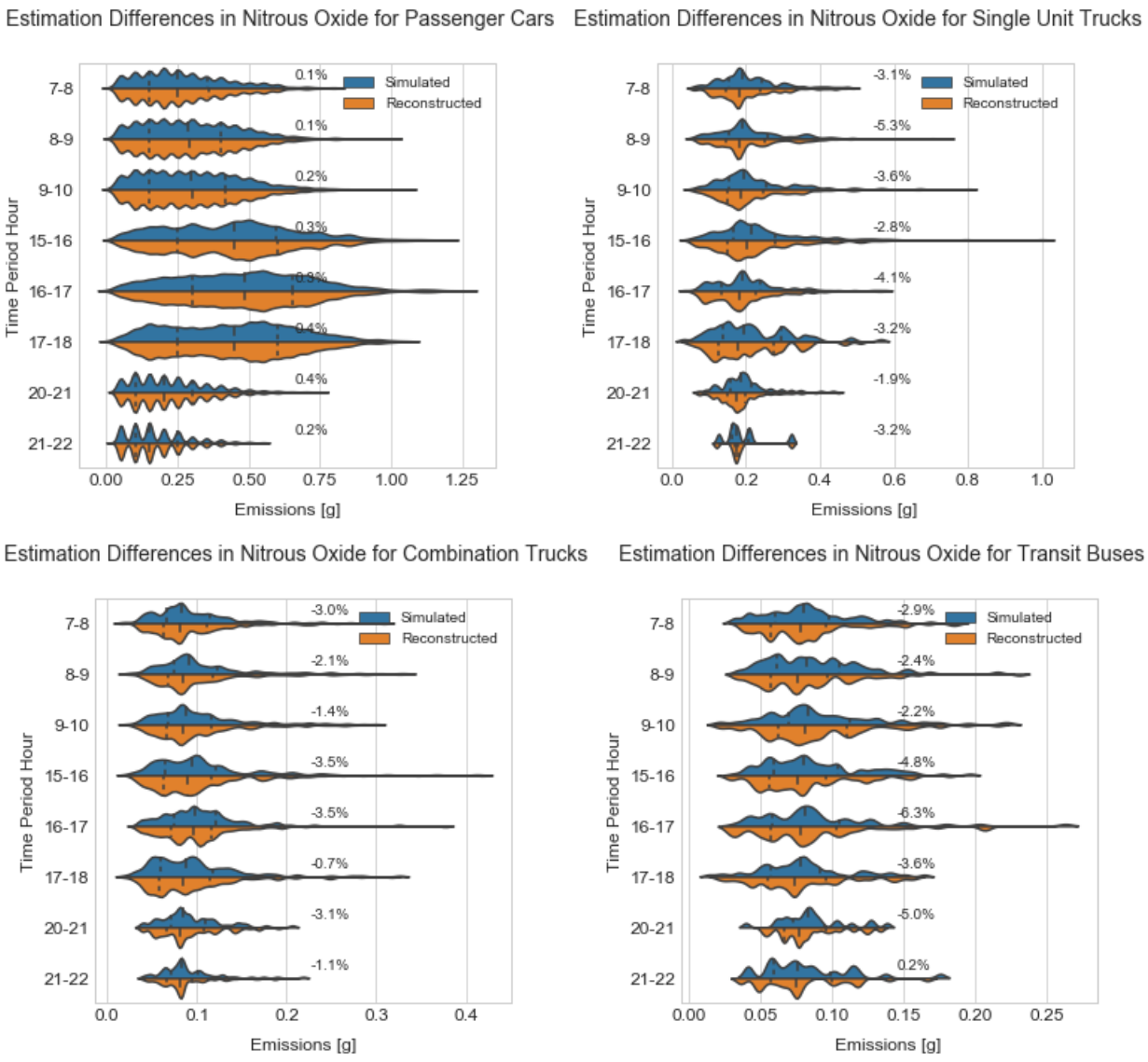

Figure 30: Performance Across Field Condition Hours for Nitrous Oxide

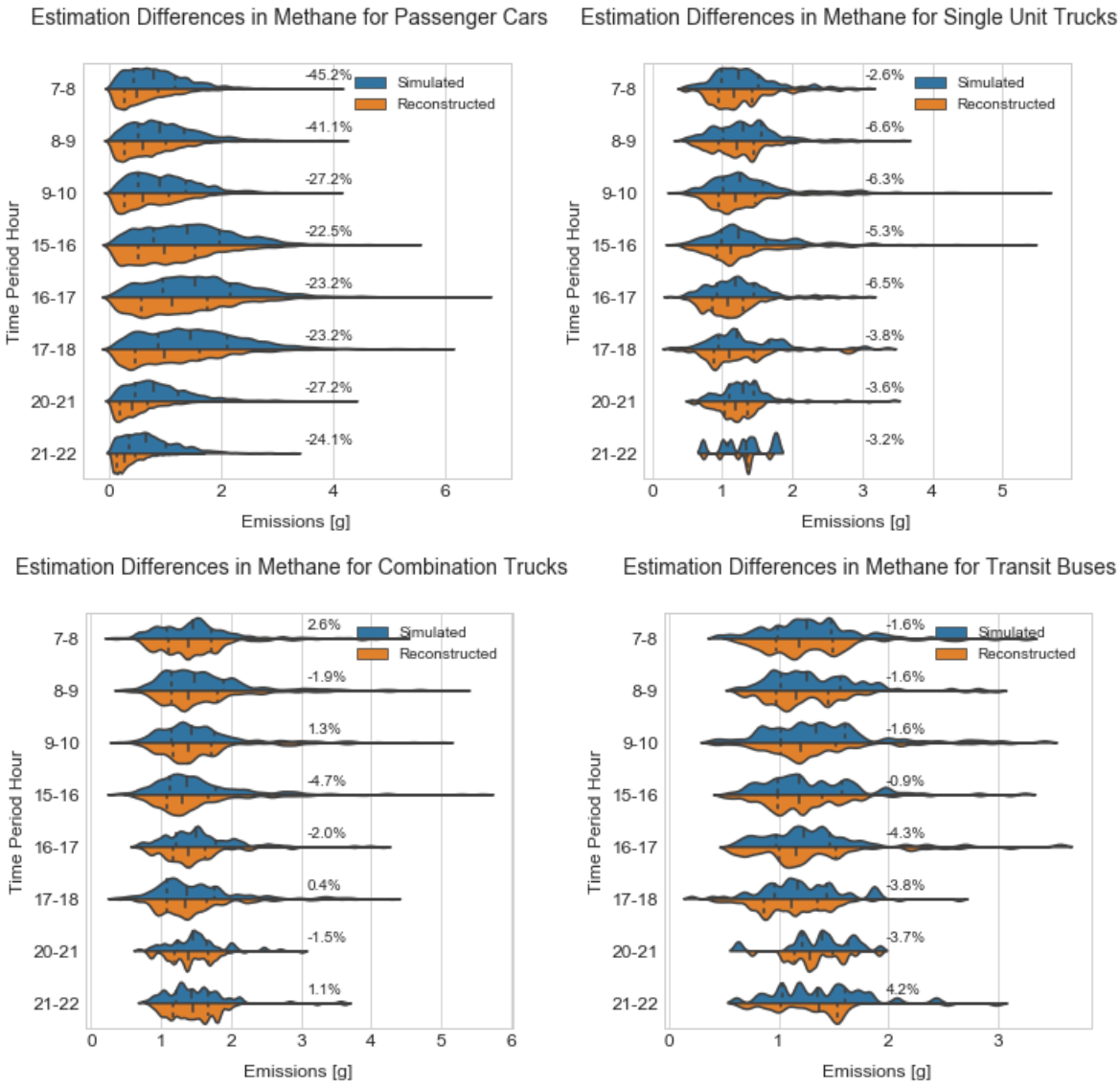

Figure 31: Performance Across Field Condition Hours for Methane

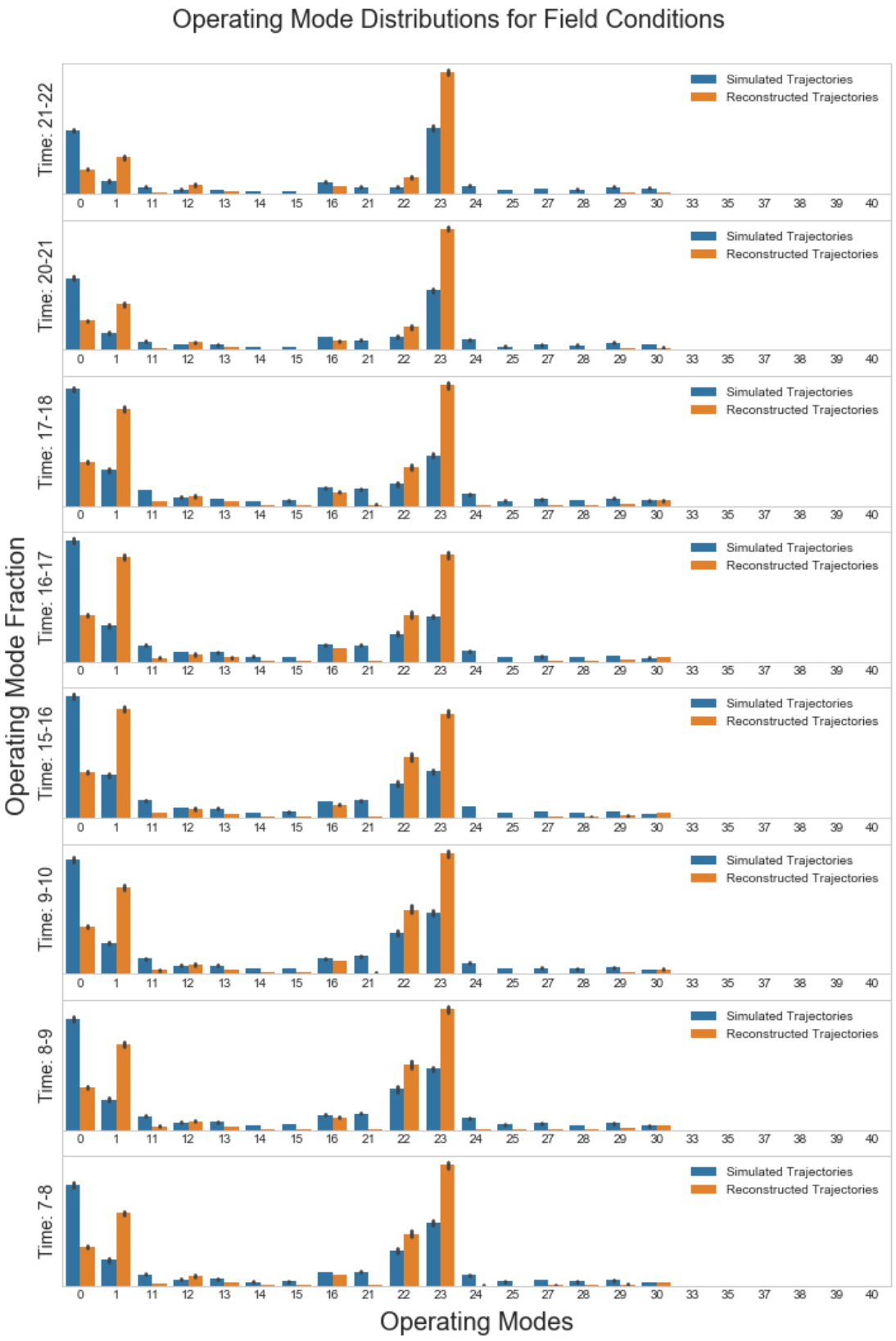

Figure 32: Operating Mode Distributions for Field Conditions

4.3.2 Effects of Detector Location and Volume Variations

As described in section 3.1.4.7, various advance detection locations were investigated to see their effects on the trajectory reconstruction process. The trajectory reconstruction using different advance detector locations were all performed on a dataset from the same Vissim simulation. The Vissim simulation was run using the model described in section 3.1.4.2 with gradually increasing vehicle input volumes. The only difference was the detector data selected. There were four sets of advance detectors placed: at 25m, 50m, 75m, and 100m setbacks.

Despite efforts to create a dataset of uniformly distributed volumes through gradually increasing input volumes, Figure 33 shows that the simulation created much more cycles with low volumes. This could be due to the stochasticity of the actuated signal phases or simply the stochasticity of the vehicle inputs. In addition, volumes in the higher end become less possible due to system capacity. For thru movements and thru shared with right-turn movements, there are very few cycles allowing 25 vehicles through. The left-turns were mostly capped off at 12 vehicles. At volumes of less than 25 veh/cycle and 13 veh/cycle for thru & right-turn and left-turn movements respectively, the sample size seems sufficient. Conducting this analysis using the volume variations simulation (described in section 3.1.4.2) also allows a comparison of the method performance across different volume levels.

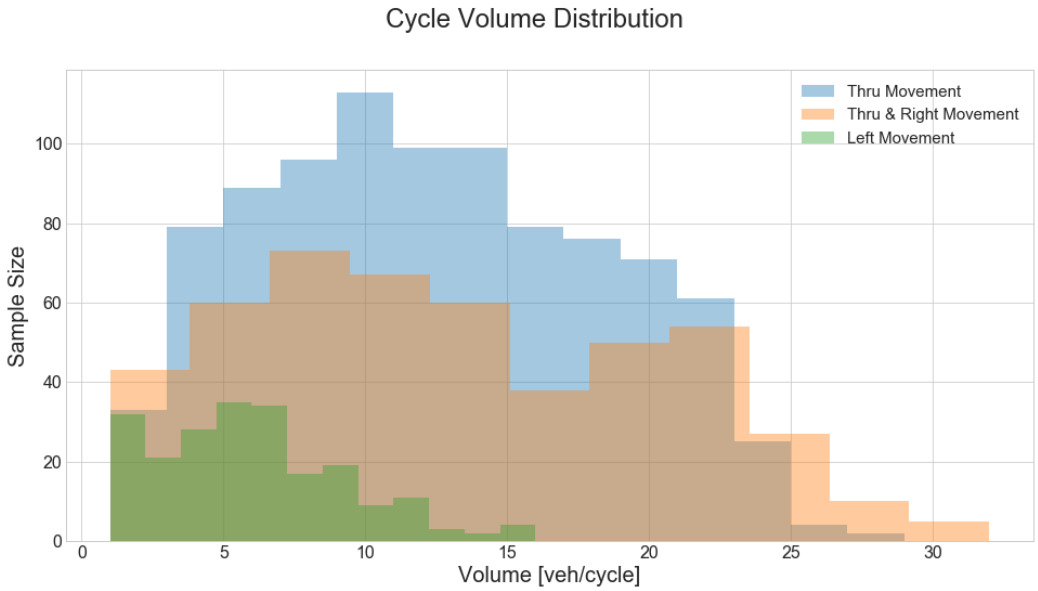

Figure 33: Cycle Volume Distribution in the Volume Variations Simulation Scenario

The estimation difference is correlated with the cycle volume, as shown in Figure 34, Figure 35, and Figure 36 bounded by shaded bands indicating the standard deviation. For all carbon dioxide and methane results, the relative differences of the emission estimates have a negative average for low volumes, meaning that emissions are underestimated. The estimation becomes more similar to those of the simulated trajectories for volumes in the mid-range of the observed volumes, that is, approximately

7-12 veh/cycle for left-turns and 10-20 veh/cycle for thru and thru shared with right-turn movements. For volumes in the high end of the observed range, the estimation becomes more variable, but this is likely just due to the higher ranges having smaller sample sizes as the system approaches capacity. For nitrous oxide estimates, the estimation difference does not change significantly over the range of different volumes. Again, this is likely due to nitrogen estimation having little to do with the trajectory reconstruction process.

For carbon dioxide estimates of passenger cars (Figure 34), using an advance detector location closer to the intersection consistently results in higher emission estimates than using further advance detector locations. This pattern is evident for the majority of the volume range. Since the estimation tends to become over-estimated for higher volumes and underestimated for lower volumes, the ideal detector location for carbon dioxide would depend on the expected volume of the intersection approach.

For estimating passenger car methane (Figure 35), the pattern observed with carbon dioxide is not constant across all turning movements. However, it can still be seen from the thru & right-turn movement figures that closer detectors result in higher estimates. The opposite is true for thru movements, but only for higher volumes. This inconsistency is likely due to the emission rates of braking modes being high for methane from passenger cars combined with the fact that the braking curve function is not calibrated to simulated braking behaviour.

For nitrous oxide (Figure 36), the detector location does not play a significant role as the emission quantity is not highly dependent on the trajectory. Furthermore, the estimates have very small differences to begin with, across all volume levels. This is not surprising considering that the emission rates output by MOVES were identical for all operating modes of the same vehicle type.

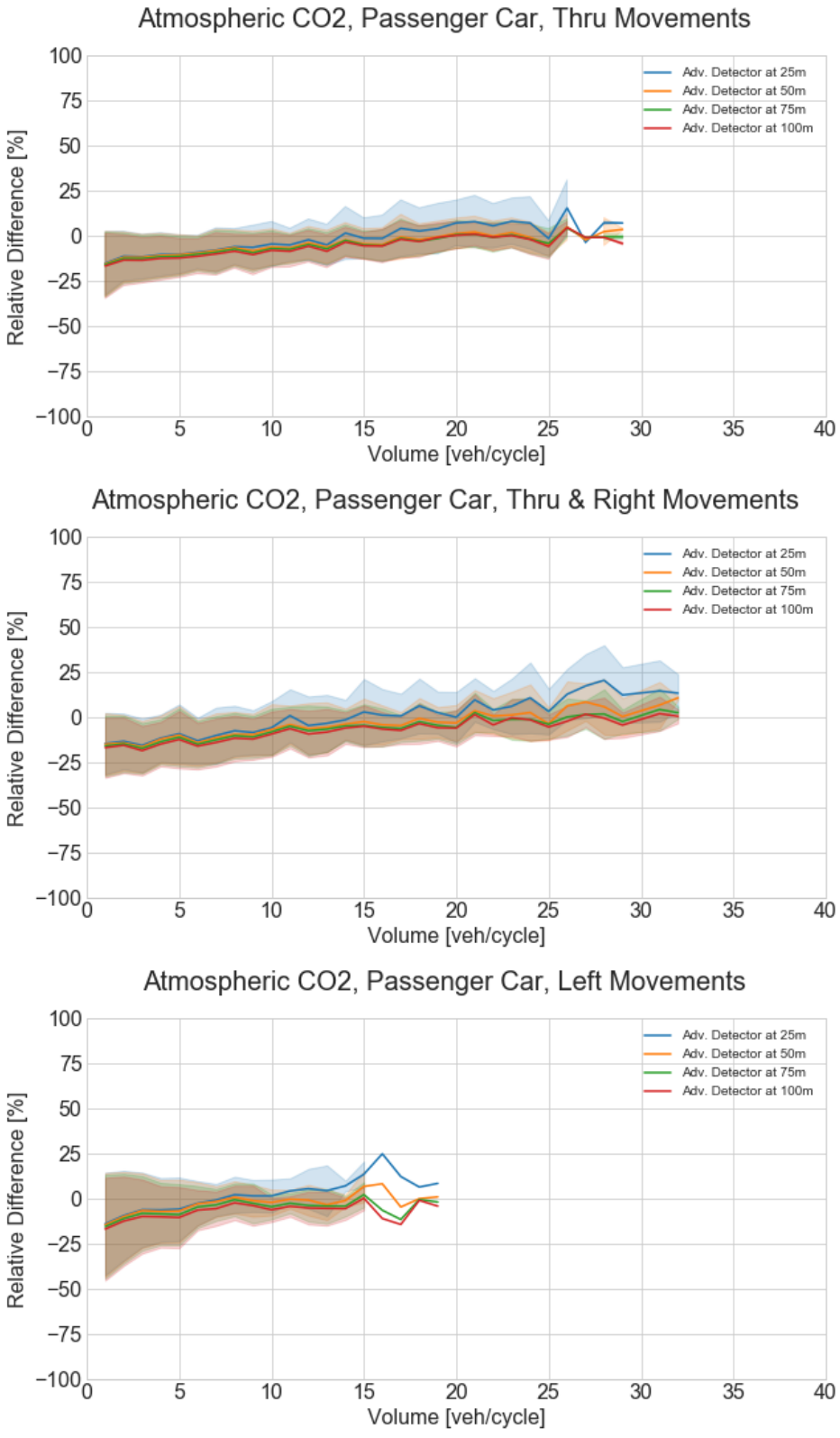

Figure 34: Performance Across Volumes and Detector Locations for CO_2 from Passenger Cars

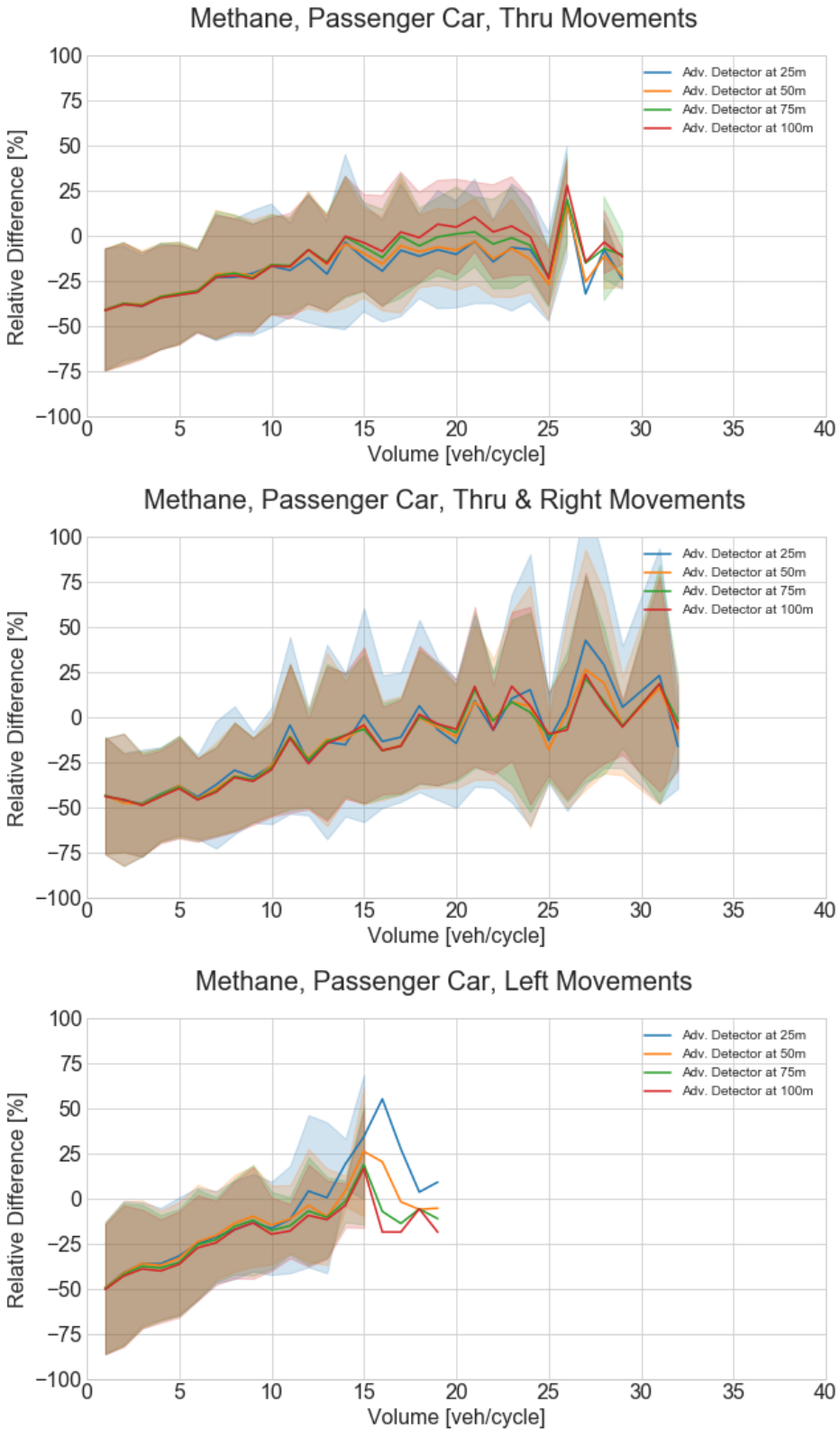

Figure 35: Performance Across Volumes and Detector Locations for CH_4 from Passenger Cars

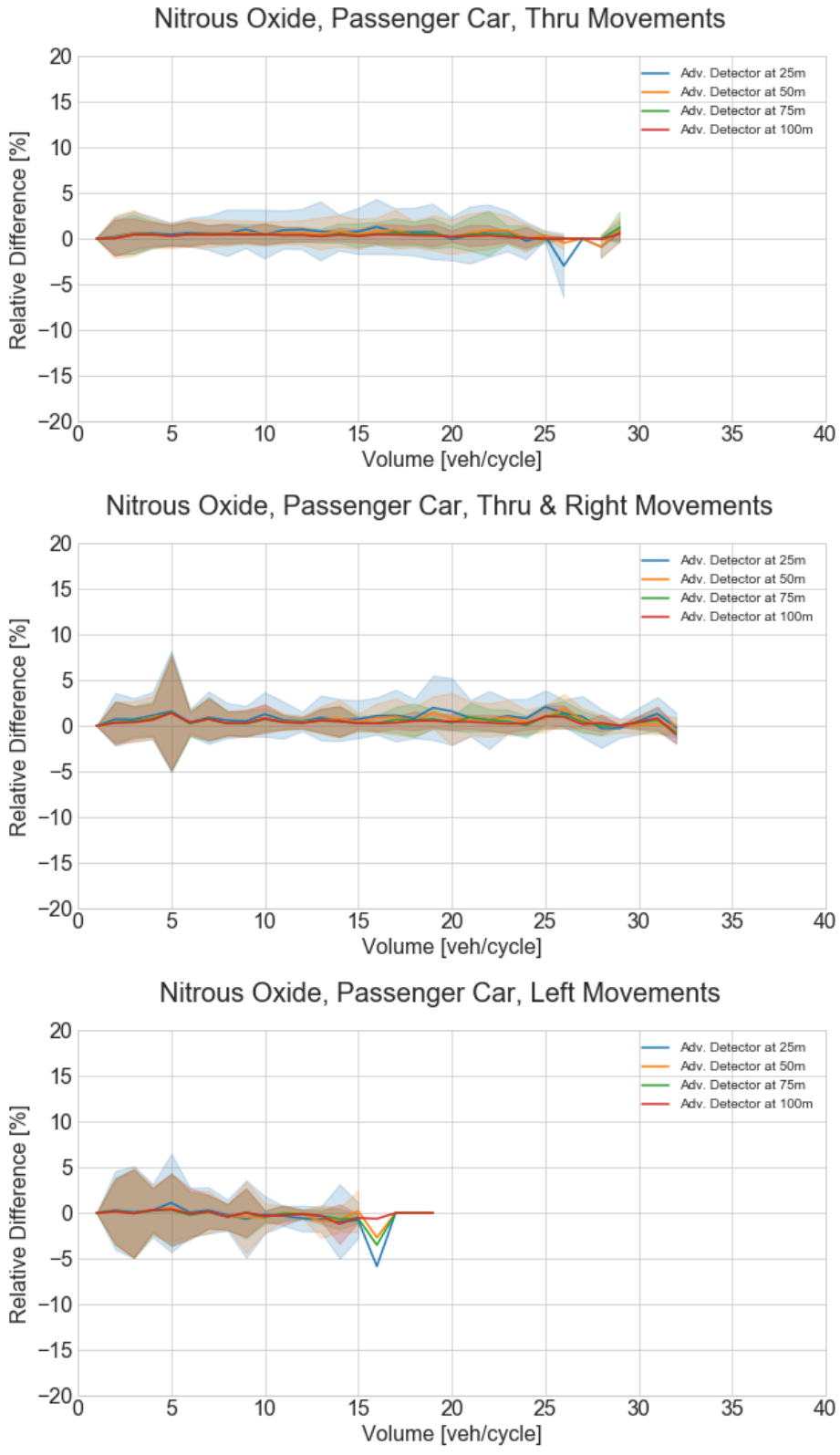

Figure 36: Performance Across Volumes and Detector Locations for NO_2 from Passenger Cars

The effects of detector location for single-unit trucks are shown in Figure 37 to Figure 39. Overall, the errors are larger and the patterns less consistent than those of passenger cars. As previously explained in section 4.3.1.2, higher differences should be expected for estimates regarding single-unit trucks, since the acceleration and deceleration modelling was focused on passenger cars. Furthermore, there is a low penetration of single-unit trucks in the volume variation simulations.

Despite the higher variability in the results, it can still be seen from the carbon dioxide estimates of left-turns (Figure 37) and the methane of thru and left-turns (Figure 38) that closer advance detector positions lead to higher estimates. The results of the remaining pollutant and movement combinations appear more random with less evident patterns in terms of performance due to different advance detector locations.

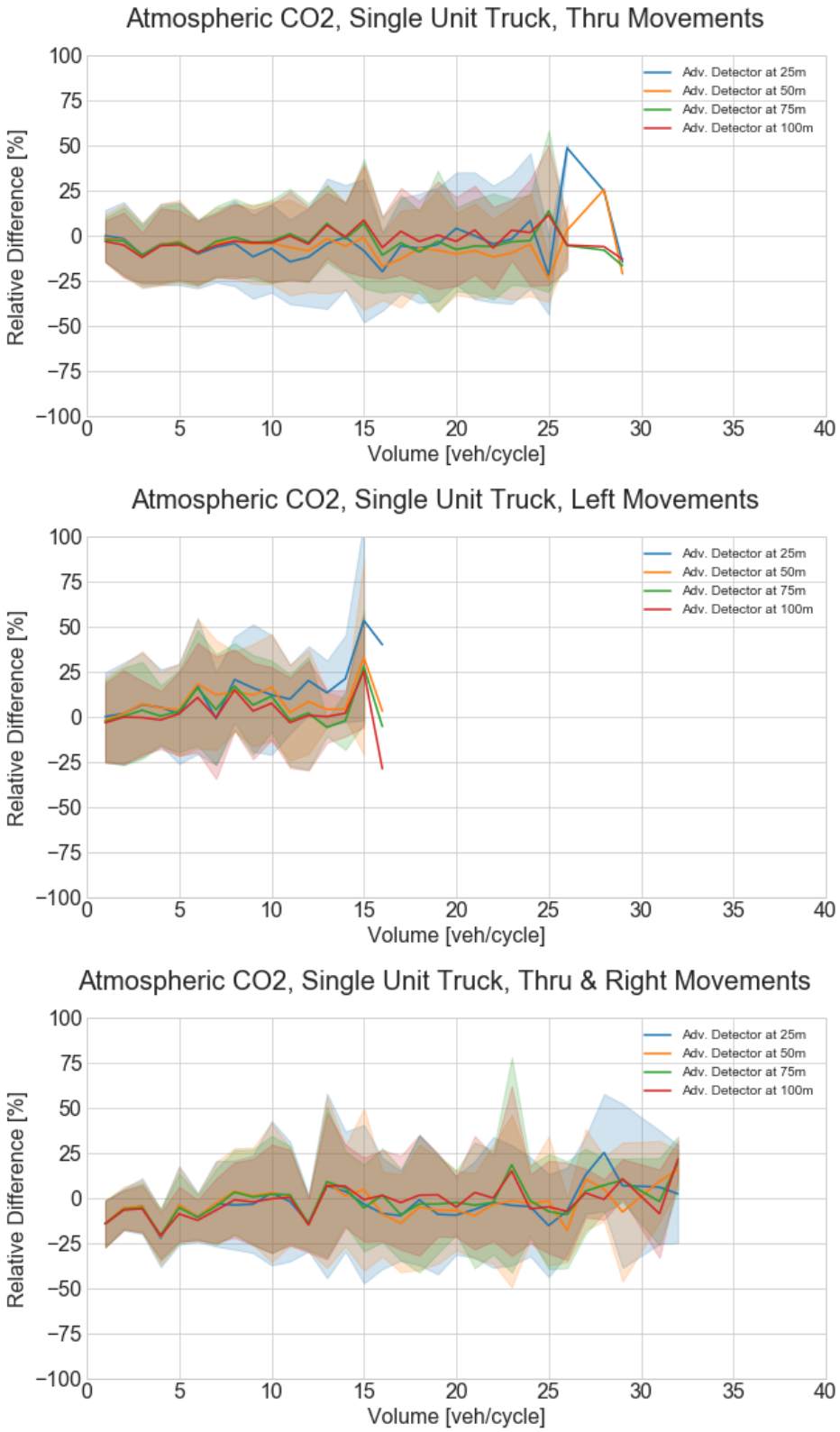

Figure 37: Performance Across Volumes and Detector Locations for CO_2 from Single-Unit Trucks

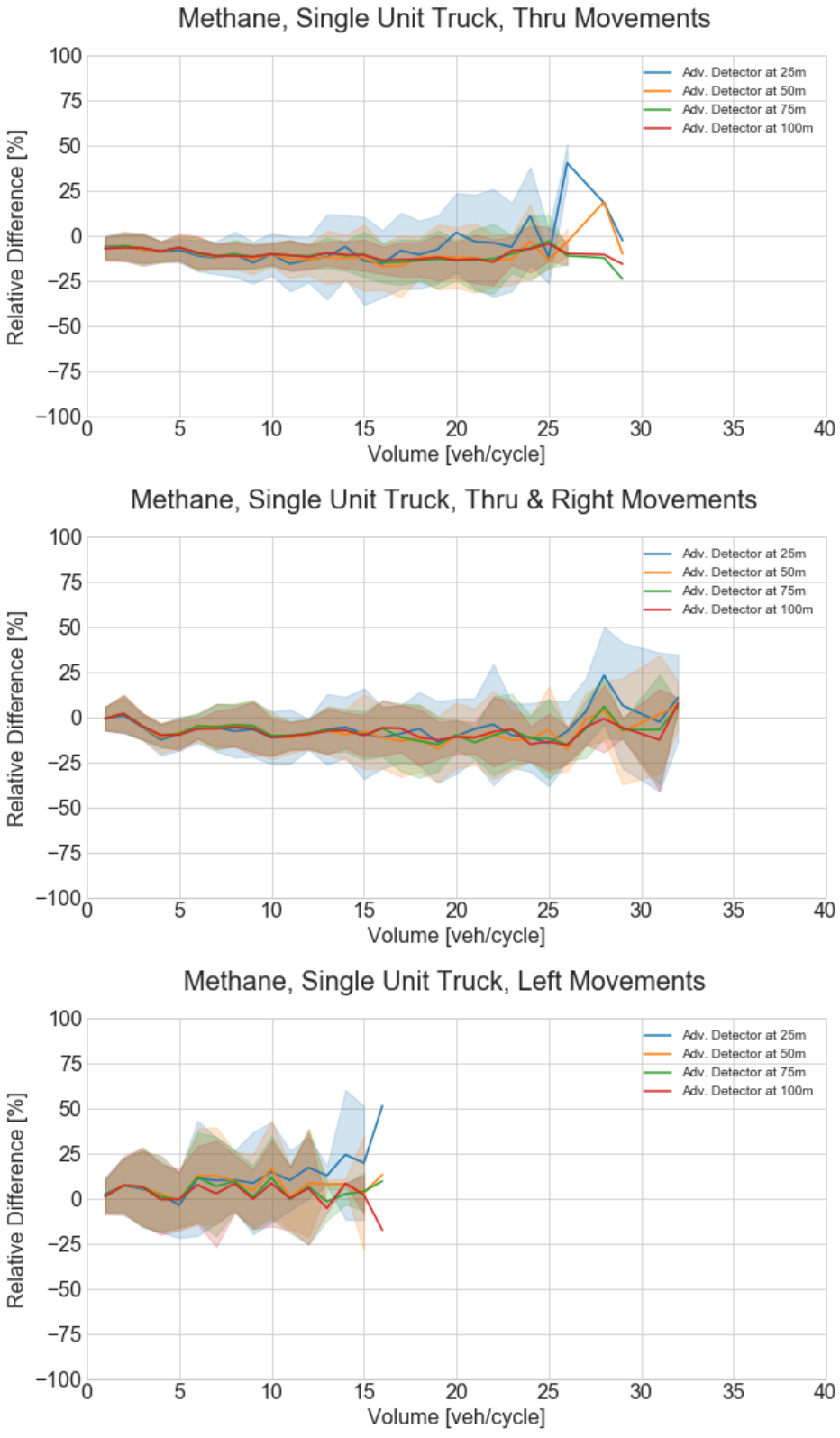

Figure 38: Performance Across Volumes and Detector Locations for CH_4 from Single-Unit Trucks

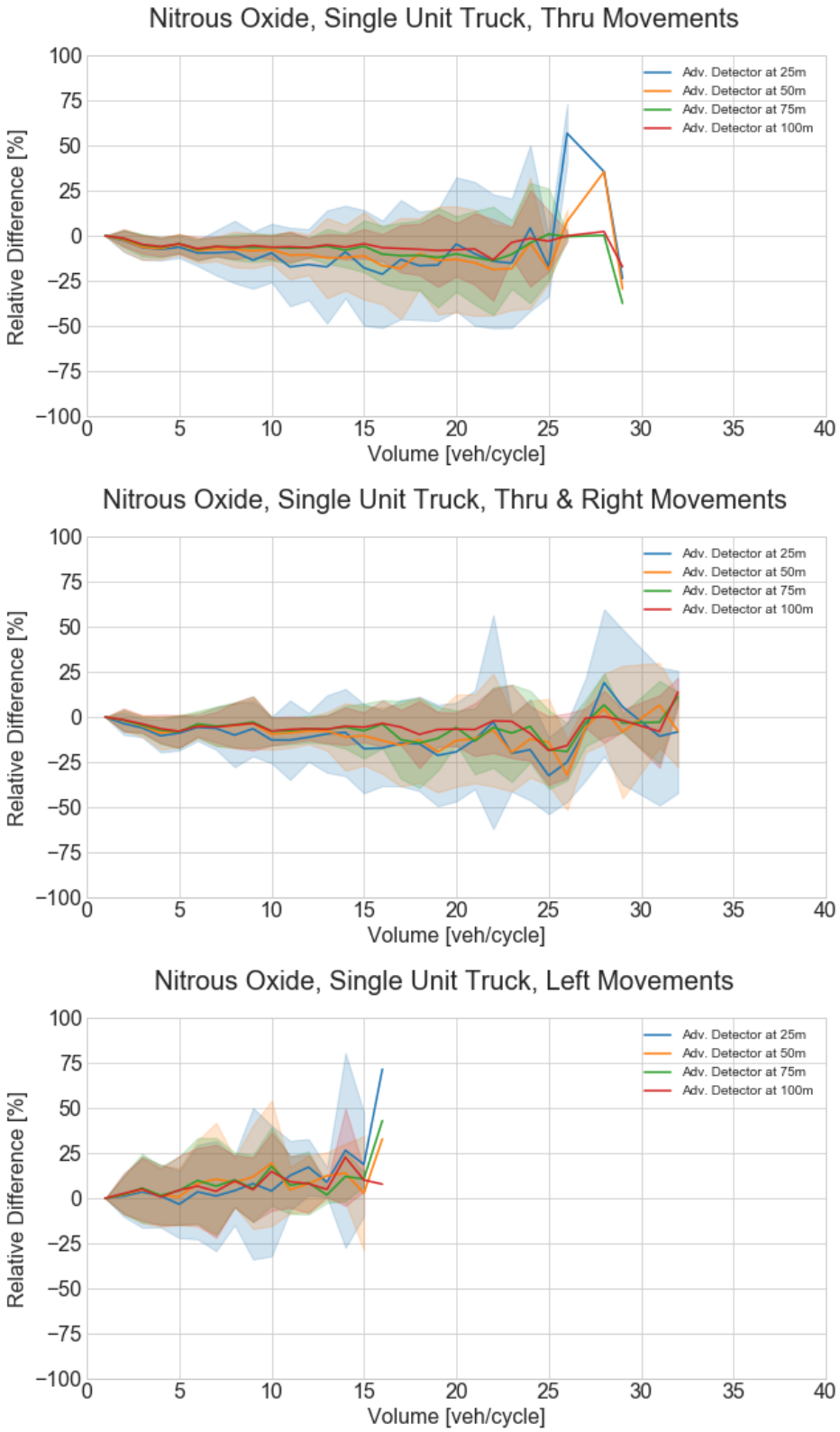

Figure 39: Performance Across Volumes and Detector Locations for NO_2 from Single-Unit Trucks

4.3.3 Effects of Aggregation

In the previous section, the performance of the proposed emission estimation method was evaluated using a highly disaggregate output measure, that is, emissions by vehicles on each individual lane over each signal cycle. However, depending on the focus of an emission estimation tool, it may be sufficient to have the emission estimates at a higher level of aggregation (e.g., total emissions by traffic passing a given intersection at an interval of more than one signal cycle). This section analyzes the effects of aggregation on the relative performance of the proposed method. In particular, we aggregated emission estimates first by approach, then by approach as well as over every 5 cycles – that is, emissions generated by vehicles on each approach of an intersection over every 5-cycle interval were summed up. This analysis was performed on the same dataset as the previous section, i.e. the volume variations simulation. To find aggregated results, the emissions from the simulated and reconstructed trajectories were first aggregated. Then, the relative difference was found using the aggregated emission estimates. The relative differences across different levels of aggregation over a range of volumes are illustrated in Figure 40 and Figure 41.

For all vehicle types and pollutants, the level of aggregation yields more precise estimates. That is, there is less variation in the range of possible estimates generated if results are aggregated at a higher level. However, the accuracy does not necessarily improve. Aggregating the reconstructed results do not necessarily bring them closer to the simulated results.

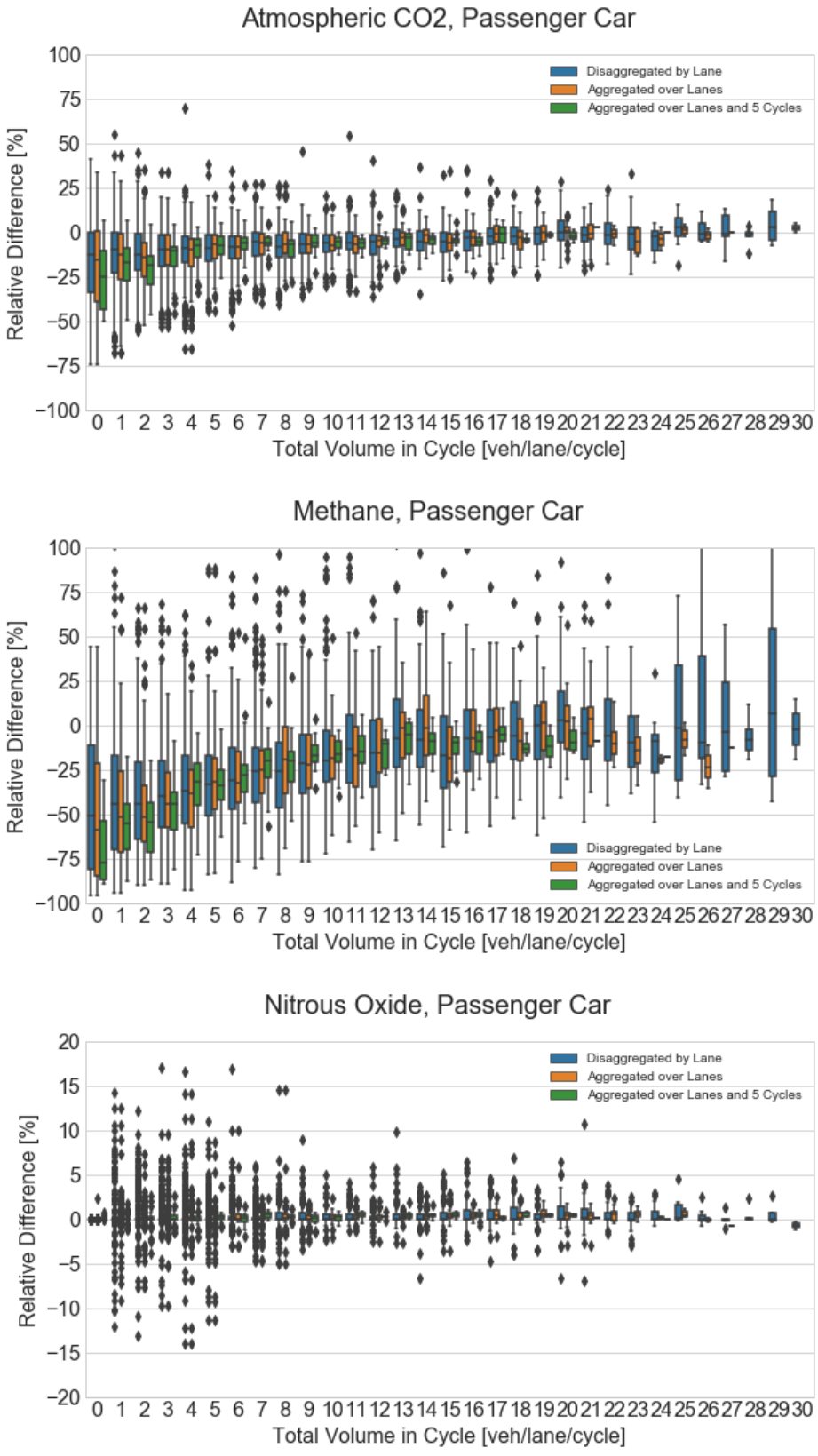

Figure 40: Performance Across Levels of Aggregation for Passenger Cars

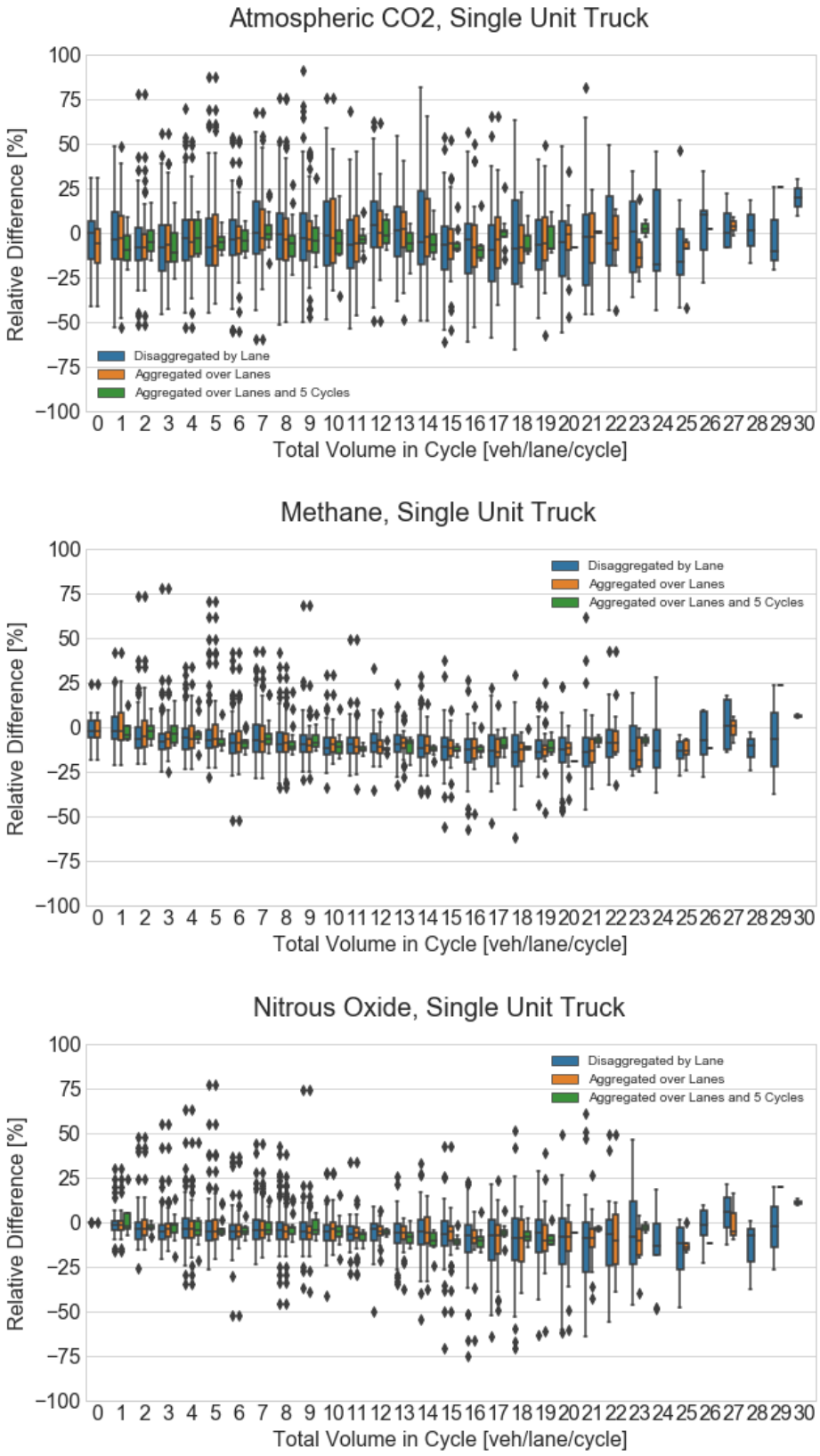

Figure 41: Performance Across Levels of Aggregation for Single Unit Trucks

4.3.4 Effects of Heavy-Duty Vehicle Penetration

To investigate the effects of heavy-duty vehicle penetration, a simulation was run with varying proportions of single-unit truck inputs, as described in section 3.1.4.3. Figure 42 shows the estimation differences of the trucks and passenger cars as the truck penetration levels increase. There is no significant change in the estimation differences for both vehicle types for all pollutants. A slight increase in the passenger car methane and nitrous oxide estimates is observed but is relatively insignificant. This indicates that changes in the vehicle type distribution does not significantly impact the performance of the trajectory reconstruction method.

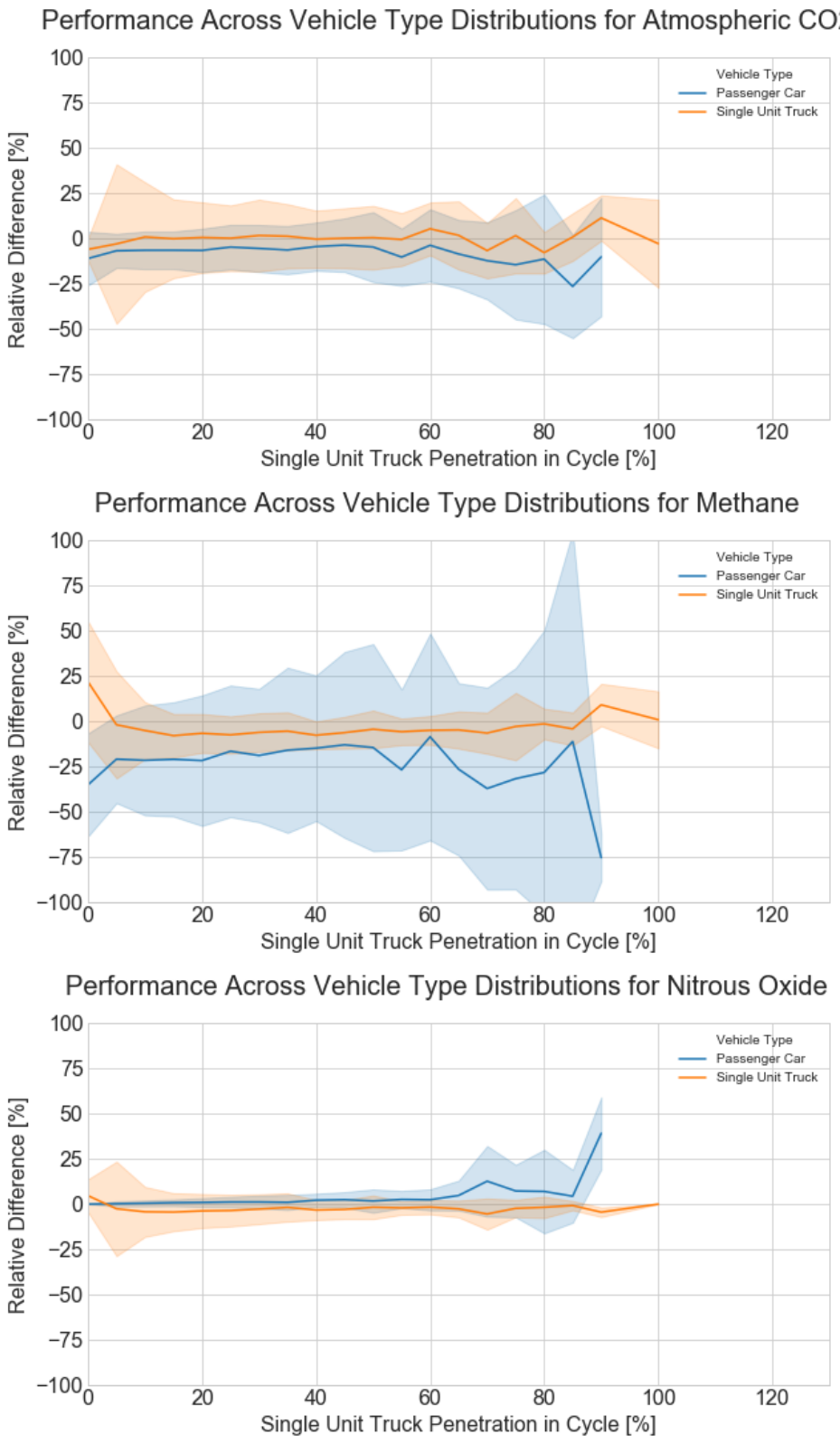

Figure 42: Effects of Truck Penetration

4.3.5 Effects of Signal Timing Variation for Thru Movements

As described in Section 1.4, one of the key requirements for a reliable emission estimation model is its ability to capture of the effects that are expected from a traffic management scheme such as signal timing. In this section, we first investigate how well the proposed method is able to capture the emission effect due to changes in signal timing at a single intersection. In order to simulate such signal timing alternations, the thru green interval of the major direction in the simulated signalized intersections described previously was set to vary from 30s to 65s at 5s intervals while keeping all other intervals unchanged, as described in Section 3.1.4.5.

To investigate the effects of signal timing changes, the emissions are aggregated over time intervals of 500s rather than compared on a per-cycle basis, since signal timing changes also change cycle lengths. Only vehicles making thru movements are included. Figure 43 and Figure 44 show the changes in the emissions per 500s time interval while Figure 45 and Figure 46 show the changes in the emissions per vehicle. The shaded regions in the line plots represent the standard variation.

Both vehicle types exhibit a slight decrease in carbon dioxide and methane production as the thru green phase is lengthened in Figure 43 and Figure 44, with passenger cars experiencing more of a decrease. The per-vehicle results in Figure 45 and Figure 46 show a similar pattern. This is expected, because the emissions produced by the vehicles of a movement should drop as its green phase is lengthened due to less frequent stopping and accelerating. The nitrous oxide emissions, however, hardly change over different signal interval lengths, since its emission rates are not sensitive to different operating modes.

In terms of the trajectory reconstruction performance, the emissions are consistently underestimated, especially for methane. However, the overall trend is captured, so the relative differences due to phase length changes can still be captured.

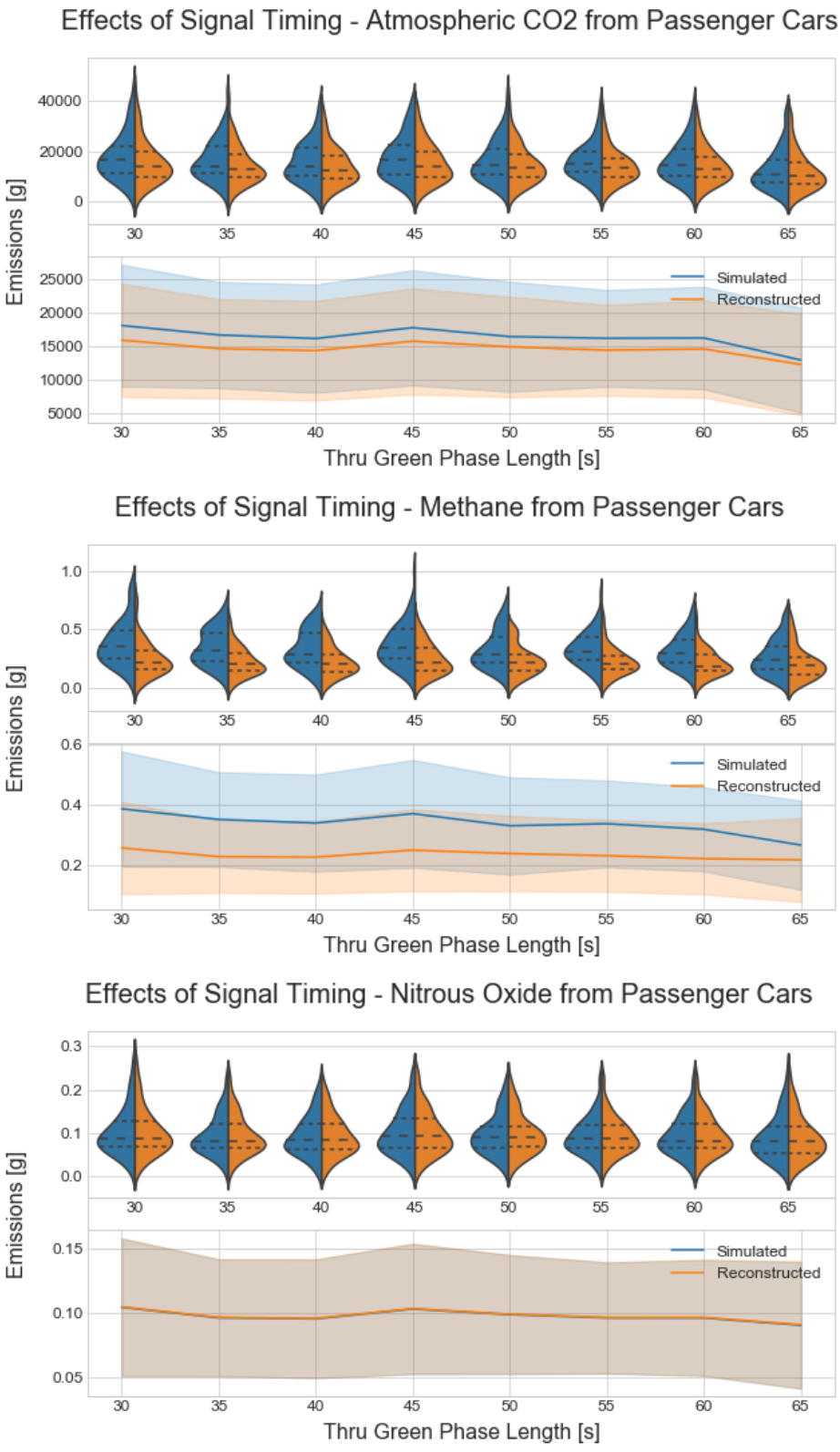

Figure 43: Effects of Signal Timing for Passenger Cars – Thru Movements Only

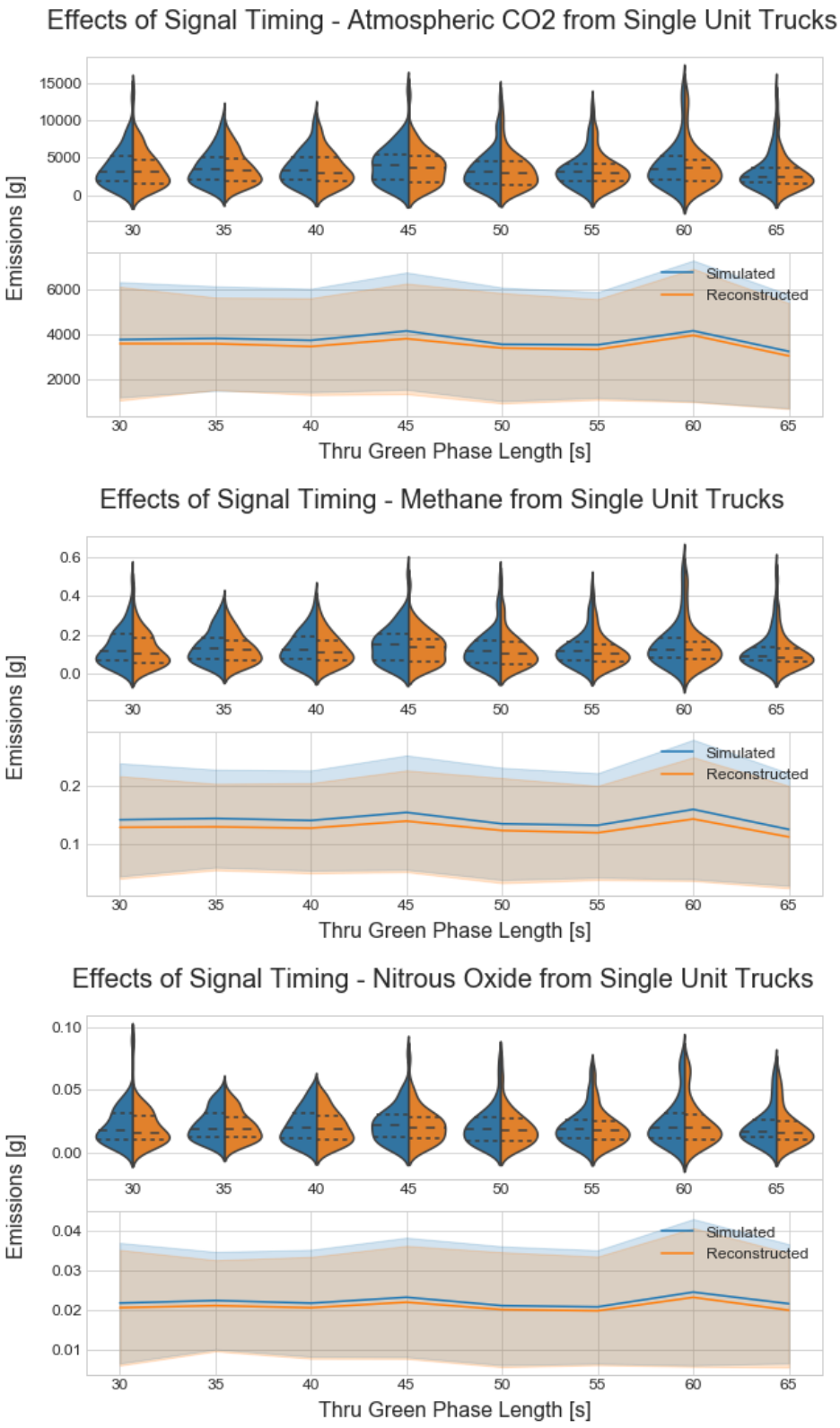

Figure 44: Effects of Signal Timing for Single-Unit-Trucks – Thru Movements Only

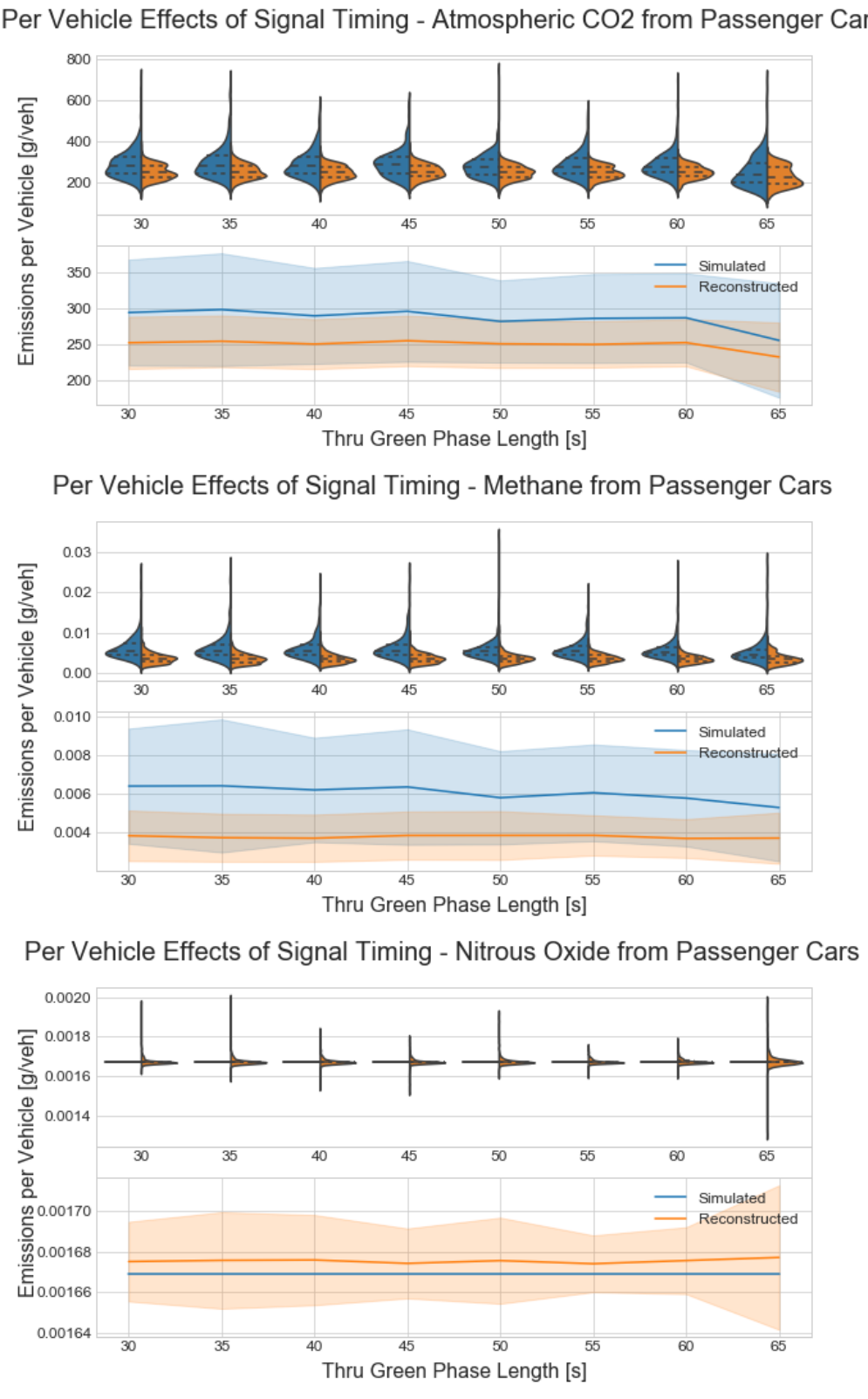

Figure 45: Per Vehicle Effects of Signal Timing for Passenger Cars – Thru Movements Only

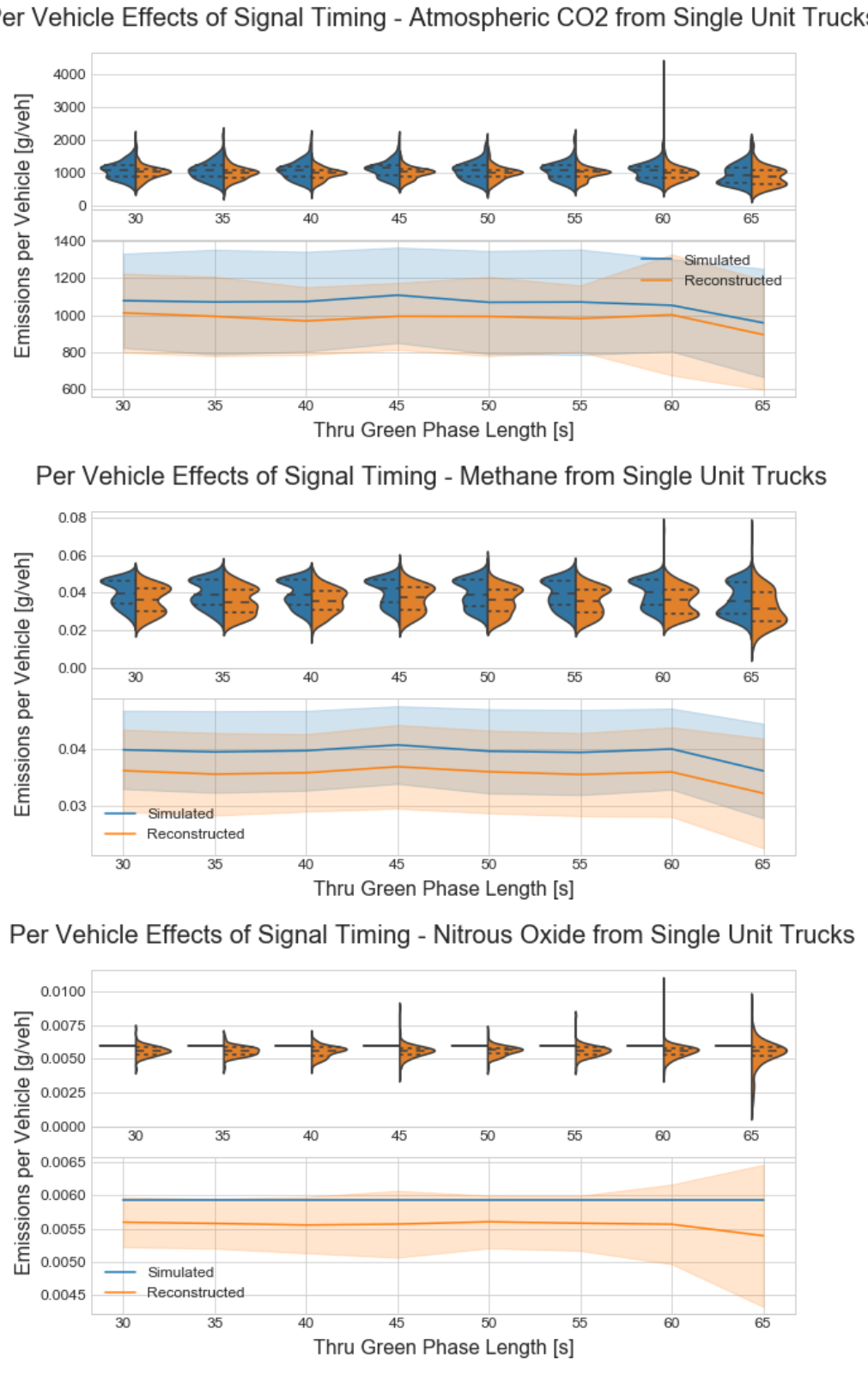

Figure 46: Per Vehicle Effects of Signal Timing for Single-Unit-Trucks – Thru Movements Only

4.3.6 Effects of Signal Coordination

In addition to optimizing signal timing at individual intersections, signal coordination is another popular traffic management scheme that could be applied for addressing traffic congestion and reducing traffic delay and number of vehicle stops. Reduction of traffic delay and stops are expected to improve vehicle fuel efficiency and emissions; as a result, a reliable emission estimation method must be able to capture such effects. In this section, we attempt to evaluate these effects of signal coordination using the traffic corridor described in 3.1.4.4, where the signal plan remains unchanged but is coordinated for the northbound direction. The emission estimates are aggregated over 20-minute time intervals and filtered to northbound thru movements.

The results comparing coordinated and uncoordinated scenarios, shown in Figure 47 to Figure 50, are for the lower end of the range of volumes simulated, since the coordination performs poorly for very high volumes. The differences between the coordinated and uncoordinated scenarios appear to be insignificant. To investigate the results, operating modes distributions for the coordinated and uncoordinated scenarios are compared in Figure 51. Referring to Table 13, the operating mode 0 refers to braking, 1 refers to idling, and 22 and 23 refers to moderate speed cruising or acceleration. The coordinated scenario shows lower fractions of braking and idling, but higher fractions of moderate speed cruising or acceleration. The lower fractions of braking and idling are due to fewer and shorter stops. The higher fractions of moderate speed cruising may be due to vehicles being able to attain higher speeds for longer periods of time when no red light is in sight.

It is possible that using operating mode distributions is not the most suitable for evaluating signal coordination. When using operating mode distributions, emissions are calculated based on fractions of time spent in each operating mode by a fleet collectively without considering the total time individual vehicles took to traverse the link. Thus, if vehicles idle for a long time, the idling operating mode will have a higher fraction. Since the idling mode has relatively low emission rates compared to other modes, this may result in less emissions estimated overall when there is a high fraction of idling such as in uncoordinated scenarios. Additionally, higher fractions of cruising in coordinated scenarios may result in higher emissions estimated. If the volume remains constant, an operating mode fraction-based method could generate higher emission estimates for free-flow behavior than for long idle times.

It is also important to note that accelerating from a stop requires high power and avoiding it would reduce emissions. When a vehicle takes off after idling, it experiences low speed acceleration first, represented by modes 12-16. These modes, which have high emission rates towards mode 16, have lower fractions in the coordinated scenario. However, their decrease in the coordinated scenario and their overall share is relatively small. It is possible that emissions savings from avoiding low speed acceleration is offset by higher fractions of moderate speed cruising.

To check that the coordination performed as intended, time-space trajectory plots from the simulation were compared between the coordinated and uncoordinated scenarios, as shown in Figure 52. The coordinated trajectories have significantly less stopping and idling, which shows that the coordination worked as intended.

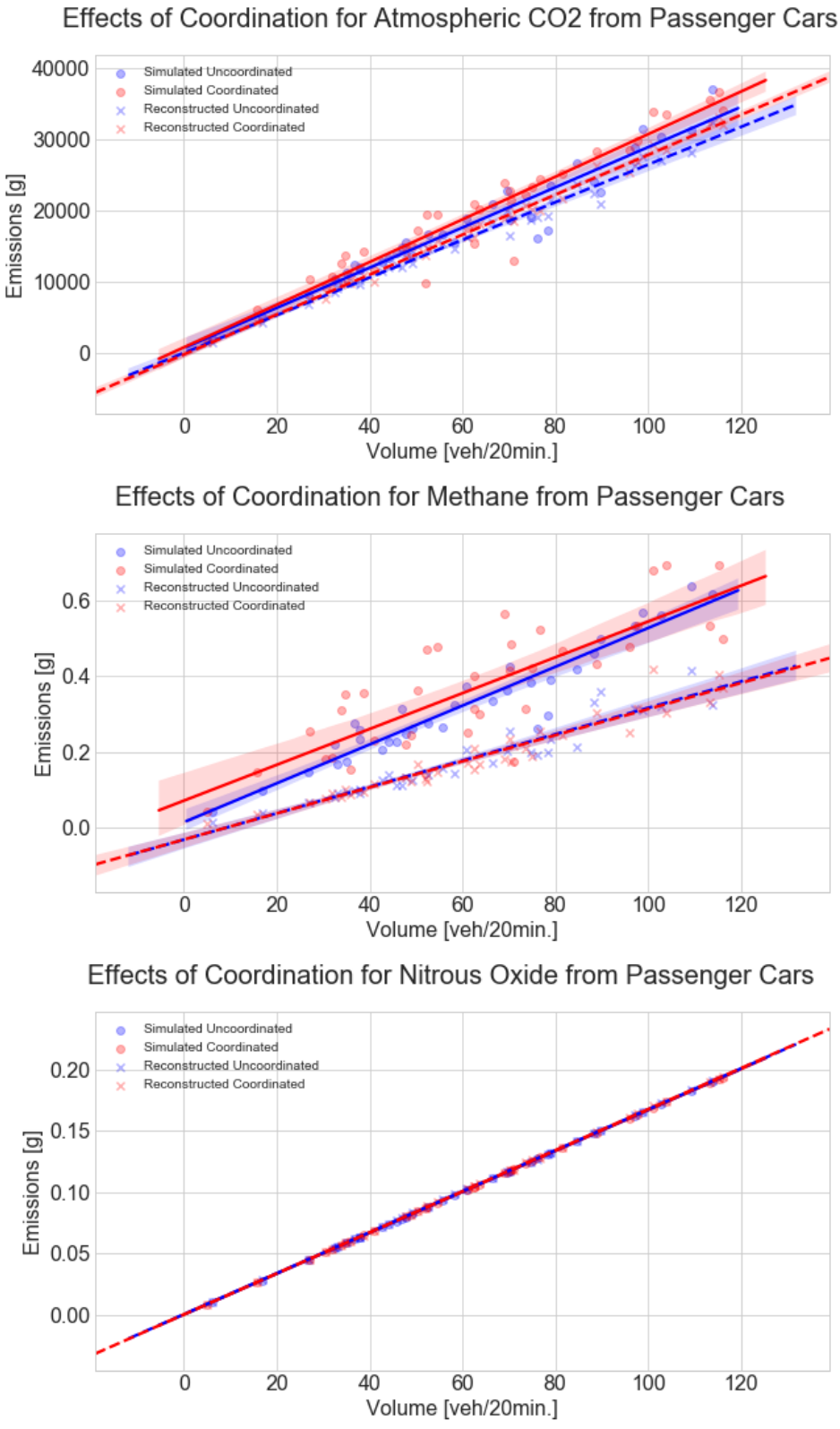

Figure 47: Effects of Signal Coordination for Passenger Cars – Northbound Thru

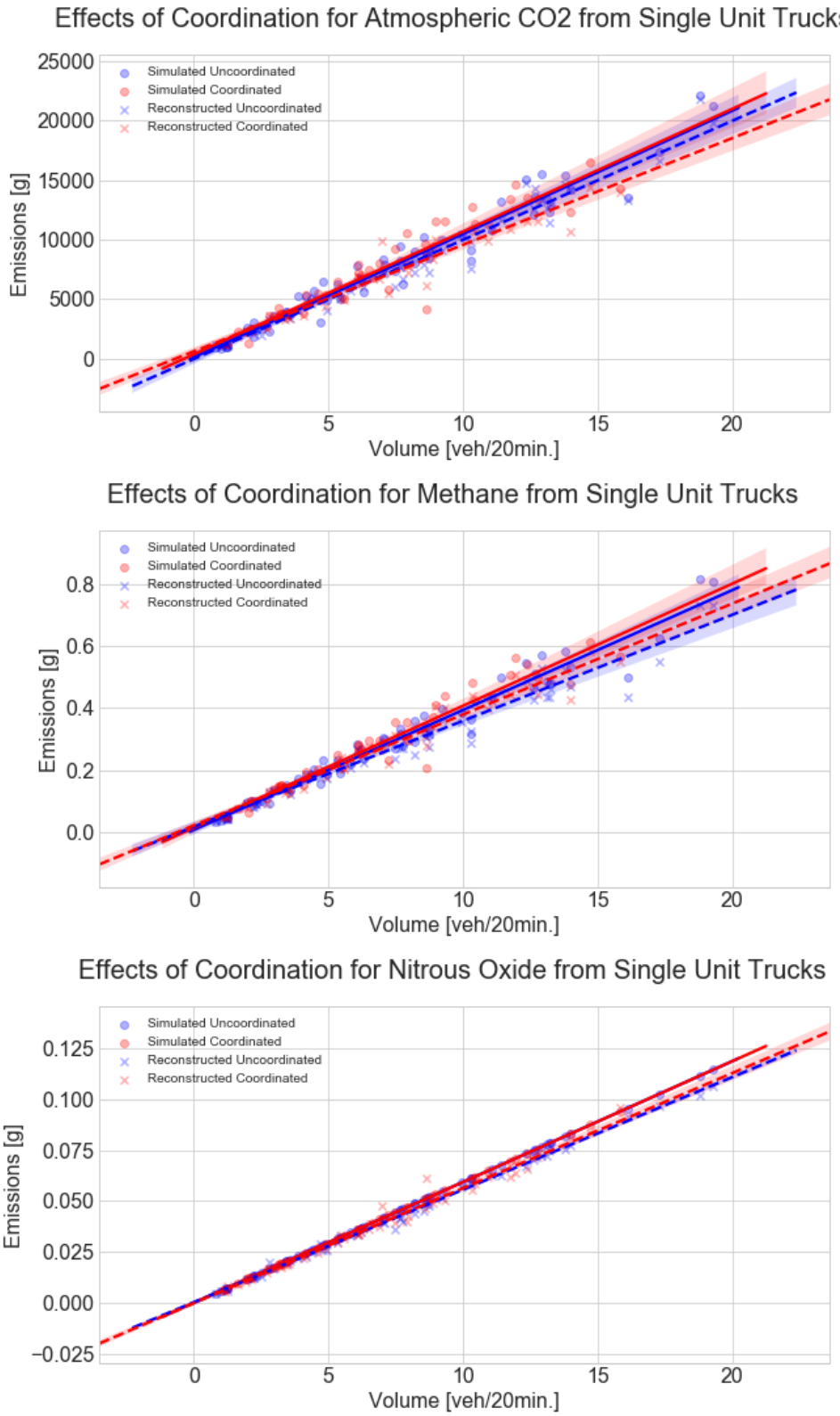

Figure 48: Effects of Signal Coordination for Single Unit Trucks – Northbound Thru

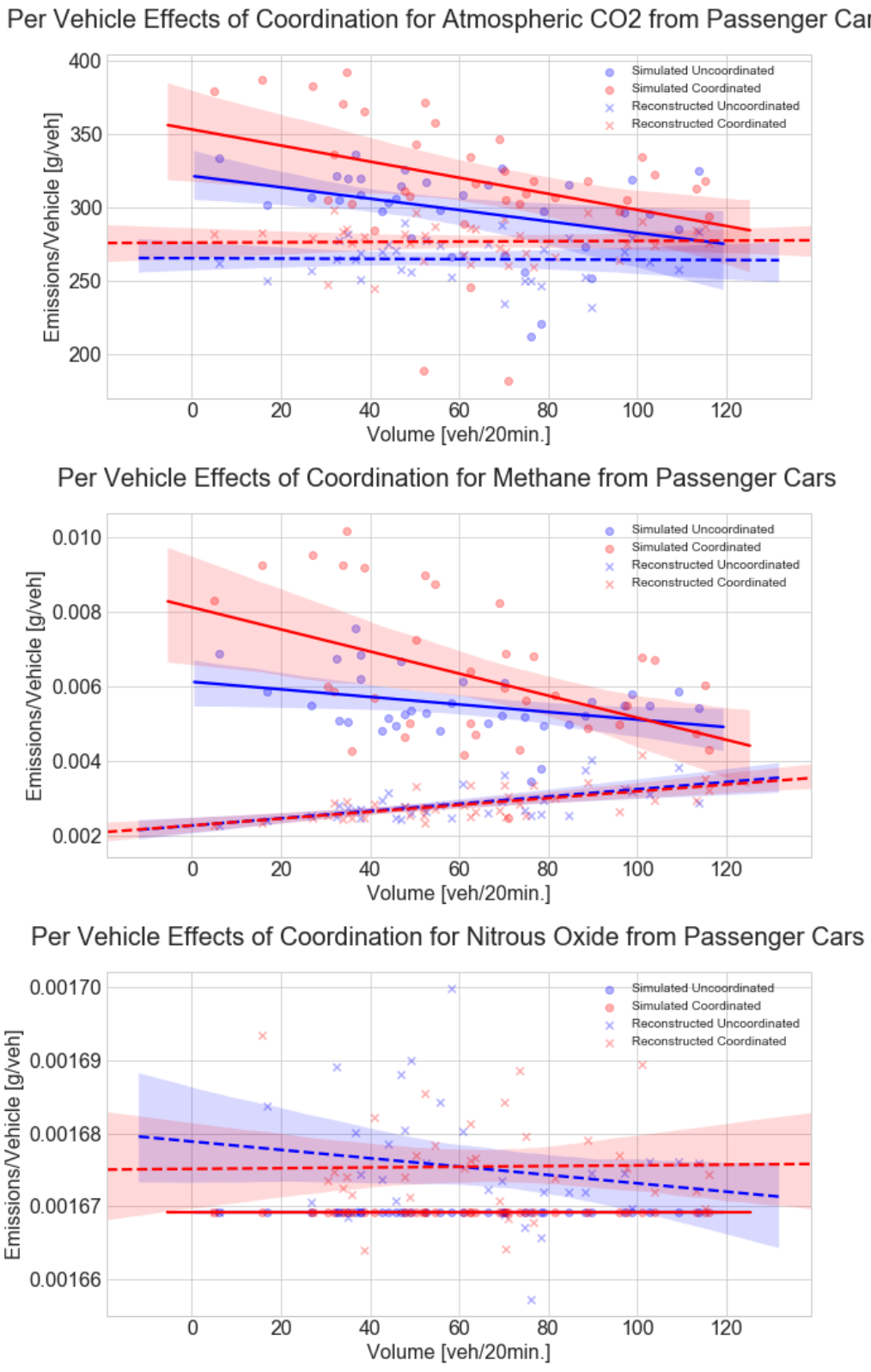

Figure 49: Per Vehicle Effects of Signal Coordination for Passenger Cars – Northbound Thru

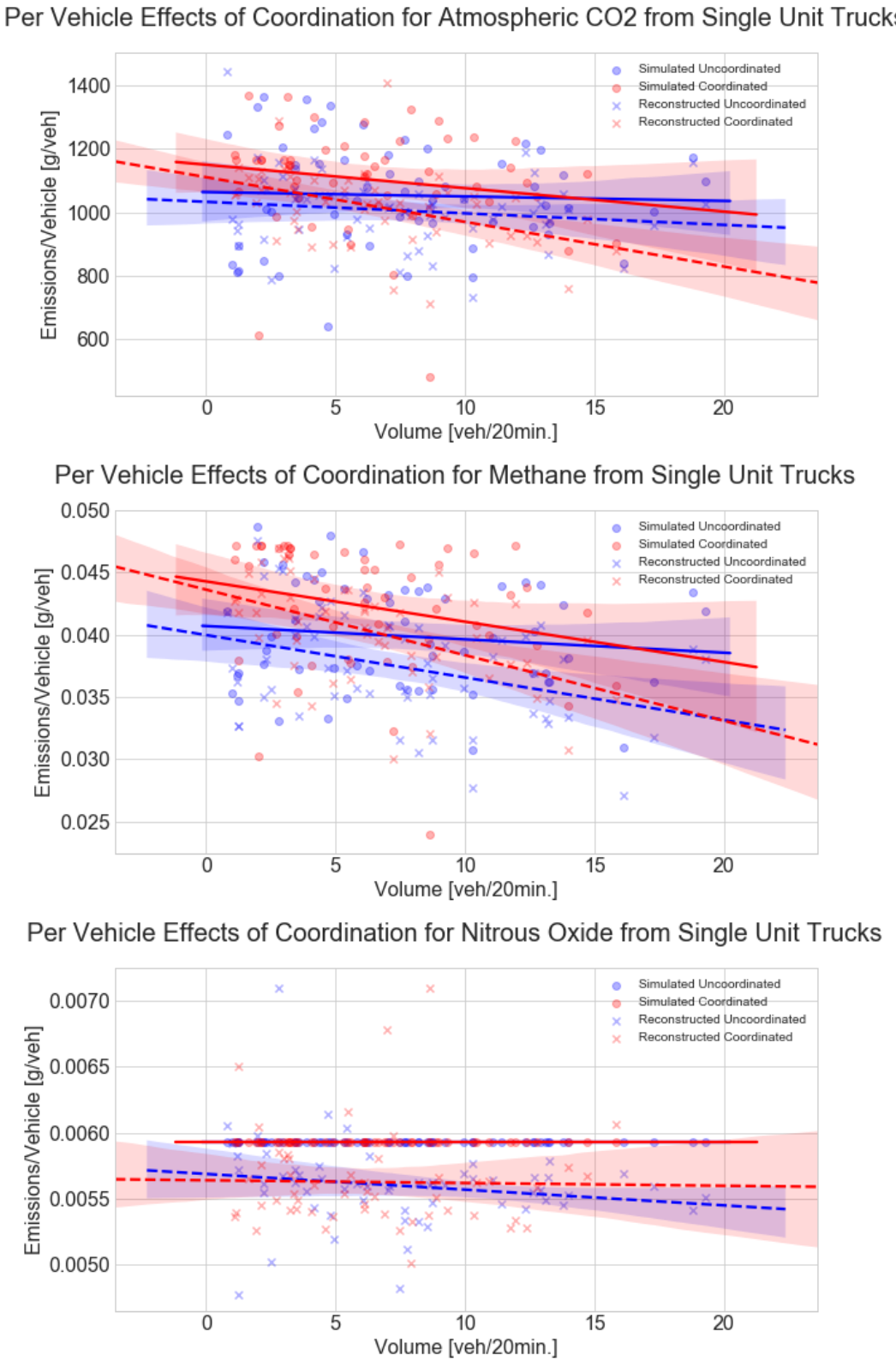

Figure 50: Per Vehicle Effects of Signal Coordination for Single-Unit Trucks – Northbound Thru

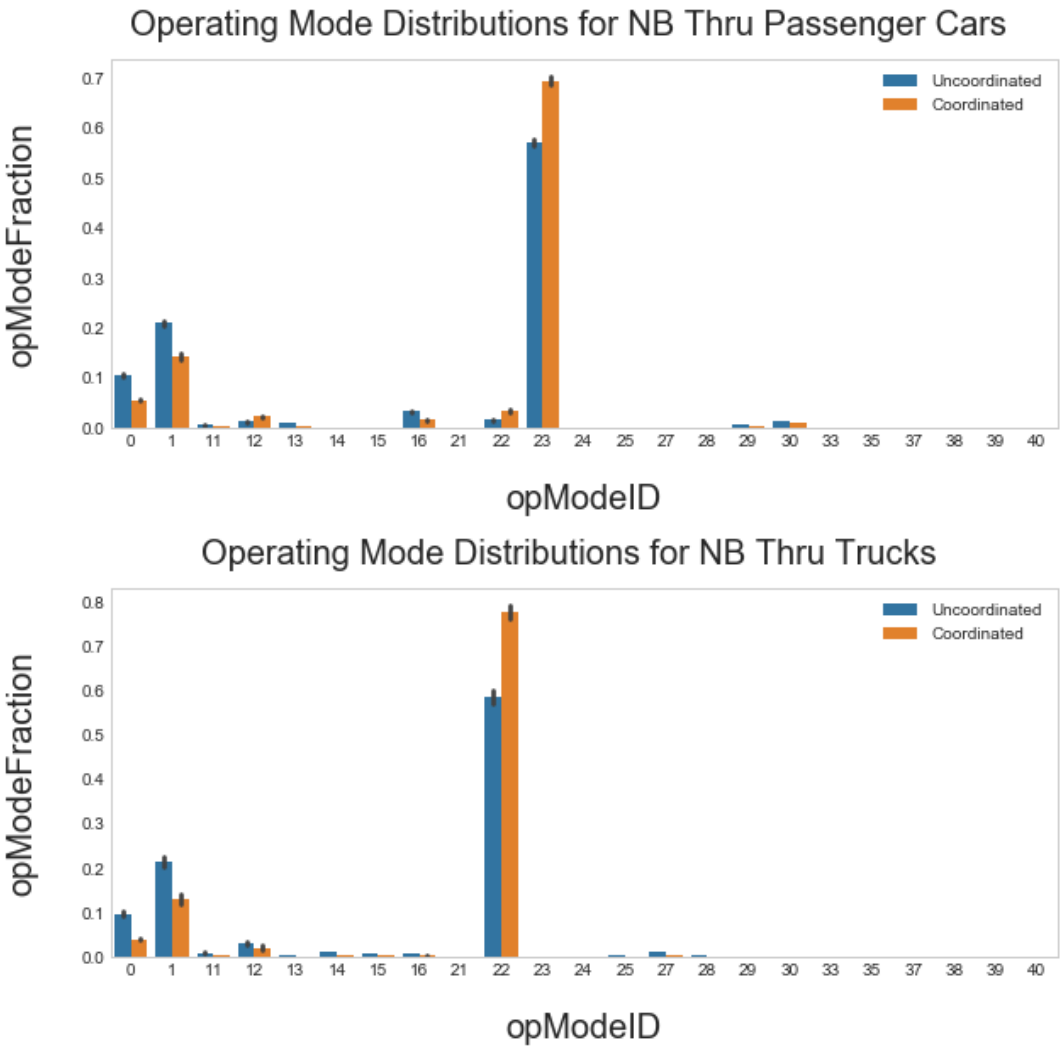

Figure 51: Operating Mode Distribution by Coordination

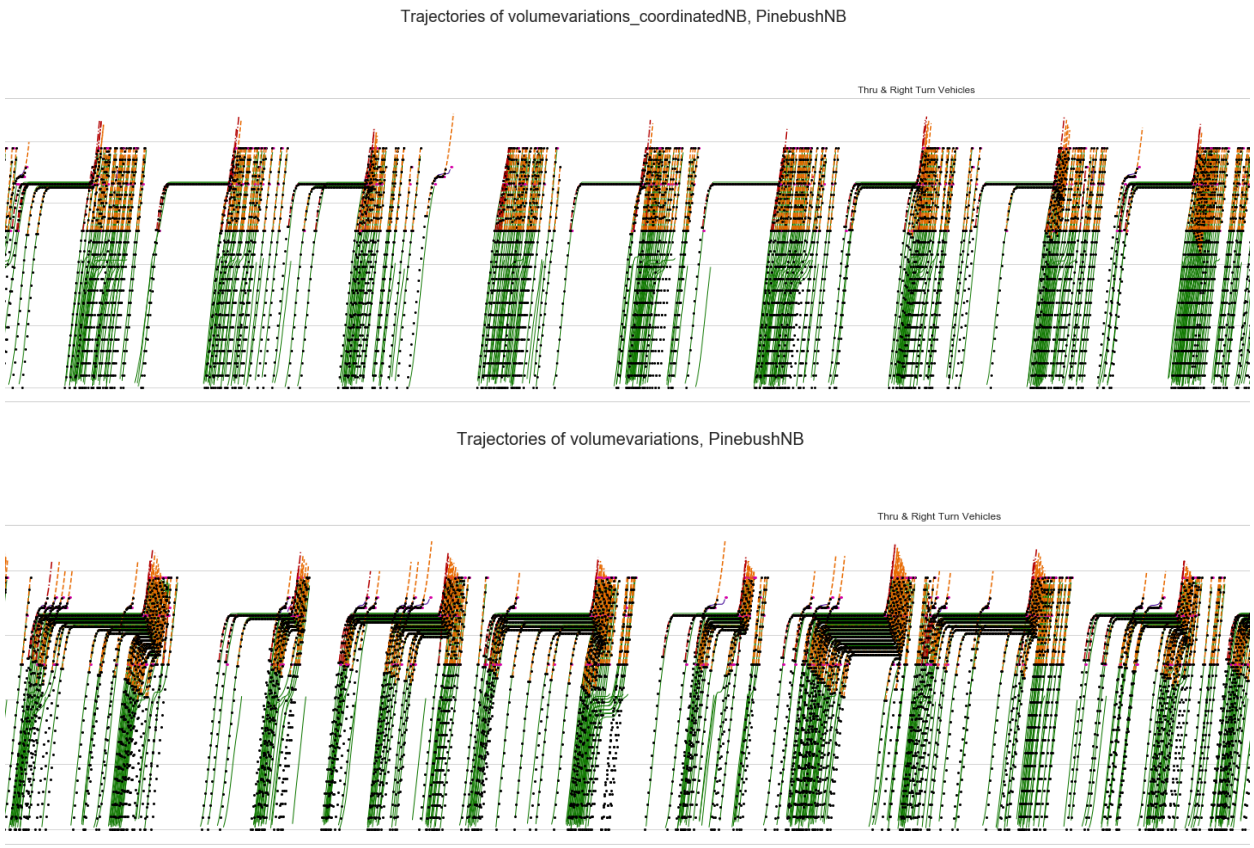

Figure 52: Coordinated (Top) and Uncoordinated (Bottom) Vehicle Trajectories

4.3.7 Effects of Speed Limits

The third traffic control scheme investigated in this research is changing speed limit. The effects of changes in speed limit were investigated using the same corridor described in Section 3.1.4.6. under a range of traffic volumes. Three speed limit scenarios were simulated, including 50km/hr, 60km/hr, and 70km/hr, as described in Section 0. With results from all simulations overlaid onto one another, the effects of speed limit changes and the performance of the trajectory reconstruction method is examined in Figure 53 and Figure 54.

The results from the simulations show that as the speed limit increases, the quantity of carbon dioxide and methane emissions produced by passenger cars also increases (Figure 54). An increase in emissions is expected as the speed increases, since many of the higher speed bins also have higher emission rates. The increase is proportional to the volume of vehicles. This pattern is not shown for the nitrous oxide, which is unsurprising since nitrous oxide emission rates are not dependent on operating modes.

The results for the reconstructed trajectories for passenger cars also show an increase in carbon dioxide and methane emissions as speed limits increase, but not as much. The increase shown by the simulated trajectories are much starker than that of the reconstructed trajectories. Evidently, even though the effects are seen, the trajectory reconstruction method is not capable of fully capturing the effects of speed limit changes for passenger cars.

In the case of trucks (Figure 54), the changes in emissions due to speed limit changes are not as obvious as with passenger cars. However, a slight increase in emissions from the simulated trajectories is still apparent when the speed limit increases. The reconstructed trajectories hardly capture what little changes there are.

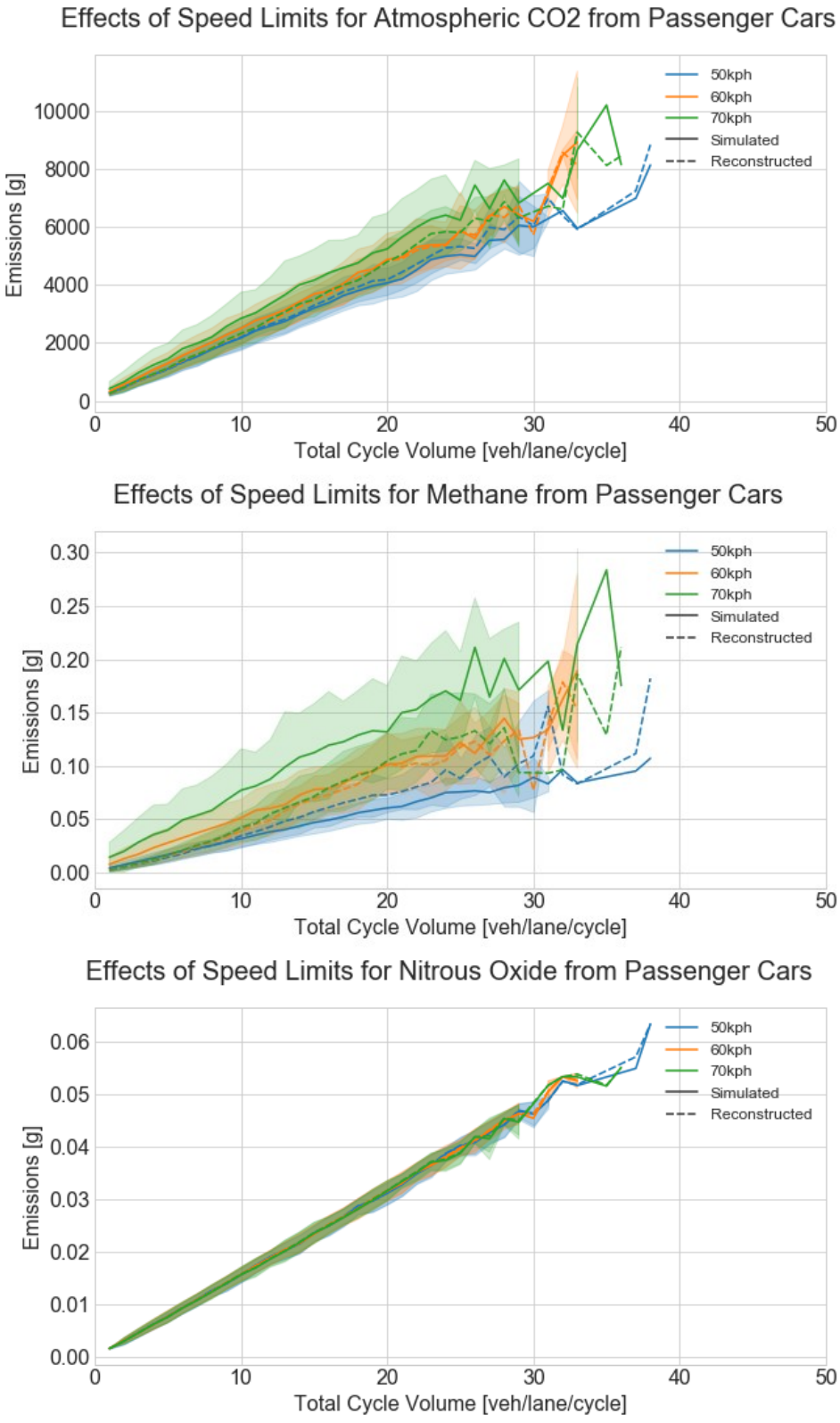

Figure 53: Effects of Speed Limits for Passenger Cars

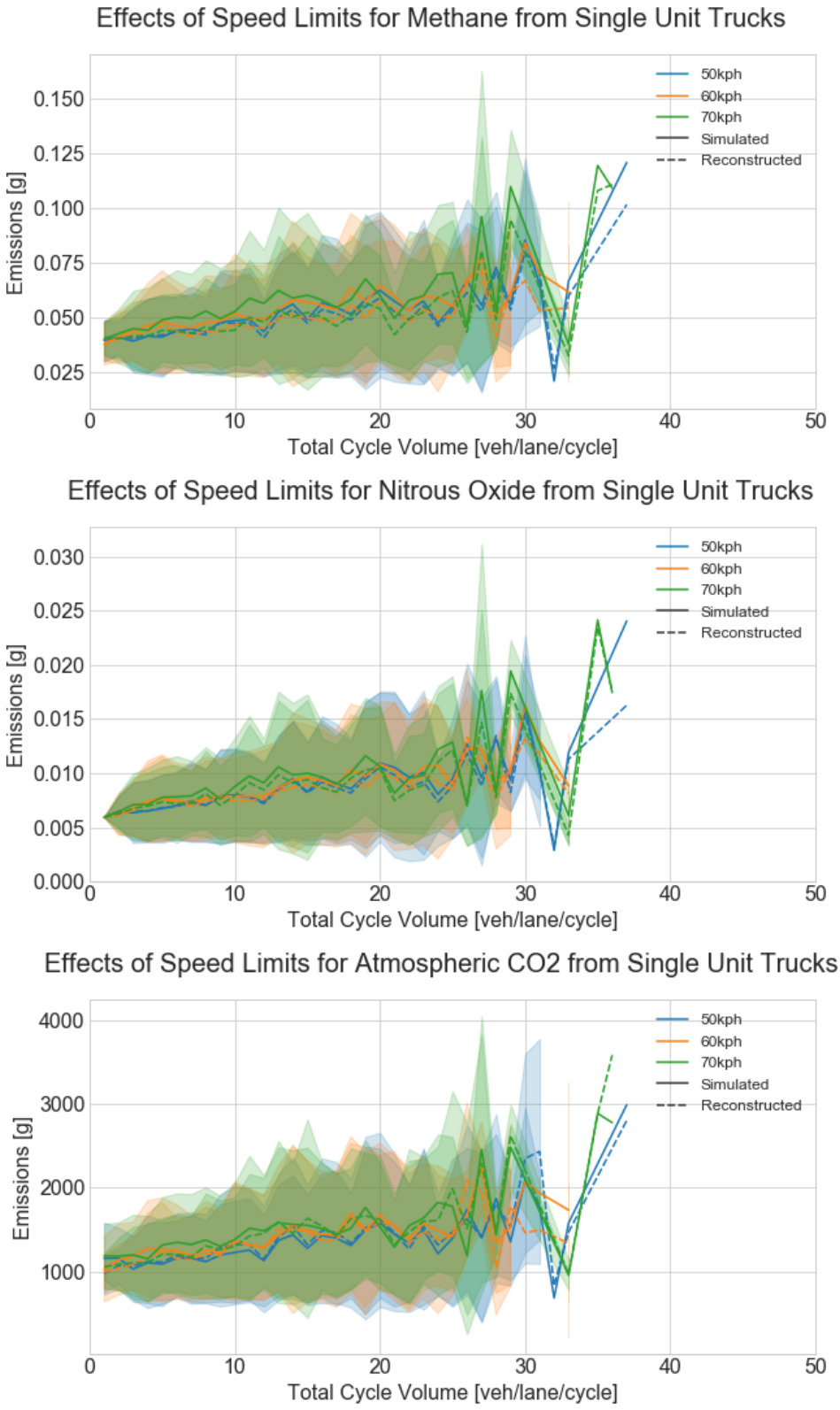

Figure 54: Effects of Speed Limits for Single-Unit Trucks

4.3.8 Summary of Model Evaluation

The results of the model evaluations are summarized in Table 14 to Table 16. The tables present statistical summaries of the relative difference between emissions estimated using the proposed method and the ground truth, such as means and standard deviations. Table 14 summarizes the performance of the proposed method in the simulation based on traffic conditions in the case study field for each vehicle type. Table 15 summarizes the effects of the advance detector location on passenger car emissions. There is no detector position that is simultaneously best for all pollutants or for both precision and accuracy. Table 16 summarizes the effects of aggregating the emission estimates. Only passenger cars are accounted for in Table 16, since most of the vehicles are passenger cars, and the effects of aggregation on trucks is similar. Consistence with the figures in section 4.3.3, aggregation leads to higher precision, but not necessarily higher accuracy. It is apparent throughout all the model evaluations that the accuracy and precision is best for nitrous oxide estimates and worst for methane estimates.

Table 14: Statistical Summaries for the Model Evaluation in Field Conditions

Mean Relative Difference			
Vehicle Type	**Carbon Dioxide**	**Methane**	**Nitrous Oxide**
Passenger Car	-9.7%	-29.2%	0.3%
Single Unit Truck	-1.7%	-4.8%	-3.4%
Combination Truck	-12.3%	-0.6%	-2.3%
Transit Bus	-6.2%	-1.7%	-3.4%

Standard Deviation of Relative Difference			
Vehilcle Type	**Carbon Dioxide**	**Methane**	**Nitrous Oxide**
Passenger Car	14.8%	34.0%	2.2%
Single Unit Truck	30.4%	15.9%	12.7%
Combination Truck	34.6%	17.0%	13.1%
Transit Bus	33.6%	21.3%	13.2%

Table 15: Statistical Summaries for the Effects of Advance Detector Positions on Passenger Car Emissions

Mean Relative Difference			
Advance Detector Setback [m]	Carbon Dioxide	Methane	Nitrous Oxide
25	-5.9%	-26.7%	0.6%
50	-7.6%	-26.5%	0.4%
75	-8.7%	-26.3%	0.3%
100	-9.8%	-26.3%	0.3%

Standard Deviation of Relative Difference			
Advance Detector Setback [m]	Carbon Dioxide	Methane	Nitrous Oxide
25	16.5%	36.6%	2.7%
50	15.0%	34.4%	2.2%
75	14.8%	34.5%	2.0%
100	14.7%	35.0%	1.9%

Table 16: Statistical Summaries for the Effects of Aggregation on Passenger Car Emissions

Mean Relative Difference			
Aggregation Level	Carbon Dioxide	Methane	Nitrous Oxide
None	-8.7%	-26.3%	0.3%
Over Lanes	-10.2%	-31.8%	0.2%
Over Lanes & Cycles	-11.3%	-35.3%	0.2%

Standard Deviation of Relative Difference			
Aggregation Level	Carbon Dioxide	Methane	Nitrous Oxide
None	14.8%	34.5%	2.0%
Over Lanes	15.7%	30.9%	1.7%
Over Lanes & Cycles	11.5%	24.0%	0.6%

4.4 Trajectory Reconstruction Using Average Speed Interpolation

An alternative, simpler method of trajectory reconstruction was explored in addition to the primarily proposed trajectory reconstruction method. This method linearly interpolates the vehicle trajectories between detectors, as explained in section 3.2.2. To evaluate this simplified method, it was performed on the volume variations simulation described in section 3.1.4.2.

The operating mode distribution created by the simplified method is shown in Figure 55 juxtaposed with those created by the simulated trajectories. Compared to the operating mode distributions created using the primary trajectory reconstruction method (Figure 32), the simplified method does not emulate the simulated trajectories as accurately. Operating mode 12 is extremely over-represented, because stop-and-go motions between detectors are all modelled as a slow average speed. Furthermore, the braking mode is not represented at all, since the average speed method does not account for acceleration or deceleration. However, these issues themselves are not of concern, as the end objective is the emission estimate and not the operating mode distribution. The performance of both methods is compared in Figure 56 to Figure 61.

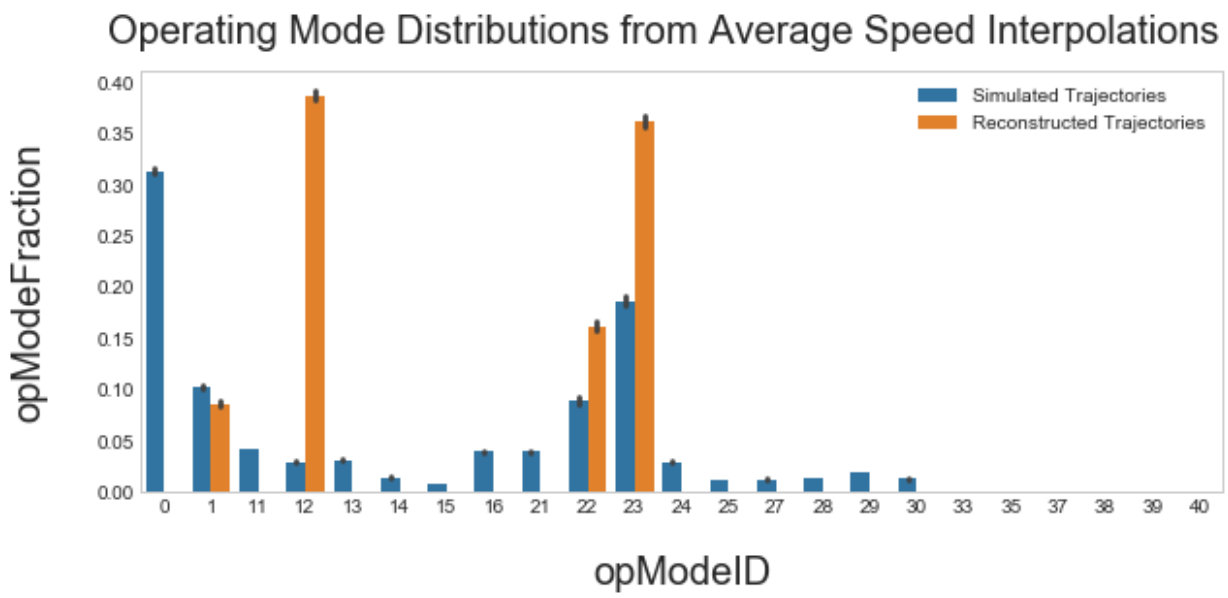

Figure 55: Operating Mode Distribution for Average Speed Trajectory Reconstruction

For passenger cars, the simplified method tends to underestimate carbon dioxide and methane emissions (Figure 56 and Figure 57), except in the case of carbon dioxide from left turn movements. For methane, the underestimation is extremely high. This is likely due to the fact that methane emission rates are high for passenger cars for the braking operating mode, but the simplified method does not account for this mode. In the case of nitrous oxide (Figure 58), there is virtually no difference between using either method, since nitrous oxide emission rates are relatively independent of operating modes.

On the contrary, the results for single-unit trucks show that the simplified method tends to overestimate the emissions as compared to the primary method. This occurs significantly for carbon dioxide from left-turns (Figure 59) and for methane from all movements (Figure 60). These results should be confirmed in a further analysis using acceleration and deceleration functions that are calibrated for heavy duty vehicles, since the current research only uses acceleration and deceleration functions calibrated to passenger cars. Again, the results for nitrous oxide emissions (Figure 61) differ very little between the primary method and the simplified method.

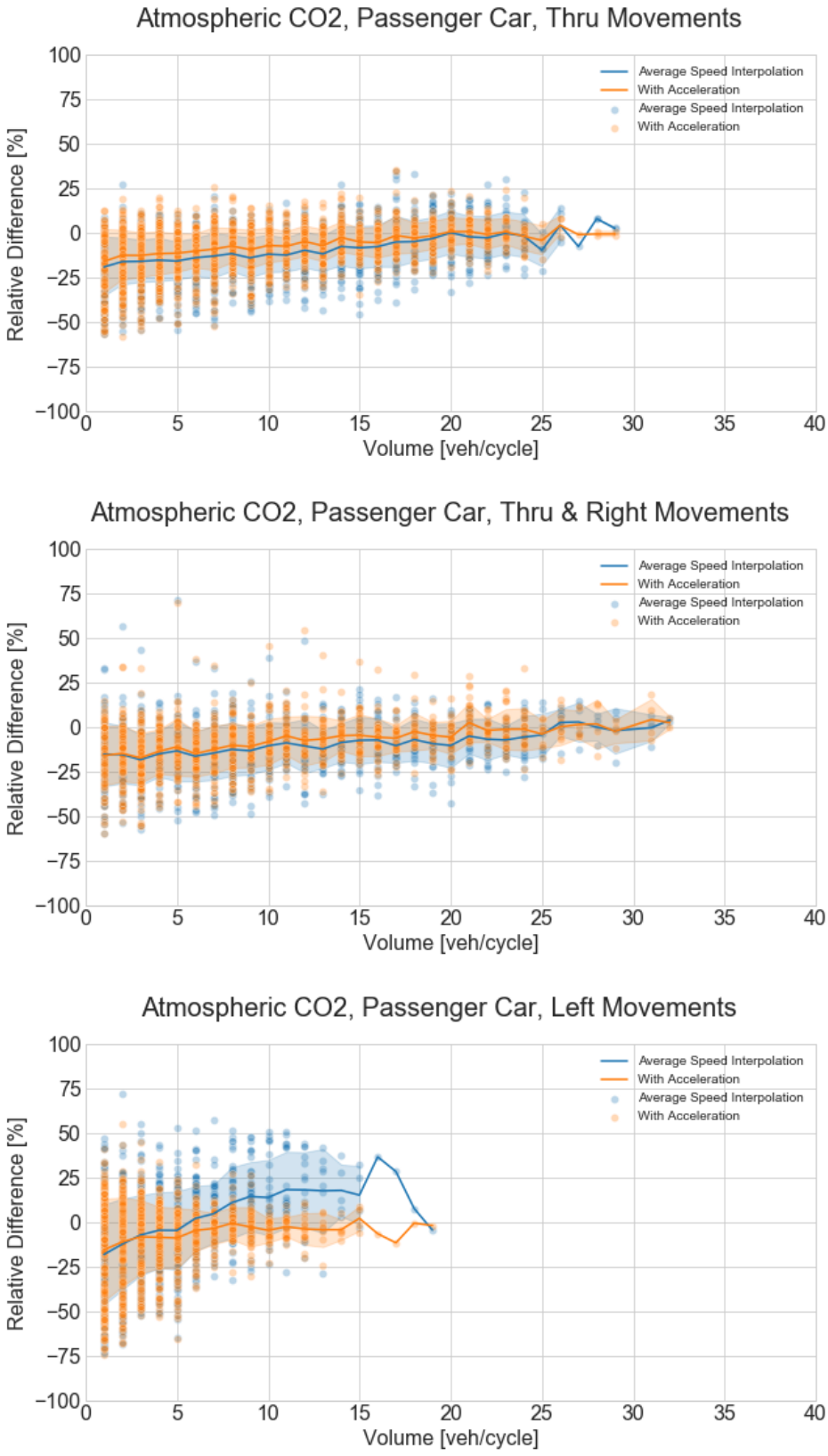

Figure 56: Comparison with Average Speed Trajectory Reconstruction for CO_2 from Passenger Cars

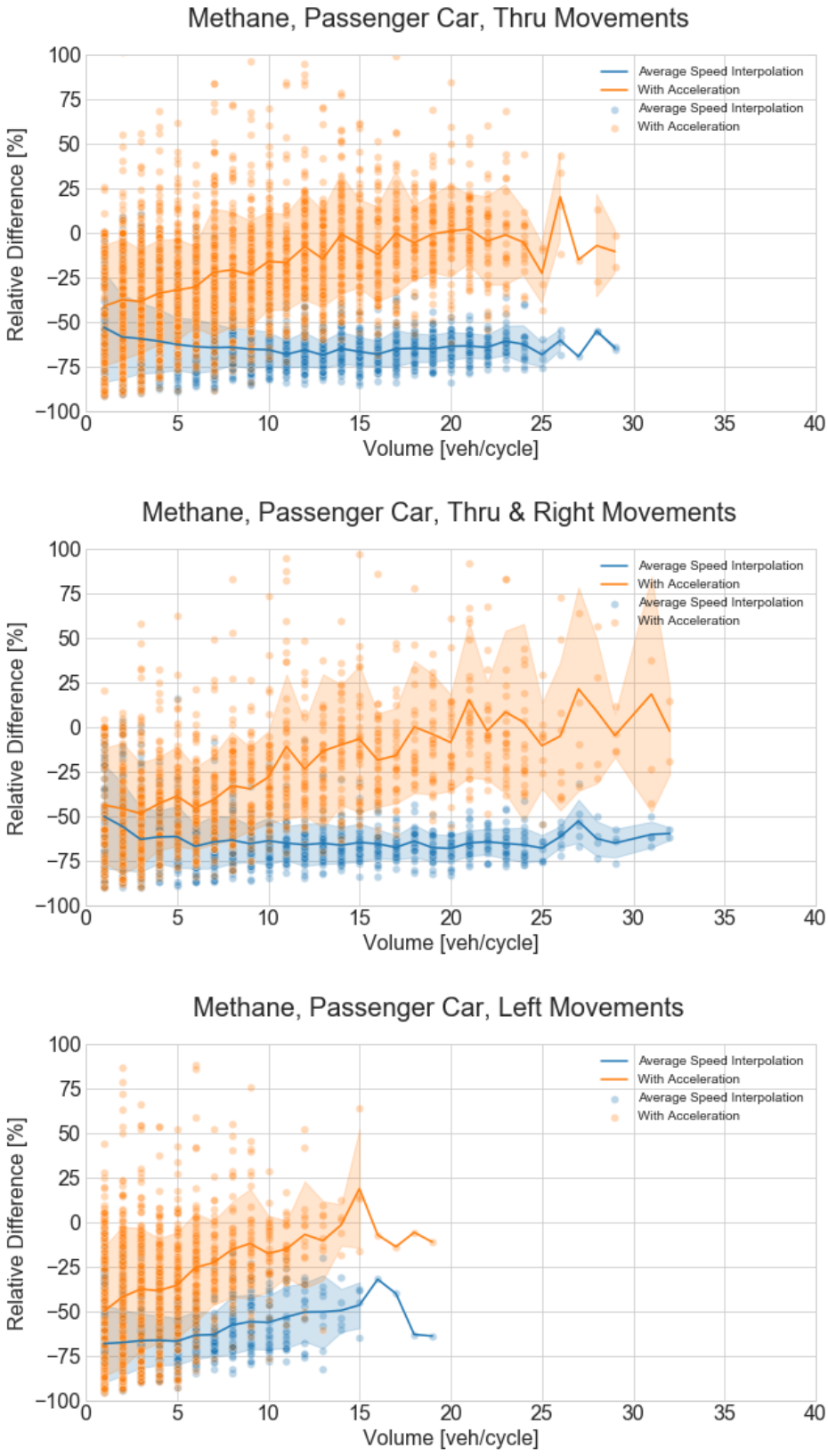

Figure 57: Comparison with Average Speed Trajectory Reconstruction for CH_4 from Passenger Cars

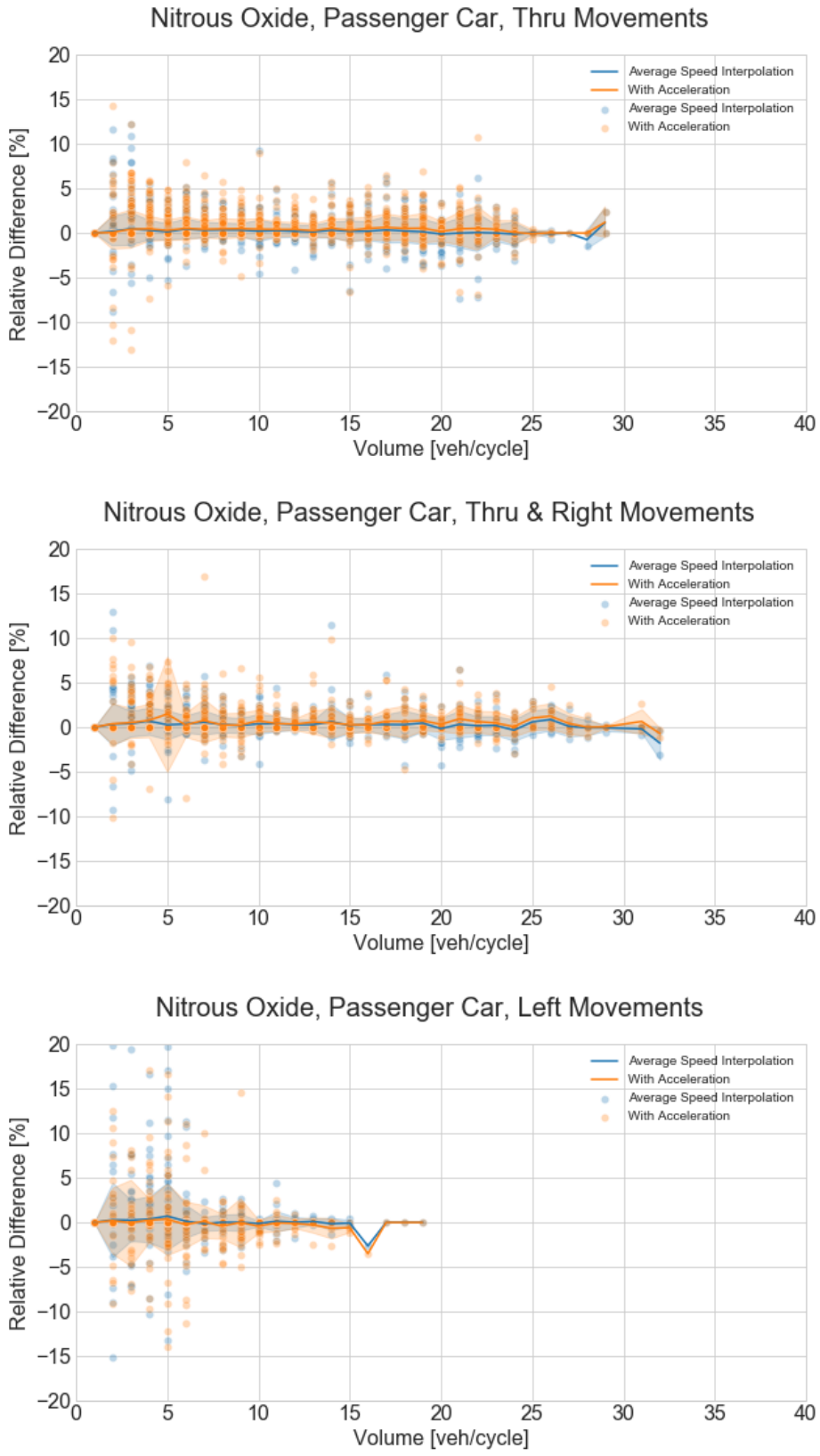

Figure 58: Comparison with Average Speed Trajectory Reconstruction for NO_2 from Passenger Cars

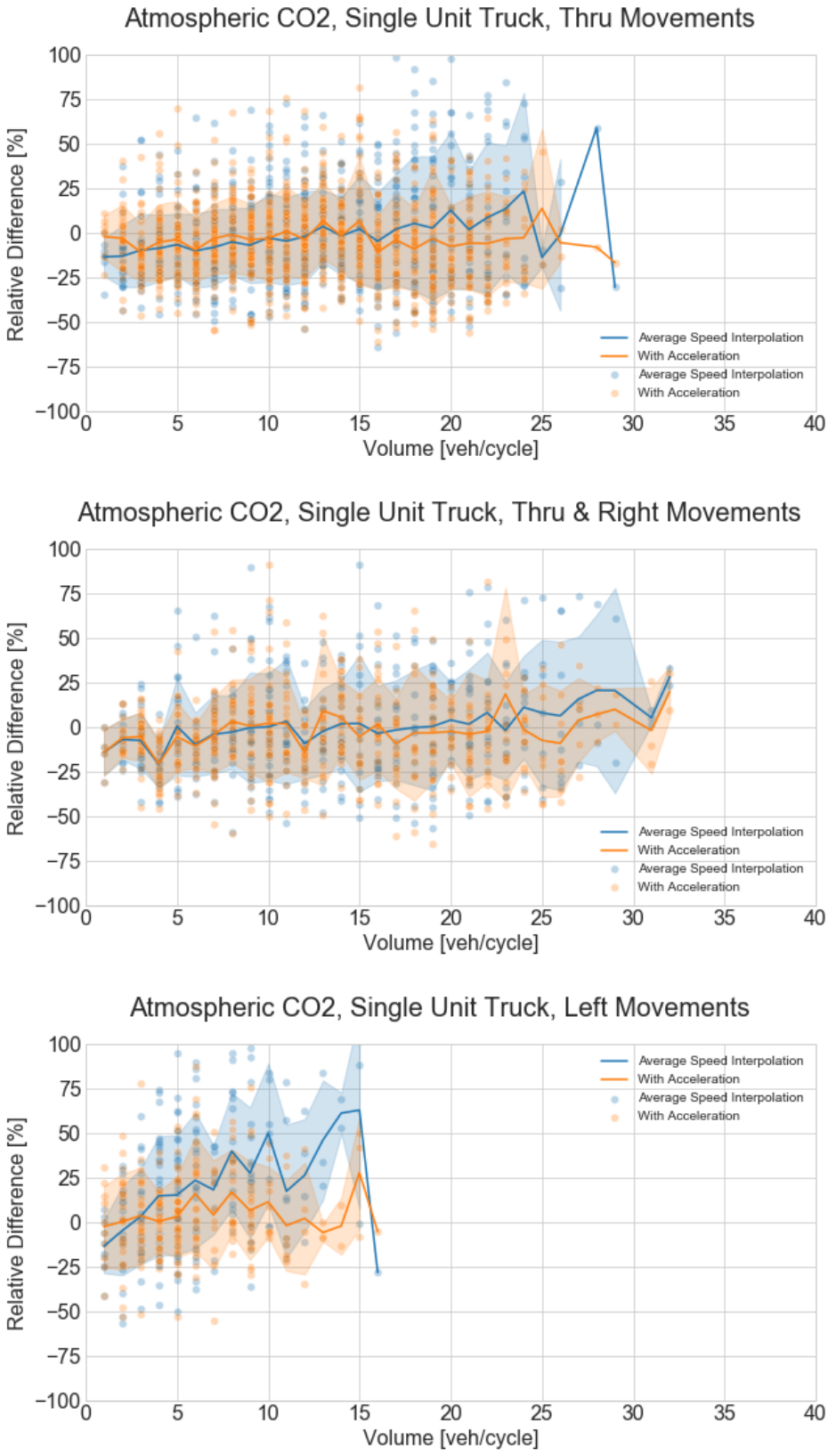

Figure 59: Comparison with Average Speed Trajectory Reconstruction for CO_2 from Trucks

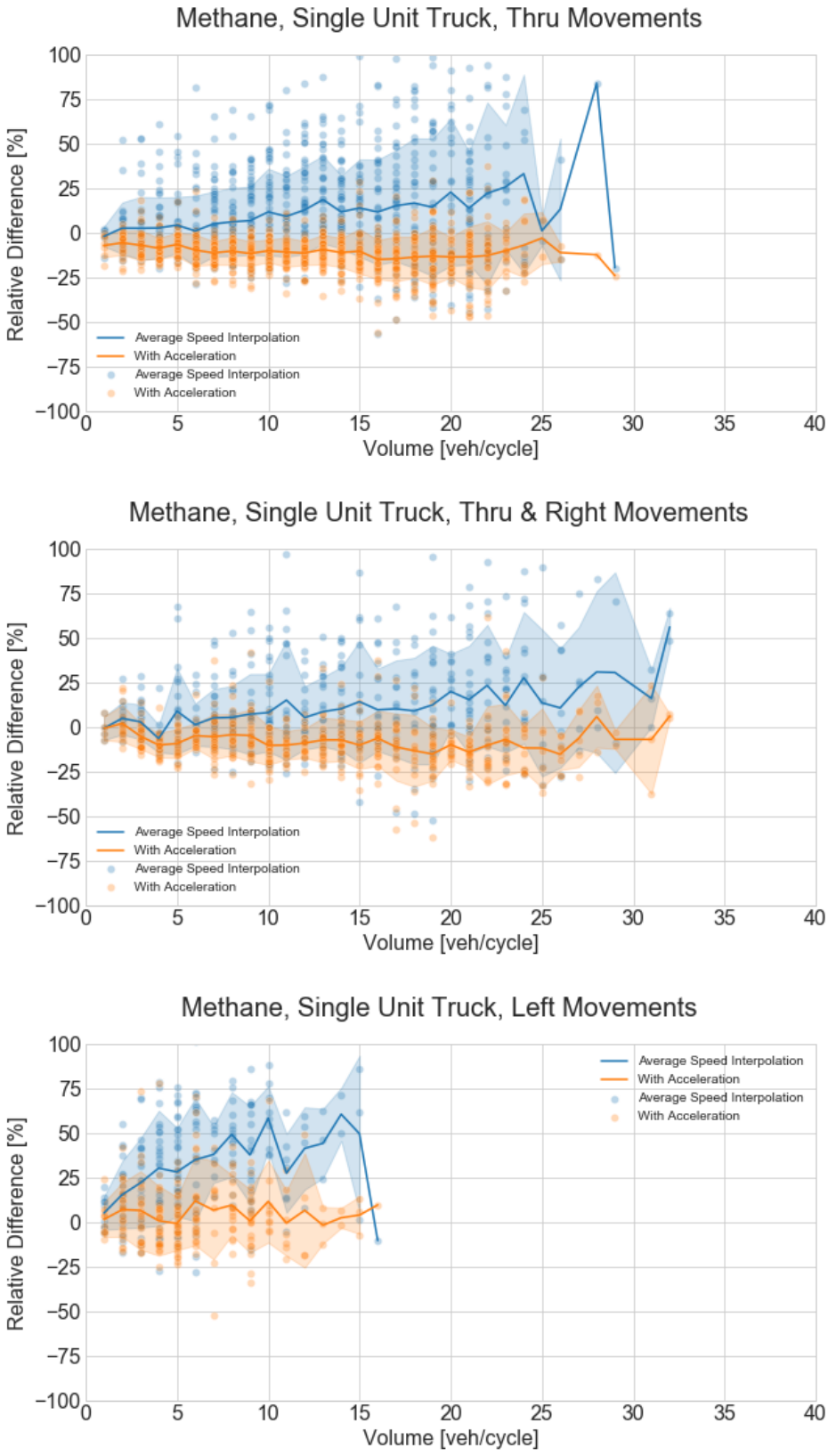

Figure 60: Comparison with Average Speed Trajectory Reconstruction for CH_4 from Trucks

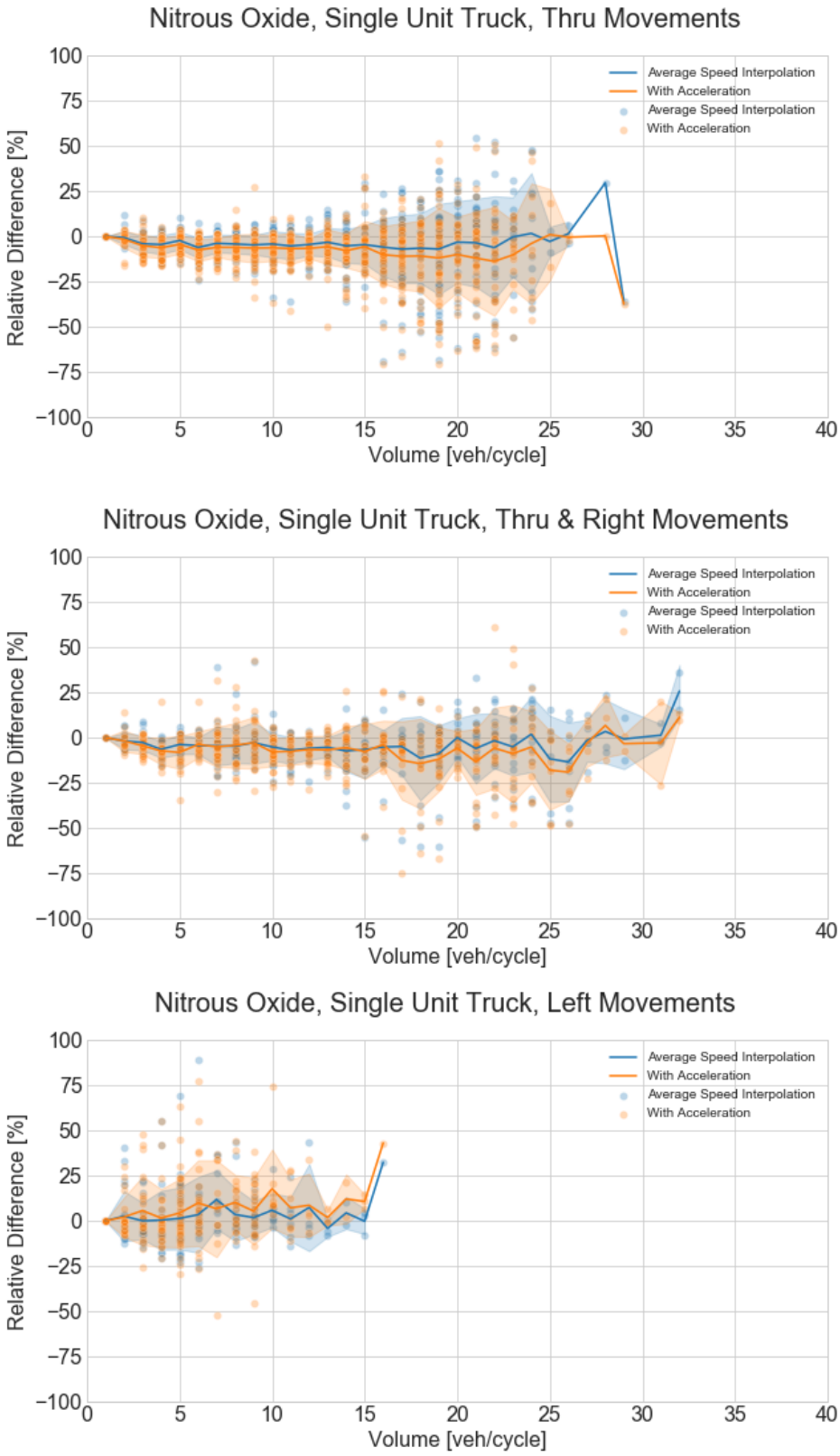

Figure 61: Comparison with Average Speed Trajectory Reconstruction for NO_2 from Trucks

Chapter 5 Conclusion

An emission modelling method was developed to produce emission estimates using high-resolution traffic data in real-time. It was developed to serve as an emission monitoring tool for traffic management applications. The research was performed in a simulation environment consisting of a Vissim model coupled with MOVES-based emission estimation. This simulation coupling provided a "ground truth" as a basis for comparison, as well as the assumed traffic data required for the developed method. The simulation model was built and validated to field conditions in an urban corridor with signalized intersections, located in Cambridge, Ontario.

The proposed method is assumed to have access to vehicle presence detection data and signal timing records as input. Using this input, it reconstructs individual vehicle trajectories at a second-by-second level of detail, including instantaneous speed and acceleration information. This information is then used to estimate emissions using a simplified emission model reconstructed from the MOVES model. This approach retains the required accuracy while significantly reducing the computation time required by the MOVES software; thus, emissions can be estimated in real-time using traffic data.

To evaluate the performance of the proposed method for evaluating alternative traffic management schemes, an extensive set of experiments were conducted on a large number of traffic scenarios. It was found that the performance of the proposed method varies depending on the traffic volume and speed limits. It is able to capture some of the effects of various traffic management strategies. Three greenhouse gases were focused on: carbon dioxide, methane, and nitrous oxide. The performance also varies depending on the type of emission being estimated.

Further research is recommended based on the results of this thesis. Due to the challenges and limitation met in this research work, recommendations are also made for other fields of research, as the challenges and limitations may be overcome through advancement in other fields.

5.1 Findings

In this thesis, a method was developed to reconstruct vehicle trajectories using traffic data, and then to estimate emission based on the reconstructed trajectories. The emission estimation method was more of a computational shortcut than a mathematical modelling endeavour and can generate results nearly identical to those of the "ground truth" method. Thus, the uncertainty lies mainly in the trajectory reconstruction process.

5.1.1 Adequacy of Traffic Modelling Techniques

The trajectory reconstruction method is able to represent the vehicle trajectories for the most part on a time-space basis. The vehicle speeds and accelerations generated from this method can create an operating mode distribution that is similar to that created from the originally simulated trajectories. The

overall performance of the developed method varies depending on the type of emission being estimated. Due to the nature of the emission model, it has been shown that it is relatively easy to reconstruct vehicle trajectories to yield accurate nitrous oxide emissions, since the nitrous oxide emission rates generated do not depend on operating modes. For carbon dioxide and methane, it becomes more important to properly model the vehicle activities. Especially in the case of methane for passenger vehicles, it is important to properly model deceleration behaviour, as the mode of deceleration has relatively high emission rates.

The methods tend to perform better for high volumes of traffic, so long as the volumes are not approaching capacity. The specified location for the advance vehicle detectors also plays a role in the performance, but not a major role. Aggregating the estimates across larger groups of vehicles over lanes and time can reduce the variation in the estimates, but accuracy is not significantly improved. Differences in the vehicle type proportions in the fleet also does not significantly affect performance.

5.1.2 Effects of Traffic Controls on Emissions

Effects in the traffic activities caused by changes in signal controls, such as introducing signal coordination or increasing phase lengths, results in changes in the overall emissions. The overall change is adequately captured by the trajectory reconstruction process. While the absolute value of the emissions generated is in many cases underestimated to varying degrees depending on the pollutant and vehicle type, the overall pattern is usually captured. That is, the increase in emissions caused by signal coordination or phase lengthening is usually more accurately captured than the absolute quantity of emissions. This is important when using the emission estimates for traffic management evaluations.

The effects of speed limits, however, is not as adequately captured. The reconstructed trajectories are able to show that increases in emissions as speeds increase, but not the same degree that the simulated trajectories show.

5.1.3 Primary versus Simplified Method

A simplified method that only consists of linearly interpolating trajectories between detections was explored. In comparison to the primary method, the performance may be similar or worse depending on the vehicle type and pollutant type being estimated. Nitrous oxide estimates were equally adequate from both methods, since nitrous oxide emissions are not heavily dependent on operating modes in the model. However, for carbon dioxide, the simplified method does not perform as well. The simplified method is especially inadequate for estimating methane from passenger cars due to its high dependence on braking behaviour, which is not modelled in the simplified method.

5.2 Discussion

The developed method works best under mid- to high-range volumes relative to the capacity. It yields highly accurate nitrous oxide emission estimates, relatively decent estimates for carbon dioxide, and needs work for methane emissions. In terms of capturing effects of traffic controls, the relative difference can usually be captured, although estimates can significant underestimate the absolute emission quantities.

To apply the proposed method, high-resolution detector data and signal timing records are required, which is increasingly available as video detection and other means become more widely used in traffic management. There will always be challenges in data collection and utilization. Aside from traffic data, meteorological data, vehicle fleet data, and fuel data is also required. However, the remaining data can be obtained at a more aggregated scale.

5.2.1 Applications

This real-time estimation method can be used in the evaluation of traffic controls, which is often dynamic and could benefit from faster feedbacks. Such applications can be useful for monitoring the effects of traffic on air quality and the greenhouse gas emissions. This would help traffic management consider the external costs that control strategies can place on surrounding residents. Furthermore, effects can be detected immediately rather than waiting for long term studies.

Some challenges of implementing a real-time emission monitoring framework need to be considered for any application. A balance must always be struck between accuracy and cost. This thesis presents two methods, one significantly simpler than the other, which can in some cases produce similar results but have completely different capabilities. Where necessary, a more complex model may be needed, but since they have more computationally intensive, complexity is only desirable if the benefits outweigh the costs.

There are many components to the model, such as individual functions used to model acceleration and deceleration behaviour, car-following model parameters, other vehicle behaviour parameters, and emission rates. The current version is calibrated to Vissim simulations, but applications in the real world may require different parameters and assumptions. There could also be differences from location to location. The model itself is easily scalable, and its generalizability is meant to be high, requiring a few parameter changes at most for different settings or driver behaviours, but whether these goals have been achieved would require further research.

The real-time emission calculation method developed requires emission rates to be pre-generated using a set of inputs that account for all the variations of the factors that the model must be sensitive to. Since traffic management deals with controlling traffic behaviours, it is vehicle activities to which the model must be sensitive. Factors that are external and not affected by traffic management should be aggregated over a larger scale and held constant over the small scale within which the traffic management evaluations take place. These external factors include meteorological, vehicle age, and fuel

related variables. The challenge in this respect is to determine the spatial-temporal scope within which external variable should be held constant. For example, to evaluate traffic controls over the course of a day, the average temperature and humidity of the day could be used, along with regional vehicle and fuel information. This would show the effects of traffic management on the emissions over the different traffic patterns of the day while holding external variables constant. However, if the temperature changes drastically over the day, the scope of constant external factors may need to be reduced, so that control strategies are evaluated using realistic relative changes.

5.2.2 Limitations

Since this research was performed in a simulated environment, the drawbacks may be underestimated. In the real world, driver behaviour has a larger variation, due to human error and changing environmental factors.

Another limitation comes from the accuracy of data available. While newer technologies such as video-detection can provide high-resolution data, there are still errors. These errors would not only compound onto the errors of the trajectory reconstruction, they may cause the algorithm to perform less optimally.

Generally, there are always limitation in microscopic emission modelling, due to numerous assumptions being made, such as driving behaviour and fleet characteristics. It is also a question to confirm whether the models used have sufficient precision for highly microscopic applications, how they compare to direct measurements, and under what circumstances certain assumptions hold. For example, there may be an issue with using operating mode fractions to estimate emissions without an absolute metric, as discussed in Section 4.3.6.

5.3 Future Research

Based on the findings, some future research is recommended. These recommendations include improvements to the proposed method, validation of the proposed method using field studies, and a broader study of vehicle emission reduction.

5.3.1 Trajectory Reconstruction Modelling Parameter Calibration

The parameters used in the trajectory reconstruction method described in Section 0 were calibrated through visual analysis of the reconstructed trajectories overlaid onto the originally simulated trajectories. A more quantitative approach could yield better results. The parameters are $_{\%cruise}$, m_{lc}, $p_{stop,cruise}$, $T_{h,discharge}$, $l_{eff,n-1}$, dt, and $T_{tolerance}$.

The parameters of the acceleration and deceleration functions originally found in the literature (Bogdanović & Ruškić, 2013; Kumar Maurya & Bokare, 2012) were

$$k_3 = 0.005$$

$k_4 = 0.154$
$k_5 = 0.493$
$\beta_0 = 3.369$
$\beta_1 = 0.072$

These values were calibrated to field data. The acceleration and deceleration behaviours in Vissim may be different. Perhaps a set of acceleration and deceleration functions calibrated to Vissim driving behaviour could allow better comparisons in a simulated environment. However, for real-world applications, functions calibrated to actual driving behaviour should be used.

In addition, the literature provided separate functions for the acceleration and deceleration behaviours of different vehicle types, but only the function for light duty passenger vehicles were used in this research due to the low penetration of other vehicle types. Since larger vehicles generate a significant amount of emissions, their trajectories should be modelled more accurately in a practical application of this method.

5.3.2 Field Validation

The trajectory reconstruction method is based on simulated vehicle behaviour. Further research could investigate how well emission modelling can be performed using reconstructed trajectories in comparison with field measurements of emissions. In addition to validating the trajectory reconstruction method, field validation would be required to see whether quality data can be collected for trajectory reconstruction. Data collection methods will continue to improve, but challenges associated with collected real-world vehicle detection data should be considered.

5.3.3 Other Means of Emission Management

It may be worthwhile to investigate the feasibility of using vehicle recorded information for emission estimation. Vehicles can already indicate their instantaneous fuel economy. If this information, along with other helpful data such as speed and acceleration or engine conditions, can be recorded, then it can be transmitted to a traffic control center for analysis. With connected vehicle technology (e.g., vehicle-to-vehicle, vehicle-to-infrastructure), large amounts of such vehicle-based data could be collected. Using this data, more accurate emission estimations can be performed. If this data can also be paired with GPS data, then a vehicle's position, along with its emissions-related information, can be known, and can then be associated with the relevant traffic controls. This method would enable a more direct flow of information between vehicle emissions and traffic controllers, cutting out some of the errors that may result in the emission modelling process.

References

Aimsum. (2010). *A Model Approach*. *Traffic Technology International*. Retrieved from http://www.aimsun.com/press/A_model_approach.pdf

Akçelik, R., Smit, R., & Besley, M. (2014). Recalibration of a Vehicle Power Model for Fuel and Emission Estimation and its Effect on Assessment of Alternative Intersection Treatments. *Roundabout Conference, Proceedings of the 4th International*, (April), 16–18. Retrieved from http://www.sidrasolutions.com/Cms_Data/Contents/SIDRA/Folders/Resources/Articles/Articles/~contents/K9TJUKAM3YMDKV5X/AKCELIK_TRBRouConf2014_Fuel-and-Emission-Estimation.pdf

Amirjamshidi, G., Mostafa, T. S., Misra, A., & Roorda, M. J. (2013). Integrated model for microsimulating vehicle emissions, pollutant dispersion and population exposure. *Transportation Research Part D: Transport and Environment*, *18*(1). https://doi.org/10.1016/j.trd.2012.08.003

Barth, M., An, F., Younglove, T., Scora, G., Levine, C., Ross, M., & Wenzel, T. (2009). Development of a Comprehensive Modal Emissions Model. *National Cooperative Highway Research Program*, 473–496.

Bogdanović, V., & Ruškić, N. (2013). The research of vehicle acceleration at signalized intersections. *Traffic and Transportation*, *25*(1), 33–42. https://doi.org/10.7307/ptt.v25i1.1245

Boulter, P., McCrae, I., & Barlow, T. (2006). A review of instantaneous emission models for road vehicles. *TRL Unpublished Report UPR/IE/030/06. TRL Limited, Wokingham*.

Bowyer, D. P., Akcelik, R., & Biggs, D. C. (1985). Guide to Fuel Consumption Analysis for Urban Traffic Management. *ARRB Transport Research*, *Special Re*, 98. Retrieved from http://www.sidrasolutions.com/Cms_Data/Contents/SIDRA/Folders/Resources/Articles/Articles/~contents/XCMJQVHWJAJ6ALYW/BowyerAkcelikBiggs_SR32_Fuel.pdf

Bretherton, D., Wood, K., & Raha, N. (2007). Traffic Monitoring and Congestion Management in the SCOOT Urban Traffic Control System. *Transportation Research Record: Journal of the Transportation Research Board*, *1634*(1), 118–122. https://doi.org/10.3141/1634-15

Choi, D., & Koupal, J. (2011). MOVES Validation. In *MOVES Workshop*. U.S. Environmental Protection Agency. Retrieved from https://www.epa.gov/sites/production/files/2016-06/documents/validation-moves-2011.pdf

Csikós, A., & Varga, I. (2012). Real-time Modeling and Control Objective Analysis of Motorway Emissions. *Procedia - Social and Behavioral Sciences*, *54*, 1027–1036. https://doi.org/10.1016/j.sbspro.2012.09.818

Datondji, S. René E., Dupuis, Y., Subirats, P., & Vasseur, P. (2016). Rotation and translation estimation for a wide baseline fisheye-stereo at crossroads based on traffic flow analysis. *IEEE Conference on Intelligent Transportation Systems, Proceedings, ITSC*, (November), 1534–1539. https://doi.org/10.1109/ITSC.2016.7795761

Datondji, Sokemi Rene Emmanuel, Dupuis, Y., Subirats, P., & Vasseur, P. (2016). A Survey of Vision-Based Traffic Monitoring of Road Intersections. *IEEE Transactions on Intelligent Transportation Systems*, *17*(10), 2681–2698. https://doi.org/10.1109/TITS.2016.2530146

Demir, E., Bektaş, T., & Laporte, G. (2011). A comparative analysis of several vehicle emission models for

road freight transportation. *Transportation Research Part D: Transport and Environment*, *16*(5), 347–357. https://doi.org/10.1016/j.trd.2011.01.011

Environment and Climate Change Canada. (2018). *Canadian Environmental Sustainability Indicators - Greenhouse Gas Emissions*. Retrieved from https://www.epa.gov/ghgemissions/sources-greenhouse-gas-emissions

European Environment Agency. (2013). *Do lower speed limits on motorways reduce fuel consumption and pollutant emissions ?* Copenhagen.

European Union. (2019). Low Emission Zones. Retrieved from http://urbanaccessregulations.eu/low-emission-zones-main/what-are-low-emission-zones

Federal Highway Administration. (2017). Chapter 6: Detectors. In *Traffic Control Systems Handbook*.

Franco, V., Kousoulidou, M., Muntean, M., Ntziachristos, L., Hausberger, S., & Dilara, P. (2013a). Road vehicle emission factors development: A review. *Atmospheric Environment*. https://doi.org/10.1016/j.atmosenv.2013.01.006

Franco, V., Kousoulidou, M., Muntean, M., Ntziachristos, L., Hausberger, S., & Dilara, P. (2013b). Road vehicle emission factors development: A review. *Atmospheric Environment*, *70*, 84–97. https://doi.org/10.1016/j.atmosenv.2013.01.006

Frey, H. C., Unal, A., Chen, J., & Song, L. (2003). Modeling Mobile Source Emissions Based Upon In-Use and Second-by-Second Data : Development of Conceptual Approaches for EPA ' s New MOVES Model. *Proceedings, Annual Meeting of the Air & Waste Management Association*, (x), 1–20.

Grote, M., Williams, I., Preston, J., & Kemp, S. (2016). Including congestion effects in urban road traffic CO2emissions modelling: Do Local Government Authorities have the right options? *Transportation Research Part D: Transport and Environment*, *43*. https://doi.org/10.1016/j.trd.2015.12.010

Hausberger, S., Rexeis, M., Zallinger, M., & Luz, R. (2009). *Emission Factors from the Model PHEM for the HBEFA Version 3*. *Graz University of Technology*. Retrieved from http://www.hbefa.net/e/documents/HBEFA32_EF_Euro_5_6_TUG.pdf

Jaikumar, R., Shiva Nagendra, S. M., & Sivanandan, R. (2017). Modal analysis of real-time, real world vehicular exhaust emissions under heterogeneous traffic conditions. *Transportation Research Part D: Transport and Environment*, *54*, 397–409. https://doi.org/10.1016/j.trd.2017.06.015

Jamshidnejad, A., Papamichail, I., Papageorgiou, M., & De Schutter, B. (2017). A mesoscopic integrated urban traffic flow-emission model. *Transportation Research Part C: Emerging Technologies*, *75*, 45–83. https://doi.org/10.1016/j.trc.2016.11.024

Jiménez-Palacios, J. L. (1999). Understanding and Quantifying Motor Vehicle Emissions with Vehicle Specific Power and TILDAS Remote Sensing, (1993), 361.

José, J., Díaz, V., Belén, A., González, R., & Wilby, M. R. (2016). Bluetooth Traffic Monitoring Systems for Travel Time Estimation on Freeways, *17*(1), 123–132. https://doi.org/10.1109/TITS.2015.2459013

Kanhere, N. K., & Birchfield, S. T. (2010). A Taxonomy and Analysis of Camera Calibration Methods for Traffic Monitoring Applications. *IEEE Transactions on Intelligent Transportation Systems*, *11*(2), 441–452. https://doi.org/10.1109/TITS.2010.2045500

Kumar Maurya, A., & Bokare, P. S. (2012). Study of Deceleration Behaviour of Different Vehicle Types.

International Journal for Traffic and Transport Engineering, *2*(3), 253–270. https://doi.org/10.7708/ijtte.2012.2(3).07

Laumbach, R. J., & Kipen, H. M. (2012). Respiratory health effects of air pollution: Update on biomass smoke and traffic pollution. *Journal of Allergy and Clinical Immunology*, *129*(1), 3–11. https://doi.org/10.1016/j.jaci.2011.11.021

Laval, J., He, Z., & Castrillon, F. (2012). Stochastic Extension of Newell's Three-Detector Method. *Transportation Research Record: Journal of the Transportation Research Board*, *2315*, 73–80. https://doi.org/10.3141/2315-08

Lejri, D., Can, A., Schiper, N., & Leclercq, L. (2018). Accounting for traffic speed dynamics when calculating COPERT and PHEM pollutant emissions at the urban scale. *Transportation Research Part D: Transport and Environment*, *63*(July), 588–603. https://doi.org/10.1016/j.trd.2018.06.023

Li, Y., Wang, W., Kan, H., Xu, X., & Chen, B. (2010). Air quality and outpatient visits for asthma in adults during the 2008 Summer Olympic Games in Beijing. *Science of the Total Environment*, *408*(5), 1226–1227. https://doi.org/10.1016/j.scitotenv.2009.11.035

Ligterink, N. (2016). Emission Factors from Emission Measurements. In *Symposium Vehicle Emissions*.

Linton, C., Grant-Muller, S., & Gale, W. F. (2015). Approaches and Techniques for Modelling CO2 Emissions from Road Transport. *Transport Reviews*, *35*(4), 533–553. https://doi.org/10.1080/01441647.2015.1030004

Liu, Hang, Tok, Y. C. A., & Ritchie, S. G. (2011). Development of a real-time on-road emissions estimation and monitoring system. *IEEE Conference on Intelligent Transportation Systems, Proceedings, ITSC*, 1821–1826. https://doi.org/10.1109/ITSC.2011.6083006

Liu, Haobing, Xu, Y., Rodgers, M. O., Akanser, A., & Guensler, R. (2016). *Improved Energy and Emissions Modeling for Project Evaluation (MOVES-Matrix)*. Retrieved from https://ncst.ucdavis.edu/wp-content/uploads/2014/09/10-10-2016-NCST_MOVESMatrix_FinalReport_version-4.pdf

Mann, H.-U. (2016). Methodenhandbuch zum Bundesverkehrswegeplan 2030. *PTV Group*, 1–493.

Mechanical Simulation. (2017). *CARSIM: Math Models*. Ann Arbor. Retrieved from https://www.carsim.com/downloads/pdf/CarSim_Math_Models.pdf

Muresan, M., Hossain, S. M. K., & Fu, L. (2016). TRB 2014 Annual Meeting Paper revised from original submittal. In *TRB 2016 Annual Meeting* (pp. 1–15). Washington DC: Transportation Research Board.

Ntziachristos, L., Samaras, Z., Kouridis, C., Samaras, C., Hassel, D., Mellios, G., … Geivanidis, S. (2018). *COPERT Guidebook 2016*.

Park, S., Ahn, K., Rakha, H. A., & Lee, C. (2015). Real-Time Emissions Modeling with Environmental Protection Agency MOVES. *Transportation Research Record: Journal of the Transportation Research Board*, *2503*(August), 60–69. https://doi.org/10.3141/2503-07

Porter, C., Kall, D., Beagan, D., Margiotta, R., Koupal, J., Fincher, S., & Stanard, A. (2015). *Input Guidelines for Motor Vehicle Emissions Simulator Model, Volume 2: Practitioners' Handbook: Project Level Inputs*. https://doi.org/10.17226/22213

PTV Group. (2015). *PTV Vissim 7 User Manual*. *PTV AG*.

PTV Vissim. (n.d.). Common Add-ons. Retrieved from http://vision-traffic.ptvgroup.com/fileadmin/files_ptvvision/Downloads_N/0_General/2_Products/2_PTV_Vissim/EN_PTV_Vissim_Modules.pdf

Rexeis, M., Hausberger, S., Kühlwein, J., & Luz, R. (2013). *Update of Emission Factors for EURO 5 and EURO 6 vehicles for the HBEFA Version 3 . 2*. *Graz University of Technology*. Graz. https://doi.org/Report No. I-25/2013/ Rex EM-I 2011/20 679

Rexeis, M., Hausberger, S., Kühlwein, J., & Luz, R. (2017). *Update of Emission Factors for EURO 5 and EURO 6 Diesel Passenger Cars for the HBEFA Version 3.3*. *Institute for Internal Combustion Engines and Thermodynamics*. https://doi.org/Report No. I-25/2013/ Rex EM-I 2011/20 679

Ross, M. (1997). Fuel Economy and the Physics of Automobiles. *Contemporary Physics*, *38*(6), 381–394.

Samaranayake, S., Glaser, S., Holstius, D., Monteil, J., Tracton, K., Seto, E., & Bayen, A. (2014). Real-Time Estimation of Pollution Emissions and Dispersion from Highway Traffic. *Computer-Aided Civil and Infrastructure Engineering*, *29*(7), 546–558. https://doi.org/10.1111/mice.12078

Scora, G., & Barth, M. (2007). *CMEM User ' S Guide*. https://doi.org/10.1111/j.1600-0447.2011.01711.x

Sensors Inc. (2016). PEMS. Retrieved from https://commons.wikimedia.org/w/index.php?curid=52237546

Shan, X., Chen, X., Hao, P., Boriboonsomsin, K., Wu, G., & Barth, M. (2018). Vehicle Energy / Emissions Estimation Based on Vehicle Trajectory Reconstruction Using Sparse Mobile Sensor Data, *479*, 2–5.

Smit, R., Ntziachristos, L., & Boulter, P. (2010). Validation of road vehicle and traffic emission models - A review and meta-analysis. *Atmospheric Environment*, *44*(25), 2943–2953. https://doi.org/10.1016/j.atmosenv.2010.05.022

Smith, M., Duncan, G., & Druitt, S. (1995). PARAMICS: microscopic traffic simulation for congestion management. *IEE Colloquium on Dynamic Control of Strategic Inter-Urban Road Networks*, 8–8. https://doi.org/10.1049/ic:19950249

So, J. (Jason), Motamedidehkordi, N., Wu, Y., Busch, F., & Choi, K. (2017). Estimating emissions based on the integration of microscopic traffic simulation and vehicle dynamics model. *International Journal of Sustainable Transportation*, *8318*, 1–13. https://doi.org/10.1080/15568318.2017.1363328

Song, Y. Y., Yao, E. J., Zuo, T., & Lang, Z. F. (2013). Emissions and fuel consumption modeling for evaluating environmental effectiveness of ITS strategies. *Discrete Dynamics in Nature and Society*, *2013*. https://doi.org/10.1155/2013/581945

Statistics Canada. (2009). Statistical Tables. Retrieved from http://www.statcan.gc.ca/pub/53-223-x/2009000/tablesectlist-listetableauxsect-eng.htm

Sun, Z., Hao, P., Ban, X. (Jeff), & Yang, D. (2015). Trajectory-based vehicle energy/emissions estimation for signalized arterials using mobile sensing data. *Transportation Research Part D: Transport and Environment*, *34*(January), 27–40. https://doi.org/10.1016/j.trd.2014.10.005

Swanson, B., Talbot, E., & Dumont, J. (2010). Analysis of Moves and Cmem for Evaluating the Emissions Impacts of an Intersection Control Change, *500*(August), 13. Retrieved from http://www.rsginc.com/sites/default/files/publications/117.Analysis of MOVES and CMEM for Evaluating the Emissions Impacts of an Intersection Control Change.pdf

Thorsen, S. (2018). Past Weather in Cambridge, Ontario, Canada — June 2016. Retrieved from https://www.timeanddate.com/weather/canada/cambridge/historic?month=6&year=2016

Treiber, M., & Kesting, A. (2013). Traffic flow dynamics: Data, models and simulation. In *Traffic Flow Dynamics: Data, Models and Simulation* (pp. 1–503). https://doi.org/10.1007/978-3-642-32460-4

U.S. Department of Transportation. (2017). Traffic Analysis Toolbox Volume VI: Definition, Interpretation, and Calculation of Traffic Analysis Tools Measures of Effectiveness. Retrieved from https://ops.fhwa.dot.gov/publications/fhwahop08054/execsum.htm#es_04

U.S. Environmental Protection Agency. (2014). *MOVES2014 Software Design Reference Manual MOVES2014 Software Design Reference Manual*.

U.S. Environmental Protection Agency. (2015). MOVES Algorithms Reference. Retrieved from https://www.epa.gov/moves/moves-algorithms

U.S. Environmental Protection Agency. (2016a). Greenhouse Gas Inventory Guidance: Direct Emissions from Stationary Combustion Sources. *Energy Economics*, *34*(5), 1580–1588. https://doi.org/10.1016/j.eneco.2011.11.013

U.S. Environmental Protection Agency. (2016b). *Population and Activity of On-road Vehicles in MOVES2014*.

U.S. EPA. (2018). Inventory of U.S. Greenhouse Gas Emissions and Sinks. Retrieved from https://www.epa.gov/sites/production/files/2018-01/documents/2018_complete_report.pdf

US EPA. (2015). *MOVES2014a User Guide*. Retrieved from https://www.epa.gov/moves/moves2014a-latest-version-motor-vehicle-emission-simulator-moves

Vieira da Rocha, T., Leclercq, L., Montanino, M., Parzani, C., Punzo, V., Ciuffo, B., & Villegas, D. (2015). Does traffic-related calibration of car-following models provide accurate estimations of vehicle emissions? *Transportation Research Part D: Transport and Environment*, *34*, 267–280. https://doi.org/10.1016/j.trd.2014.11.006

Wu, X., Zhang, S., Wu, Y., Li, Z., Zhou, Y., Fu, L., & Hao, J. (2015). Real-world emissions and fuel consumption of diesel buses and trucks in Macao: From on-road measurement to policy implications. *Atmospheric Environment*, *120*. https://doi.org/10.1016/j.atmosenv.2015.09.015

Xu, X., Liu, H., Anderson, J. M., Xu, Y. (Ann), Hunter, M. P., Rodgers, M. O., & Guensler, R. L. (2016). Estimating Project-Level Vehicle Emissions with Vissim and MOVES-Matrix. *Transportation Research Record: Journal of the Transportation Research Board*, *2570*, 107–117. https://doi.org/10.3141/2570-12

Yao, Z., Wei, H., Ma, T., Li, G., Ai, Q., & Liu, H. (2012). Developing Operating Mode Distribution Inputs for MOVES using Computer Vision-based Vehicle Data Collector, *9*(513).

Zhang, K., & Batterman, S. (2014). Air pollution and health risks due to vehicle traffic. *Science of the Total Environment*, (2), 307–316. https://doi.org/10.1016/j.scitotenv.2013.01.074.Air

Zhang, Y., Lv, J., & Wang, W. (2013). Evaluation of vehicle acceleration models for emission estimation at an intersection. *Transportation Research Part D: Transport and Environment*, *18*(1), 46–50. https://doi.org/10.1016/j.trd.2012.09.004

Zhao, Y., & Sadek, A. W. (2013). Computationally-Efficient Approaches to Integrating the MOVES

Emissions Model with Traffic Simulators. *Procedia - Procedia Computer Science*, *19*, 882–887. https://doi.org/10.1016/j.procs.2013.06.118

Appendix A – Operating Mode Bins

opModeID	opModeName	Bin Boundaries					
		VSPLower	VSPUpper	speedLower [mph]	speedUpper [mph]	brakeRate1Sec [mph/s]	brakeRate3Sec [mph/s]
0	Braking	0	0	0	0	-2	-1
1	Idling	0	0	-1	1	0	0
11	Low Speed Coasting; VSP< 0; 1<=Speed<25	0	0	1	25	0	0
12	Cruise/Acceleration; 0<=VSP< 3; 1<= Speed<25	0	3	1	25	0	0
13	Cruise/Acceleration; 3<=VSP< 6; 1<=Speed<25	3	6	1	25	0	0
14	Cruise/Acceleration; 6<=VSP< 9; 1<=Speed<25	6	9	1	25	0	0
15	Cruise/Acceleration; 9<=VSP<12; 1<=Speed<25	9	12	1	25	0	0
16	Cruise/Acceleration; 12<=VSP; 1<=Speed<25	12	0	1	25	0	0
21	Moderate Speed Coasting; VSP< 0; 25<=Speed<50	0	0	25	50	0	0
22	Cruise/Acceleration; 0<=VSP< 3; 25<=Speed<50	0	3	25	50	0	0
23	Cruise/Acceleration; 3<=VSP< 6; 25<=Speed<50	3	6	25	50	0	0
24	Cruise/Acceleration; 6<=VSP< 9; 25<=Speed<50	6	9	25	50	0	0
25	Cruise/Acceleration; 9<=VSP<12; 25<=Speed<50	9	12	25	50	0	0
26	Cruise/Acceleration; 12<=VSP; 25<=Speed<50	12	0	25	50	0	0
27	Cruise/Acceleration; 12<=VSP<18; 25<=Speed<50	12	18	25	50	0	0
28	Cruise/Acceleration; 18<=VSP<24; 25<=Speed<50	18	24	25	50	0	0
29	Cruise/Acceleration; 24<=VSP<30; 25<=Speed<50	24	30	25	50	0	0
30	Cruise/Acceleration; 30<=VSP; 25<=Speed<50	30	0	25	50	0	0
33	Cruise/Acceleration; VSP< 6; 50<=Speed	0	6	50	0	0	0
35	Cruise/Acceleration; 6<=VSP<12; 50<=Speed	6	12	50	0	0	0
36	Cruise/Acceleration; 12 <= VSP; 50<=Speed	12	0	50	0	0	0
37	Cruise/Acceleration; 12<=VSP<18; 50<=Speed	12	18	50	0	0	0
38	Cruise/Acceleration; 18<=VSP<24; 50<=Speed	18	24	50	0	0	0
39	Cruise/Acceleration; 24<=VSP<30; 50<=Speed	24	30	50	0	0	0
40	Cruise/Acceleration; 30<=VSP; 50<=Speed	30	0	50	0	0	0
300	All Running	0	0	0	0	0	0

Appendix B – Sample of Signal Plan

#803 - HESPELER ROAD @ DUNBAR ROAD **T08-50/24C**

Semi-Actuated Operation.
Actuated protected/permissive NB/SB/WB left-turn phases.
Intersection equipped with Transit Signal Priority.

Signal timing in effect: **06:00 – 10:00 Monday to Friday**

Hespeler Road					
NB Green Arrow	Min.	7.0 seconds	SB Green Arrow	Min.	7.0 seconds
	Ext.	3.0 seconds		Ext.	3.0 seconds
	Max.	11.6 seconds		Max.	8.0 seconds
N/S Amber Arrow		3.0 seconds			
All Red		1.0 second			
Green		57.6 seconds	Walk – 40.6 seconds		
Amber		4.0 seconds	FDW – 17.0 seconds		
All Red		2.0 seconds			
Dunbar Road					
WB Green Arrow	Min.	7.0 seconds			
	Ext.	3.0 seconds			
	Max.	9.2 seconds			
WB Amber Arrow		3.0 seconds			
All Red		1.0 second	Pedestrian Call		
Green	Min.	8.0 seconds	Green/Walk – 10.0 seconds		
	Ext.	3.0 seconds	Green/FDW – 23.0 seconds		
	Max.	21.6 seconds	Green/SDW – 1.8 seconds		
Amber		4.0 seconds			
All Red		2.0 seconds			
TOTAL		**120.0 seconds**			

Signal timing in effect: **10:00 - 14:00 & 19:00 - 22:00 Monday to Friday;**
09:00 - 22:00 Saturday; 11:00 - 18:00 Sunday;

Hespeler Road					
NB Green Arrow	Min.	7.0 seconds	SB Green Arrow	Min.	7.0 seconds
	Ext.	3.0 seconds		Ext.	3.0 seconds
	Max.	8.0 seconds		Max.	10.4 seconds
N/S Amber Arrow		3.0 seconds			
All Red		1.0 second			
Green		56.4 seconds	Walk – 39.4 seconds		
Amber		4.0 seconds	FDW – 17.0 seconds		
All Red		2.0 seconds			
Dunbar Road					
WB Green Arrow	Min.	7.0 seconds			
	Ext.	3.0 seconds			
	Max.	11.6 seconds			
WB Amber Arrow		3.0 seconds			
All Red		1.0 second	Pedestrian Call		
Green	Min.	8.0 seconds	Green/Walk – 10.0 seconds		
	Ext.	3.0 seconds	Green/FDW – 23.0 seconds		
	Max.	21.6 seconds	Green/SDW – 4.2 seconds		
Amber		4.0 seconds			
All Red		2.0 seconds			
TOTAL		**120.0 seconds**			

Cont'd...P2

Appendix C – Signal Actuation Detector Loop Layout

Sent: November 9, 2017 4:11 PM
Subject: RE: Traffic Signal Plans Request

Hi Anjie,

We use a standard detector length of 30m. All side streets along Hespeler Rd have detection in every lane as they are actuated. The only lanes where detectors are set back 7.5m from the stop bar are left-turn lanes on the main street with protected/permissive phasing. The reasoning for that is to only display the left-turn phase if 2 or more vehicles are in the lane. If the left-turn is fully-protected the detector is not set back. This would be the case at Hespeler @ Eagle/Pinebush.

Hope this helps. If you have any other questions, let me know.

Sent: Thursday, November 09, 2017 9:54 AM
Subject: RE: Traffic Signal Plans Request

Hi Patricia,

Would it be possible for me to get information on the vehicle detector layouts of these intersections as well? Such as setbacks, detector lengths, etc.

Thank you,

Anjie

Appendix D – Sample of Turning Movement Count Data

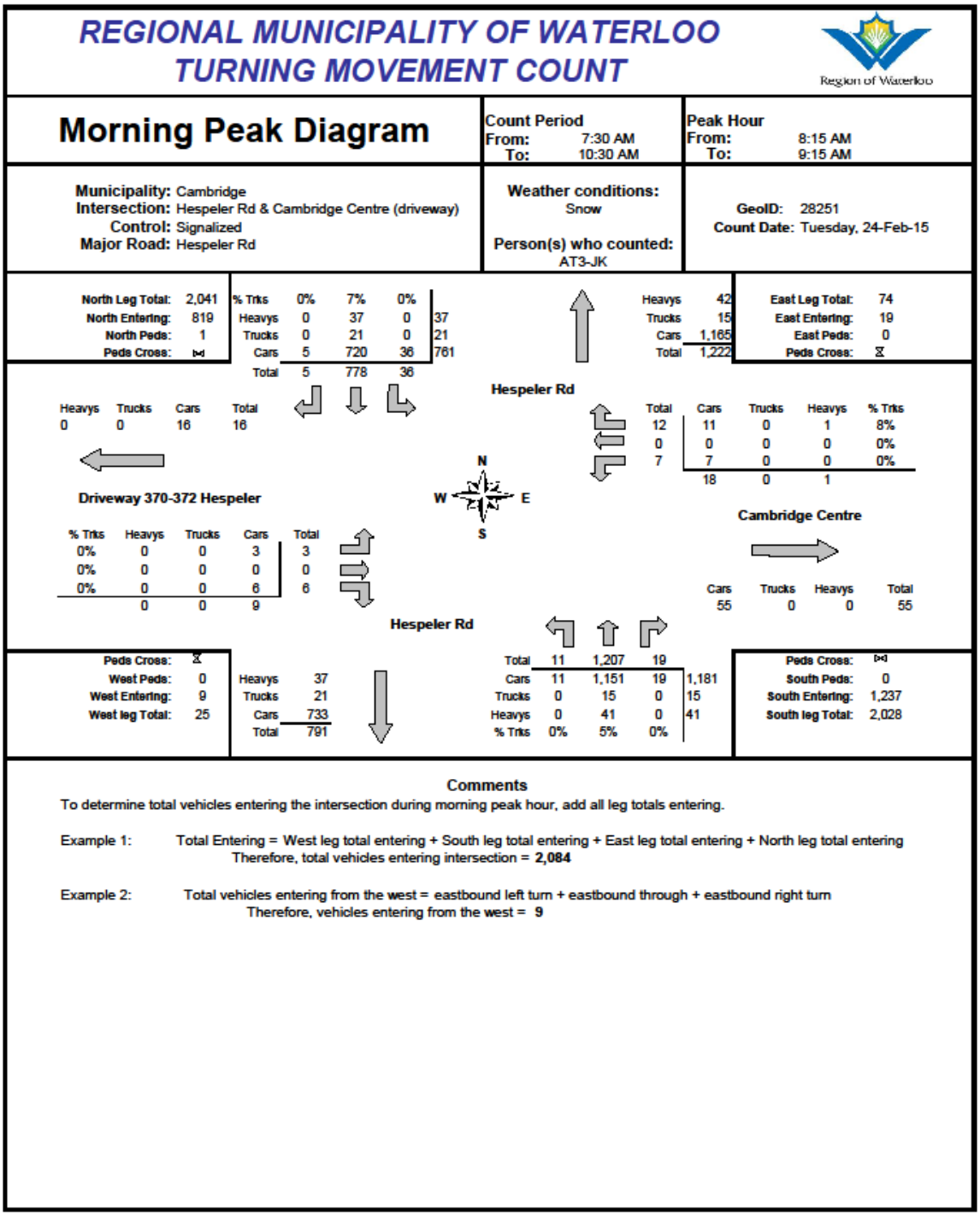

REGIONAL MUNICIPALITY OF WATERLOO
TURNING MOVEMENT COUNT

Region of Waterloo

Morning Peak Diagram

Count Period
From: 7:30 AM
To: 10:30 AM

Peak Hour
From: 8:15 AM
To: 9:15 AM

Municipality: Cambridge
Intersection: Hespeler Rd & Cambridge Centre (driveway)
Control: Signalized
Major Road: Hespeler Rd

Weather conditions: Snow

Person(s) who counted: AT3-JK

GeoID: 28251
Count Date: Tuesday, 24-Feb-15

North Leg Total: 2,041
North Entering: 819
North Peds: 1
Pede Cross: ⋈

% Trks	0%	7%	0%	
Heavys	0	37	0	37
Trucks	0	21	0	21
Cars	5	720	36	761
Total	5	778	36	

Heavys	Trucks	Cars	Total
0	0	16	16

Driveway 370-372 Hespeler

% Trks	Heavys	Trucks	Cars	Total
0%	0	0	3	3
0%	0	0	0	0
0%	0	0	6	6
	0	0	9	

Pede Cross: ⧖
West Peds: 0
West Entering: 9
West leg Total: 25

Heavys	37			
Trucks	21			
Cars	733			
Total	791			

Hespeler Rd

Total	11	1,207	19	
Cars	11	1,151	19	1,181
Trucks	0	15	0	15
Heavys	0	41	0	41
% Trks	0%	5%	0%	

Pede Cross: ⋈
South Peds: 0
South Entering: 1,237
South leg Total: 2,028

Heavys	42		
Trucks	15		
Cars	1,165		
Total	1,222		

East Leg Total: 74
East Entering: 19
East Peds: 0
Pede Cross: ⧖

Hespeler Rd

Total	Cars	Trucks	Heavys	% Trks
12	11	0	1	8%
0	0	0	0	0%
7	7	0	0	0%
	18	0	1	

N
W E
S

Cambridge Centre

Cars	Trucks	Heavys	Total
55	0	0	55

Comments

To determine total vehicles entering the intersection during morning peak hour, add all leg totals entering.

Example 1: Total Entering = West leg total entering + South leg total entering + East leg total entering + North leg total entering
Therefore, total vehicles entering intersection = **2,084**

Example 2: Total vehicles entering from the west = eastbound left turn + eastbound through + eastbound right turn
Therefore, vehicles entering from the west = **9**

Appendix E – Comparison of Field and Simulation Travel Times

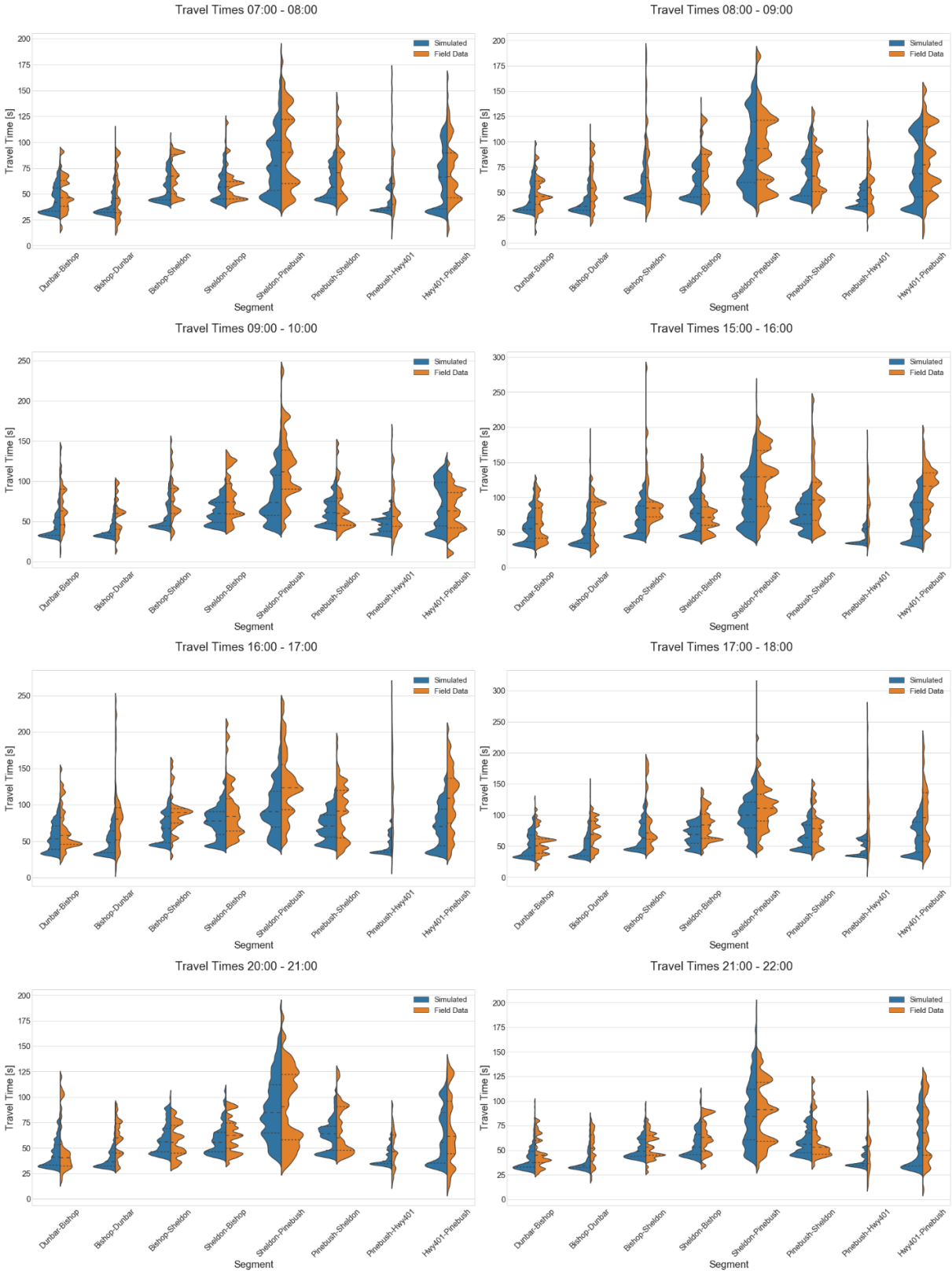

Comparison of Field and Simulation Travel Time Scaled by Sample Sizes

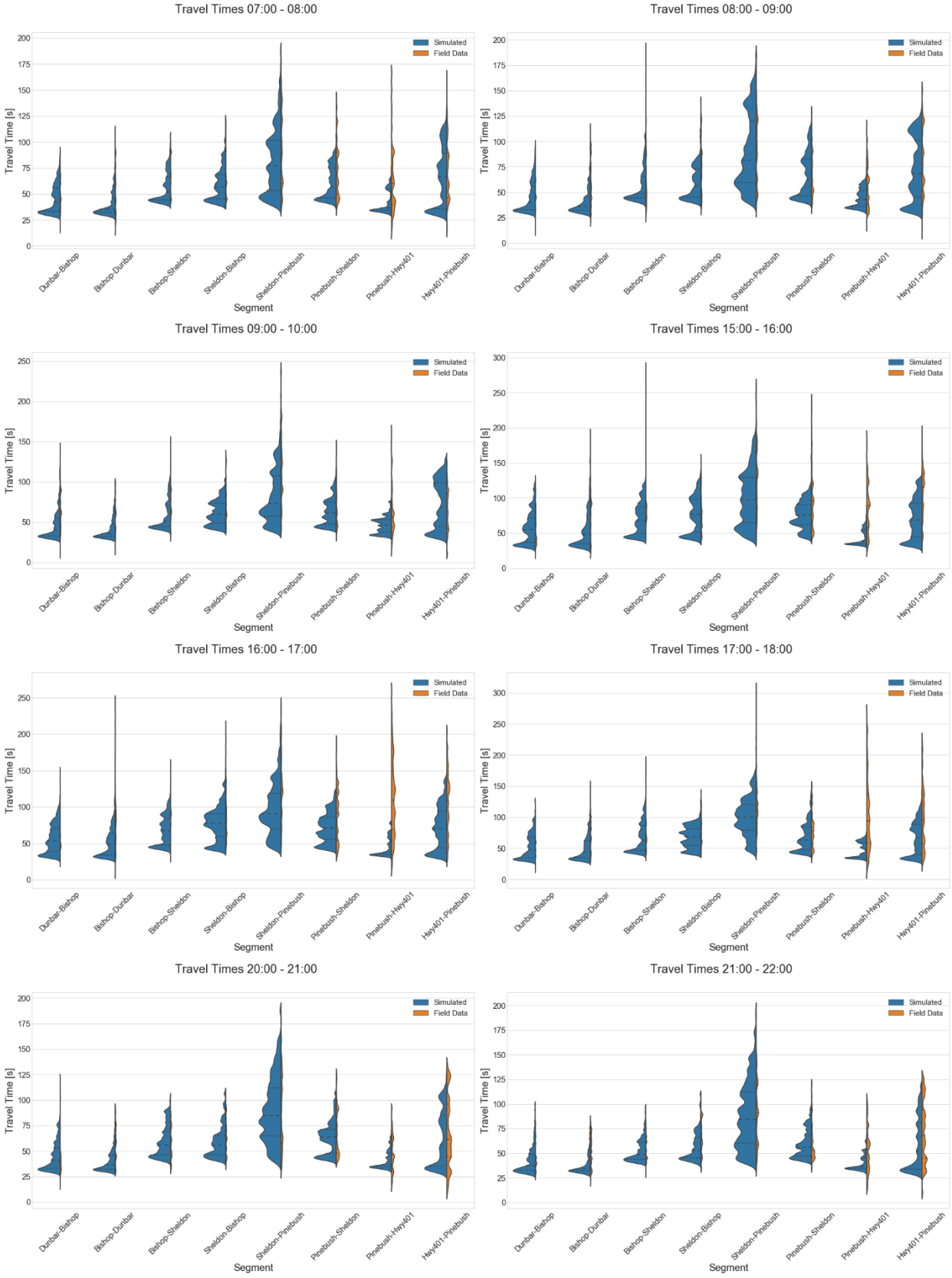

Appendix F – Vehicle Age Distribution Extrapolation

Age	Age Proportion
0	0.047412297
1	0.077551647
2	0.081137376
3	0.074652732
4	0.075186485
5	0.067807862
6	0.080344456
7	0.075363515
8	0.064434485
9	0.06879337
10	0.053266193
11	0.050479411
12	0.041851768
13	0.027045465
14	0.026046501
15	0.019670907
16	0.014898813
17	0.012768849
18	0.00885373
19	0.007332129
20	0.005767657
21	0.004536999
22	0.00356893
23	0.00280742
24	0.002208395
25	0.001737185
26	0.001366518
27	0.001074941
28	0.000845579
29	0.000665156
30	0.00052323

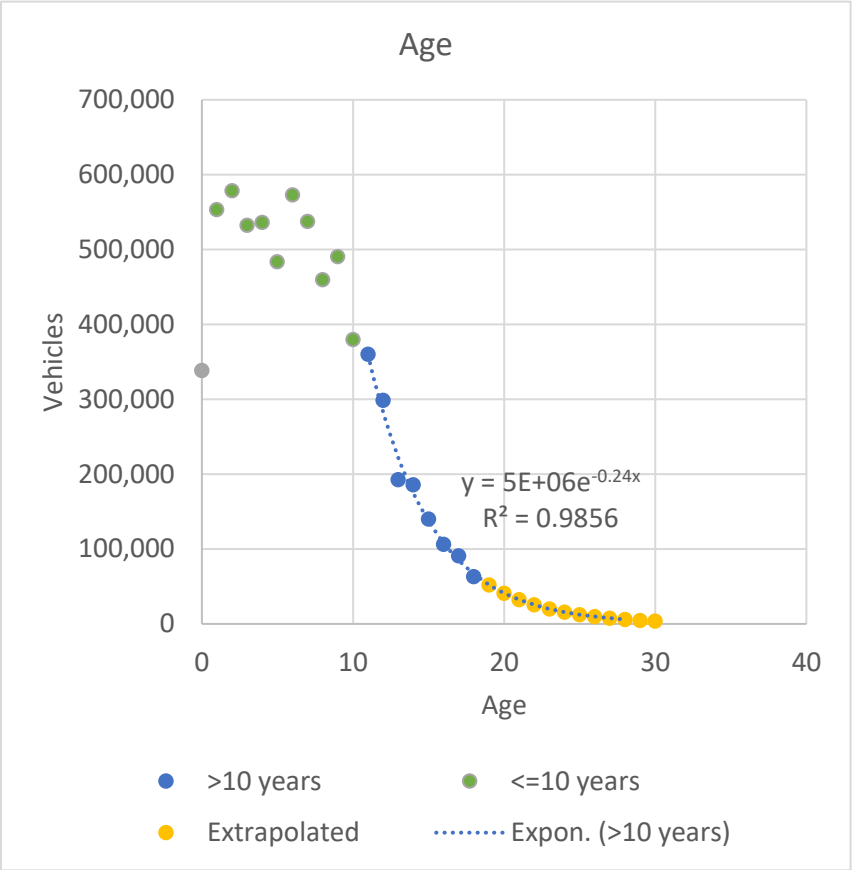

Extrapolation of age distribution for vehicles 19 years and older was based on available data for vehicles older than 10 years.

Appendix G – Partial Visualization of the MOVES Algorithm

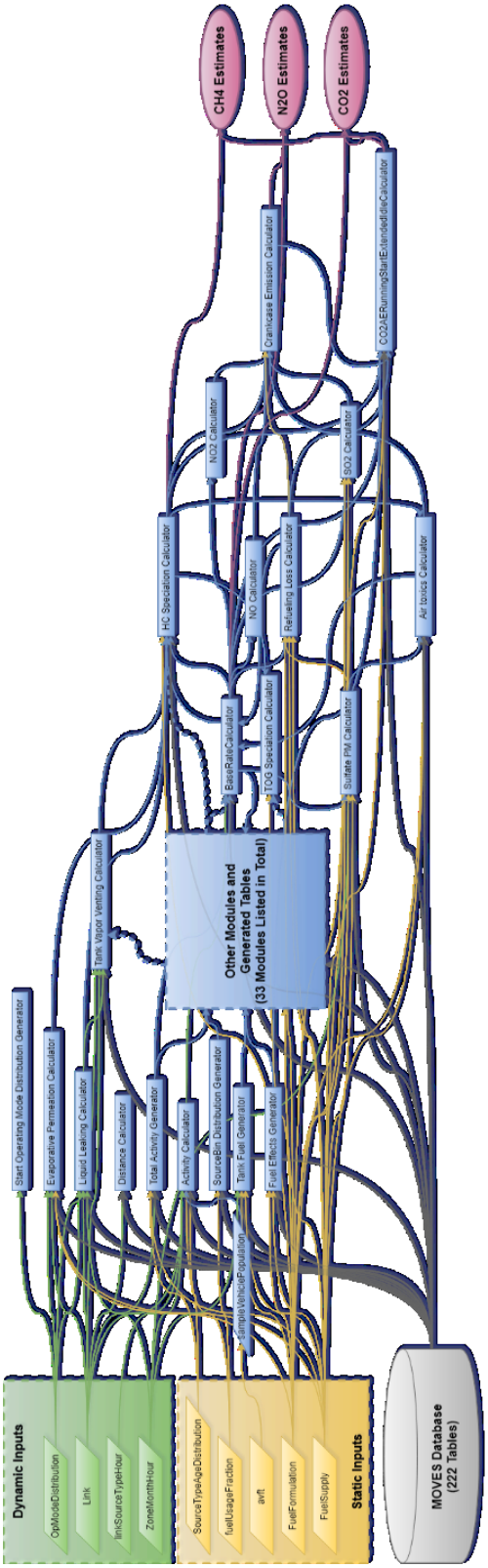

Based on

(U.S. Environmental Protection Agency, 2015)

Appendix H – Emissions from Simulated Trajectories of Field Conditions

Passenger Cars

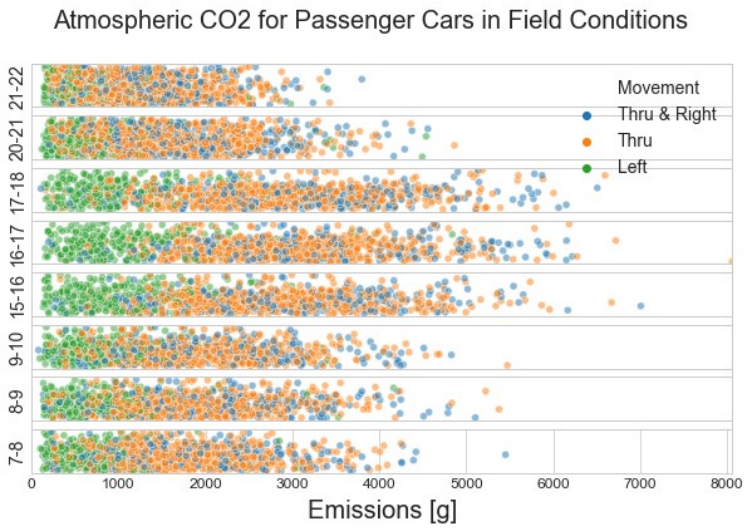

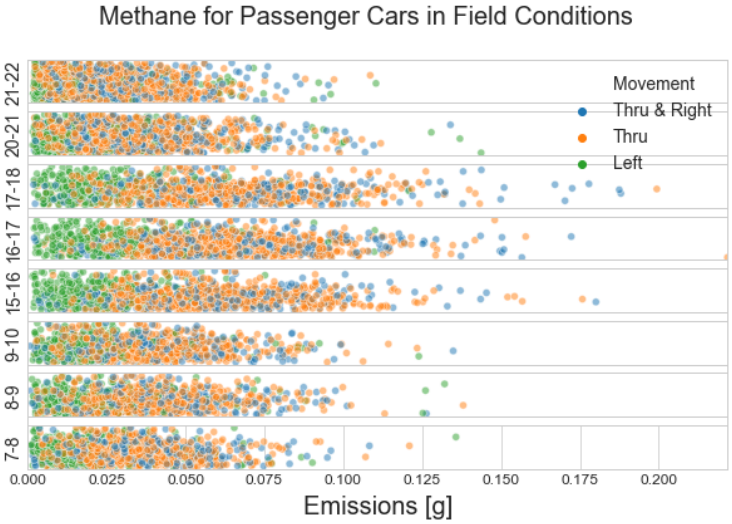

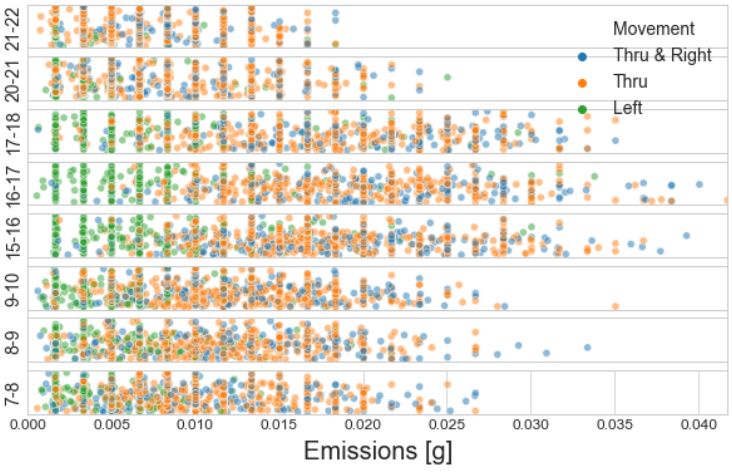

Single Unit Trucks

Atmospheric CO2 for Single Unit Trucks in Field Conditions

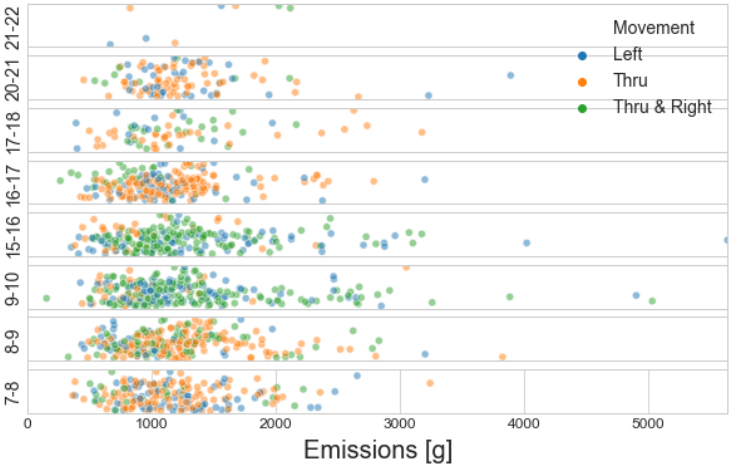

Methane for Single Unit Trucks in Field Conditions

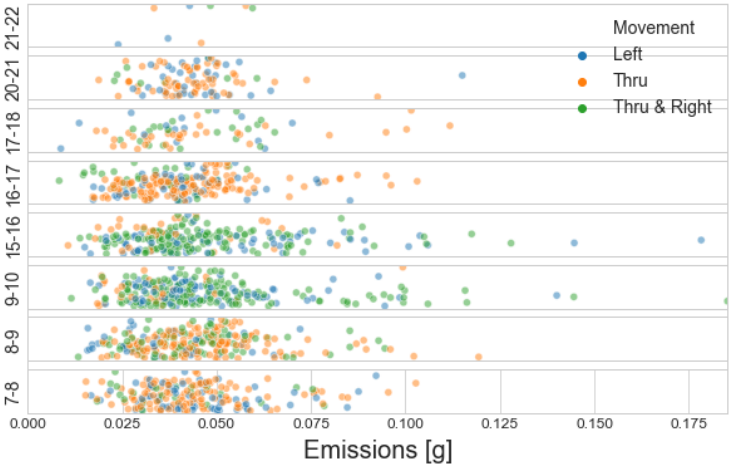

Nitrous Oxide for Single Unit Trucks in Field Conditions

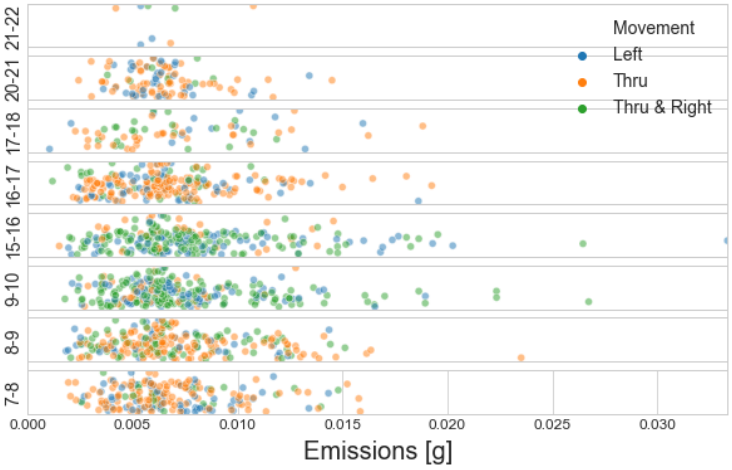

Combination Trucks

Nitrous Oxide for Combination Trucks in Field Conditions

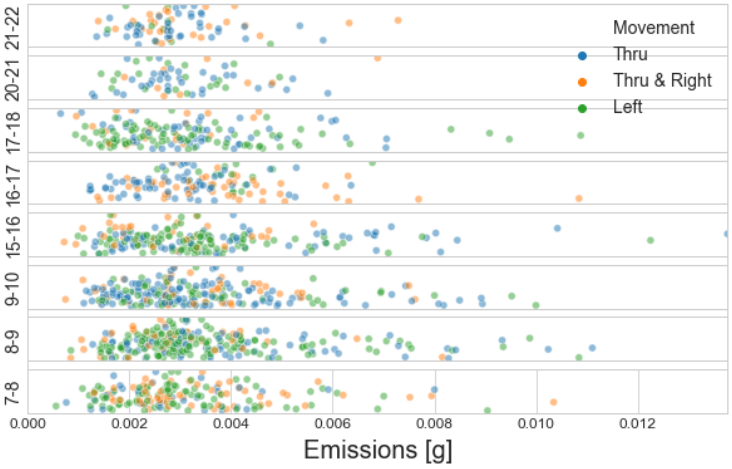

Atmospheric CO2 for Combination Trucks in Field Conditions

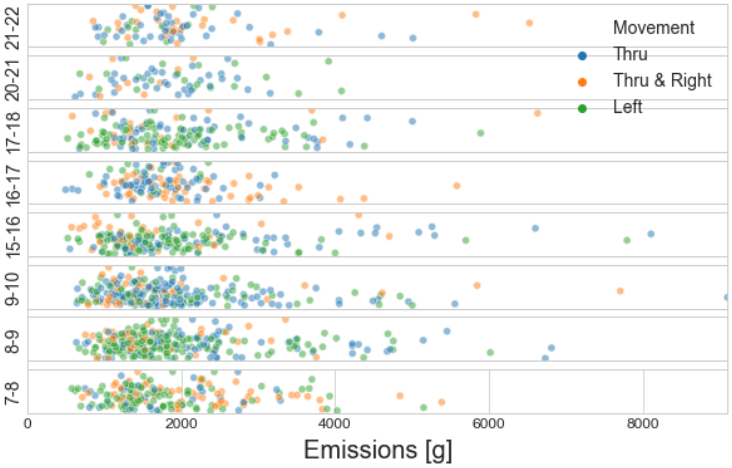

Methane for Combination Trucks in Field Conditions

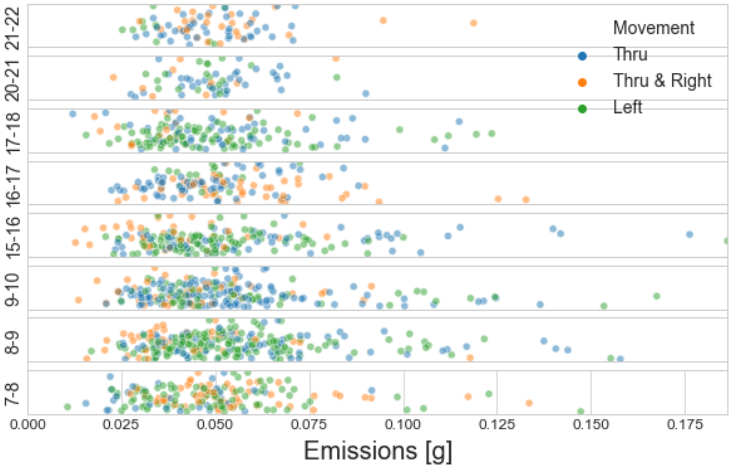

Transit Buses

Atmospheric CO2 for Transit Buses in Field Conditions

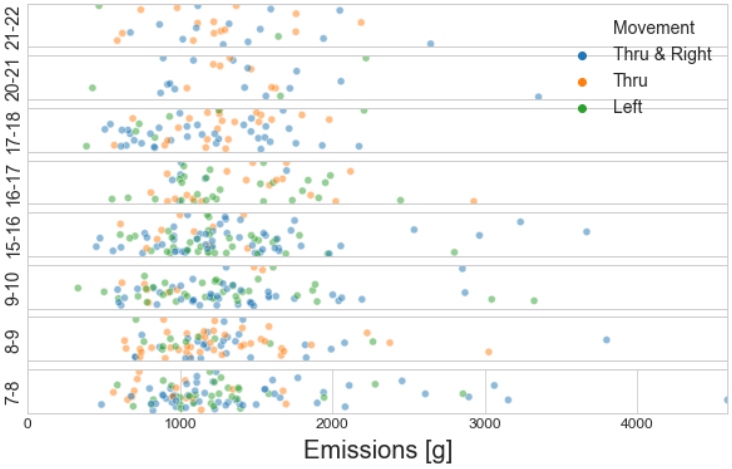

Methane for Transit Buses in Field Conditions

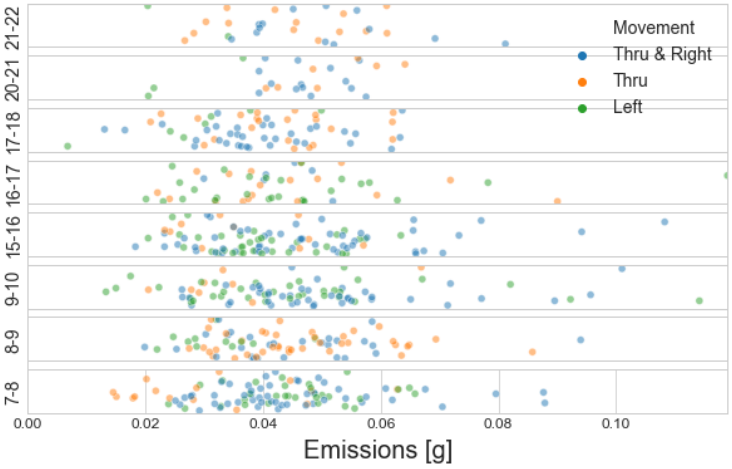

Nitrous Oxide for Transit Buses in Field Conditions